AMINO ACID BASED GREEN INHIBITORS FOR THE CORROSION OF MILD STEEL AND COPPER IN DIFFERENT MEDIA

Thesis
Submitted to the University of Calicut
For the award of the degree of

DOCTOR OF PHILOSOPHY IN CHEMISTRY

MATHEW KURUVILLA

DEPARTMENT OF CHEMISTRY
UNIVERSITY OF CALICUT
KERALA-673635
INDIA

MARCH 2016

CERTIFICATE

This is to certify that the thesis entitled **"Amino acid based green inhibitors for the corrosion of mild steel and copper in different media"** submitted by **Mathew Kuruvilla** to Calicut University for the award of the degree of Doctor of Philosophy in Chemistry, is the result of bonafide research work carried out by him in the Department of Chemistry, University of Calicut under my guidance and supervision. I also certify that the thesis or part therefore has not been formed earlier as base for the award of any degree, diploma or associateship of any other university or institution.

University of Calicut **Dr. Abraham Joseph**

March - 2016

DECLARATION

I hereby declare that the content of the thesis is the result of investigations carried out by me under the supervision of **Dr. Abraham Joseph**, Professor, Department of Chemistry, University of Calicut and the same has not been previously formed the basis for the award of any degree or diploma from any university/institute.

The investigations described or cited wherever in the thesis are based on the findings of other researchers, due acknowledgement has been given in tune with the general practice of reporting scientific observations/inferences. However, errors and unintentional oversights, if any, are regretted.

Mathew Kuruvilla

ACKNOWLEDGEMENT

I am deeply indebted to my supervising teacher **Dr.Abraham Joseph**, Professor, Department of Chemistry, University of Calicut for his dynamic guidance, constant support and encouragements during the course of this investigation.

It is with immense pleasure I place on record my profound gratitude to Dr. K. Muraleedharan, Head of the Department of Chemistry, for providing me the facilities in the department required for the conduct of research work.

I am grateful to Prof. V. M. Abdul Mujeeb, former Head of the department of Chemistry, Dr. N. K. Renuka, Assistant Professor, Dr. Pradeepan Periyat, Assistant Professor, all other faculty members & technical staff in the department of Chemistry, University of Calicut for their support and encouragements.

Thanks are also due to Dr. V. V. Radhakrishnan, Associate Professor, Dept.of Botany, University of Calicut and Dr.Anup Thomas, Assistant Professor, SCET for their encouragements and valuable assistance.

The unstinted support rendered by Dr.Bincy Joseph, Dr.Sam John, Ms.Rugmani Ammal Ms.Prajila, Ms. Remya, Ms. Revathy, Miss. Anupama, Miss. Shainy, Miss.Anupama R Prasad and all other fellow researchers in the department of Chemistry is gratefully acknowledged.

Financial assistance received from the University Grant Commision, New Delhi for the project entitled ‘Amino acid derived green inhibitors for the corrosion of mild steel and copper in acid solutions’ which forms part of this thesis is also acknowledged.

I also express my sincere gratitude to all those who have extended their support directly or indirectly for the successful completion of my research work.

I bow my head to the Almighty for abundant blessings poured on me during the course of the investigations enabling me to submit the thesis in time.

Mathew Kuruvilla

CONTENTS

PREFACE

Corrosion is a spontaneous process and is generally addressed as a hundred billion dollar thief. It contains the reaction of a metallic material and its environment. The corrosion of metals leads to large loss and the nations all over the world witness great losses due to this phenomenon in terms of economics, safety and environmental damage. A corrosion inhibitor is a chemical substance that, upon addition to a corrosive environment, reduces the corrosion rate to a threshold level. These inhibitors are always used in low concentration. Protection from corrosion can be achieved by addition of inhibitors and by the use of protective coatings. Corrosion protection of metals and alloys is therefore a subject of great technological and industrial importance and an enormous amount of research works have been initiated towards the study on corrosion and the stability of the materials in various environments. Organic inhibitors are widely used to protect metals and alloys from corrosion. However, most of these compounds are synthetic in nature and are expensive, toxic and causes hazardous impact to living creatures and the environment. Considering the demerits of synthetic inhibitors, the isolation of efficient and eco-friendly corrosion inhibitors became highly necessary as an alternative of toxic inhibitors. In recent years the research is oriented to the identification of green corrosion inhibitors like amino acids and its schiff bases with good inhibition efficiency and minimum environmental pollution. The information on the effect of amino acids

and amino acid derived schiff bases on corrosion behaviour of metals such as mild steel and copper is very little and therefore studies were undertaken to find out the effect of amino acids such as cysteine, alanine and Schiff bases viz, MOAB[(Z) – 3 – methyl – 2- (2-oxoindolin–3–ylideneamino) butanoic acid], HMIB [(E) - 2 – (2-hydroxynaphthalene – 1-yl) methyleneamino) - 4 –(1H – imidazolyl – 5 –yl) butanoic acid, HMMB (E – 2- ((2- hydroxy – 4a,8a – dihydronaphthalene- 1- yl)methyleneamino)- 4- (methylthio) butanoic acid), HHDMP [Z -3-hydroxy-2-((2-hydroxy-4a,8a,-dihydro-naph-thalene-1-yl) methyleneamino) propanoic acid, HDMMA [(E)–2-((2-hydroxyl–4a,8a–dihydronaphthalene –1- yl)methyleneamino) – 3-mercaptopropanoic acid] etc. derived from the amino acids on mild steel and copper under hydrochloric acid and sulphuric medium at varying temperatures.

The thesis is divided into ten chapters containing two parts Part – A and Part – B. First two chapters include introduction and materials and methods. Part – A deals with corrosion inhibition of copper using amino acid schiff bases and Part – B deals with corrosion inhibition of mild steel using amino acid schiff bases.

CHAPTER I - INTRODUCTION

This chapter contains a brief introduction to corrosion, classification of corrosion, common corrosion prevention methods, corrosion inhibitors and corrosion monitoring techniques such as gravimetric methods, electrochemical techniques and surface morphological techniques. The

application of quantum chemical methods and review of literature are also included.

CHAPTER II - MATERIALS AND METHODS

This chapter highlights about various inhibitor molecules, metals, materials and methods used in the investigations. The methodology adopted includes weight loss, polarization studies, quantum mechanical calculations etc.

CHAPTER III - ELECTROCHEMICAL STUDIES ON THE INTERACTION AND CORROSION INHIBITION BEHAVIOUR OF L – CYSTEINE WITH COPPER IN SULPHURIC ACID.

This chapter explains the inhibitory effect of a sulphur containing amino acid, L - cysteine, on copper in different concentrations of sulphuric acid (0.5M, 1.0M and 1.5M) at different temperatures (303K, 308K & 313K). Techniques like weight loss method, electrochemical impedance spectroscopy (EIS), potentiodynamic polarization (Tafel) and adsorption studies were employed. The structure of the inhibitor is given in figure.1

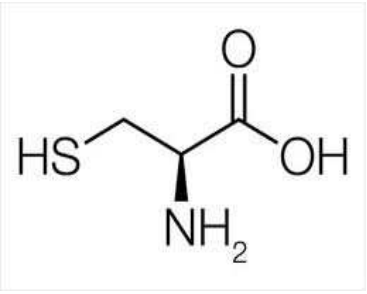

Figure. 1

Results revealed that L - cysteine do offer attractive inhibition efficiency. However, with an increase in the concentration of the inhibitor, corrosion rate decreased irrespective of the temperature gradients. This is due to the adsorption of the inhibitor molecules on the metal surface which has contributed to decrease the double layer capacitance and increase the polarization resistance. With the increase in the concentration of the medium, the corrosion rate also increased and this is due the liberation of high quantum of H^+ ions. Based on Tafel studies, it can be concluded that L - cysteine could act as a mixed type inhibitor.

CHAPTER IV - ELECTRO CHEMICAL INTERACTIONS OF HHDMP, A L- SERINE BASED SCHIFF BASE, WITH COPPER IN SULPHURIC ACID

Corrosion inhibition effect of L-serine based schiff base HHDMP on copper under 1M sulphuric acid at a temperature gradient of 303K, 308K & 313 K is described. Various techniques such as weight loss method, electrochemical impedance spectroscopy (EIS), potentiodynamic polarization (Tafel), basic computational calculations and adsorption studies were employed to study the inhibitory effect. A perusal of the results revealed that schiff base HHDMP do offer attractive inhibition efficiency and the inhibition effect advanced with the increase in concentration of the inhibitor. This trend is not maintained in the case of temperature regimes. With the increase of temperature the inhibition efficiency declined. The polarization studies showed that increasing the inhibitor concentration reduces both the cathodic and the anodic current, and there is no definite trend in the

shift of E_{corr} values. The displacement in E_{corr} values in the absence and presence of the inhibitors, were less than 85 mV and therefore, the inhibitor was considered as mixed type. The ΔG^0_{ads} values, derived from the adsorption studies support that adsorption involved is physisorption. Structure of the molecule is given in Figure.2

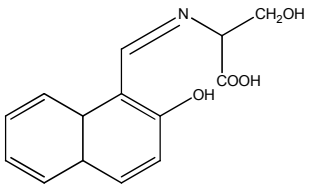

Figure.2

CHAPTER V - ELECTROCHEMICAL INTERACTIONS OF HDMMA, A CYSTEINE BASED SCHIFF BASE, WITH COPPER IN HYDROCHLORIC ACID

Studies undertaken to find out the inhibitory effect of cysteine based schiff base HDMMA [(E)–2-((2- hydroxyl–4a,8a–dihydronaphthalene –1- yl)methyleneamino) – 3- mercaptopropanoic acid] on mild steel in 1M hydrochloric acid at a temperature regime of 303K,308K & 313K.Techniques such as weight loss method, electrochemical impedance spectroscopy (EIS), potentiodynamic polarization (Tafel),scanning electron microscopy (SEM), basic computational calculations and adsorption studies were employed to understand the corrosion behaviour. The structure of the inhibitor molecule is given in Figure.3.

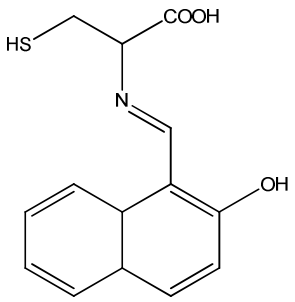

Figure.3

Weight loss studies revealed that the inhibition efficiency became high upto 24 hour interval irrespective of various concentrations of the inhibitor and subsequently the efficiency declined. Electrochemical results indicated that the electrochemical parameters vary with the inhibitor concentration and also with the temperature. Tafel polarization studies revealed that HDMMA can act as a mixed type inhibitor.

CHAPTER VI- ELECTROCHEMICAL STUDIES ON THE INTERACTION AND CORROSION INHIBITION BEHAVIOUR OF CYSTEINE /ALANINE PAIR ON COPPER IN SULPHURIC ACID

The synergistic interaction of cysteine and alanine on the corrosion inhibition of copper in 1M of sulphuric acid at various temperatures are outlined. Electrochemical studies revealed that I_{corr} value shows a decreasing trend with increased concentration of the inhibitor in all temperature regimes (303K, 308K & 313K). It is evidenced that as the concentration of the inhibitor increases, inhibition efficiency also

increases and reaches to maximum at a combination of cysteine 150ppm and alanine 50ppm. Synergism parameter S_θ was calculated from electrochemical data and it is clear that the values of S_θ were greater than unity only at high temperature. The structure of the inhibitor molecule is given in Figure.4.

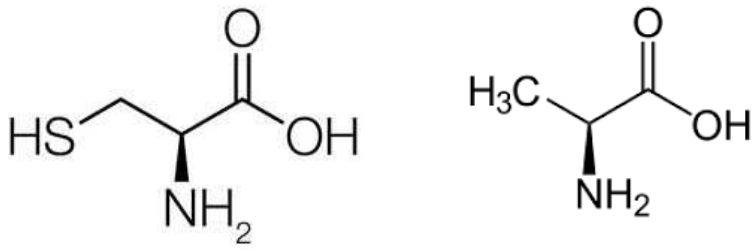

(a) (b)

Figure.4 .Structure of the inhibitor molecules (a) cysteine (b) alanine

CHAPTER VII- ELECTROCHEMICAL STUDIES ON THE INTERACTION AND CORROSION INHIBITION BEHAVIOUR OF MOAB, A VALINE BASED SCHIFF BASE, WITH COPPER IN SULPHURIC ACID

The inhibitory behaviour of valine derived schiff base MOAB on copper in 1M sulphuric acid at temperature regimes of 303 K,308 K & 313 K are explained. The structure of the inhibitor molecule is given in Figure.5.

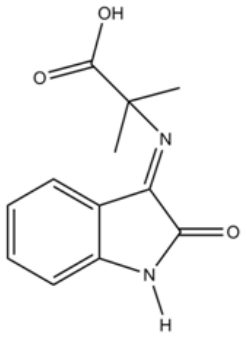

Figure.5

Various techniques such as weight loss method, electrochemical impedance spectroscopy (EIS), potentiodynamic polarization (Tafel), scanning electron microscopy (SEM), basic computational calculations and adsorption studies were employed to understand the electrochemical interactions. The values of electrochemical parameters, corrosion potential (E_{corr}), corrosion current density (i_{corr}) and Tafel slopes (β_a and β_c) varied with the inhibitor concentration as well as temperature. Adsorption studies reveal that adsorption involved is physisorption.

CHAPTER VIII - ELECTROCHEMICAL STUDIES ON THE INTERACTION AND CORROSION INHIBITION OF SCHIFF BASE HMMB WITH MILD STEEL IN HYDROCHLORIC ACID

This chapter explains the inhibitory effect of Schiff base HMMB derived from the amino acid DL –Methionine on mild steel in hydrochloric acid at varying temperatures (303K, 308K &313K). Techniques such as weight loss method, electrochemical impedance

spectroscopy (EIS), potentiodynamic polarization (Tafel), scanning electron microscopy (SEM), basic computational calculations and adsorption studies were employed in the present investigations. The structure of the inhibitor molecule is given in Figure.6.

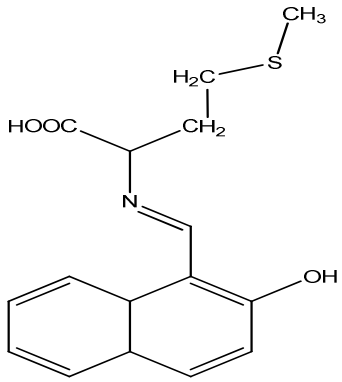

Figure.6

Weight loss results revealed that the inhibition efficiency is high at 24 hour interval irrespective of concentration of the inhibitor and subsequently the efficiency declined. The inhibition efficiency increased with the increase in concentration of the inhibitor. Polarization studies revealed that both the anodic metal dissolution and cathodic hydrogen evolution would exhibit Tafel type behaviour and HMMB can act as a mixed type inhibitor. It is noted from Nyquist plots that R_{ct} values increased with inhibitor concentration, which can be attributed to the formation of a protective layer at the metal surface and this layer acts as a barrier for the mass and the charge transfers.

CHAPTER IX - ELECTROCHEMICAL STUDIES ON THE INTERACTION AND CORROSION INHIBITION OF MILD STEEL WITH HMIB IN HYDROCHLORIC ACID

This chapter deals with the study of Schiff base HMIB derived from L –Histidine on mild steel in hydrochloric acid medium at varying temperatures. Polarization studies revealed that both the anodic metal dissolution and cathodic hydrogen evolution would exhibit Tafel type behaviour and the inhibitor HMIB acts as a mixed type. It was found that as the concentration of the inhibitor increases, efficiency also increases and efficiency is found to be maximum for 150ppm of inhibitor HMIB and its efficiency decreases with the increase in the acid concentration. The structure of the molecule is given in Figure.7.

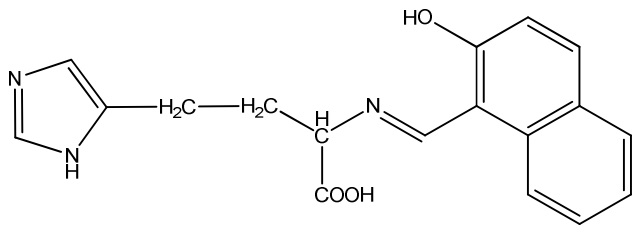

Figure.7

CHAPTER X - ELECTROCHEMICAL AND THEORETICAL STUDIES ON THE INTERACTION OF DL-METHIONINE WITH MILD STEEL IN SULPHURIC ACID

This chapter describes the inhibition effect of DL – methionine at various concentrations on mild steel in sulphuric acid at various temperature regimes. Potentiodynamic polarization studies of the mild steel at 0.5M, 1.0M and 1.5M sulphuric acid with and without inhibitor at 303K, 308K and 313K were carried out. Results indicated that the

electrochemical parameters such as E_{corr} & I_{corr} vary with the inhibitor and acid concentrations. With the variation in temperature, the potentiodynamic polarization behaviour also showed varied response. EIS results revealed that I_{corr} value showed decreasing trend with increased concentration of the inhibitor and this trend was observed in all the concentrations of the acid. Similar observations were made in all the temperature conditions. The structure of the molecule is given in Figure.8.

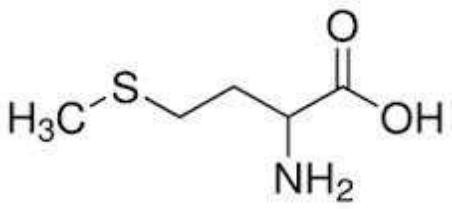

Figure.8

Chapter

1

INTRODUCTION

Contents

1.1 Introduction

The term “corrosion” originated from the Latin word “corrodere” which means “gnawing to pieces.” The phenomenon of corrosion manifests in daily life in different forms. Metallic corrosion has become a very serious problem with the initiation of common metals use in all walks of life from the beginning. There are many reasons to take up studies on corrosion by the scientists. Among the various reasons, four of them are very important and received the attention of the chemists in the past. Three of these reasons are associated with societal issues regarding (i) human life and safety (ii) the cost of

corrosion (iii) conservation of materials. The fourth one is that corrosion is inherently a difficult phenomenon to understand and their study has become a challenge and an interesting pursuit.

1.2 Forms of corrosion

Corrosion may be defined in general terms or in specific terms depending up on the perspectives. For instance, in aqueous media corrosion is defined an electrochemical process. In more general terms, corrosion is defined as the degradation of material caused by an aggressive environment. The corrosive environment could be water, air, carbon dioxide, organic liquids, molten salts or gaseous sulphur. Neutron beams, ultraviolet light, nuclear fission fragments, and gamma radiation are a few among the less aggressive environmental factors.

An array of materials is subjected to corrosion and it includes engineering materials such as metals, plastics, rubber, and ionic and covalent solids; aggregates such as concrete, composite materials and wood. The eight forms of corrosion defined by Fontana [1] are general corrosion, pitting corrosion, intergranular corrosion, parting, galvanic corrosion, crevice corrosion, stress-corrosion cracking (SCC), and erosion corrosion.

Classification of the different forms of corrosion may be based on intrinsic and extrinsic modes. Intrinsic modes of corrosion independent of design are general corrosion, pitting, intergranular corrosion, parting, and stress-corrosion cracking. Extrinsic modes of corrosion affected by design are crevice or under deposit corrosion, galvanic corrosion, erosion corrosion, fretting corrosion, and corrosion fatigue.

1.3 General Corrosion

General corrosion may be even or uneven and is the most common form of corrosion. It is characterized by a chemical or electrochemical reaction that takes place on the exposed surface. The metal becomes thinner and eventually results in perforation and failure. General corrosion accounts for the greatest loss of metal on a tonnage basis. This mode of corrosion does not present a great threat from a technical standpoint since the life of the equipment can be estimated from the corrosion rates obtained from immersion of the sample materials in the medium of interest.

1.4 Local corrosion

1.4.1 Galvanic Corrosion

Galvanic corrosion occurs when a potential difference exists between two dissimilar metals immersed in a corrosive medium. The potential difference indicates the results in the flow of electrons between the metals. The less corrosion resistant metal becomes the anode and the more corrosion resistant metal would act as cathode. Galvanic corrosion is generally more prominent at the junction of two dissimilar metals and the severity of attack decreases with increasing distance from the junction. The distance affected is determined by the conductivity of the solution. Further, the cathode to anode ratio plays an important role in this form of corrosion. Severity of galvanic corrosion further increases with increase in surface area of cathode and decrease in the surface area of anode. Corrosion of leaded or non

leaded solders in copper pipes carrying drinking water is an example of this form of corrosion.

Some of the preventive measures to combat galvanic corrosion are (a) selection of metals which are very close to each other in galvanic series (b) maintenance of cathode/anode surface area ratio to the smallest possible minimum (c) providing insulation between the two dissimilar metals (d) use of coatings that are kept in good condition (e) to reduce the corrosivity of the medium using appropriate corrosion inhibitors (f) avoiding of threaded joints between the two dissimilar metals (g) employment of suitable design for the easy replacement of anodic part and (h) use of a third metal which is anodic to both the metals in galvanic contact.

1.4.2 Pitting corrosion

Pitting corrosion is a form of localized attack that results in localized penetration of the metal. This is one of the most destructive and insidious forms of corrosion. Pitting can cause equipment failure due to perforation, accompanied by a small percentage weight loss of the whole structure. Areas where a brass valve is incorporated in to steel or galvanized pipe line are prone to pitting corrosion. The junction between the two areas is often pitted, and if the pipe is threaded, the thread will make close contact with the brass valve pits rapidly, resulting in a leak. This occurs frequently in industrial units, homes and farms. It is difficult to measure pitting corrosion in laboratory tests because of the varying number of pits and the depth under identical conditions. Pits usually grow in the gravitational direction. Most pits

develop and grow downwards from horizontal surfaces. Pitting usually requires an extended initiation period on the order of months to years. Because of the localized and intense nature, pitting corrosion failures may occur suddenly. Pitting can be considered as a unique type of anodic reaction as well as an auto catalytic type of process. The metal in the pit dissolves along with the reduction of oxygen level, as is the case with crevice corrosion. The rapid dissolution of metal in the pit results in the build up of excessive positive charge in the pit followed by the migration of chloride ions into the pits to maintain the electro neutrality conditions. Due to high ionic potential of ferrous or ferric ion, hydrolysis of a ferric or ferrous ion results in lowering of the pH in the pit, which, together with the high chloride ion concentration in the pit, increases the corrosion rate. The preventive measures reported for crevice corrosion also apply to pitting corrosion.

1.4.3 Crevice corrosion

This form of corrosion usually occurs within the crevices and shielded areas on the metal surface in contact with corrosive media. Crevice corrosion is also known as deposit or gasket corrosion. The mechanism of crevice corrosion consists of the oxidation of the metal and the reduction of oxygen, yielding hydroxyl ion. Subsequently the oxygen in the crevice is consumed and converted into hydroxyl ion. The metal continues to be attacked and the excess positive charge is balanced by the migration of chloride anion from the bulk into the crevice. Thus, ferric or ferrous chloride builds up in the crevice. The ferric chloride can hydrolyze in the crevice and give rise to iron hydroxide and hydrochloric acid. Crevice corrosion can be controlled by (a) use of

welded butt joints in place of riveted or bolted joints (b) closure of crevices in lap joints by continuous welding (c) caulking or soldering (d) vessel design that allows complete drainage without stagnation (e) removal of solid deposits (f) use of non absorbent gaskets such as Teflon and (g) flushing of the equipment with an inhibitor solution.

1.4. 4. Intergranular Corrosion

This form of corrosion consists of localized attack at adjacent to the grain boundaries, causing relatively little corrosion of grains leading to disintegration of the alloy and loss of strength. The impurities at the grain boundaries, enrichment of one of the alloying elements or depletion of one of the elements in the grain boundary areas causes intergranular corrosion.

1.4.5 Dealloying or selective leaching

Selective leaching refers to the removal of an element from an alloy by corrosion. Selective removal of zinc from brass, known also as “dezincification” is an example of this form of corrosion.

1.5 Mechanically assisted corrosion

1.5.1 Stress-Corrosion Cracking (SCC)

Stress-corrosion cracking involves cracking of susceptible material caused by the simultaneous presence of tensile stress and a specific corrosive environment. During SCC the metal may be virtually unattacked over most of the surface, but fine cracks progress through the metal. Stress-corrosion cracking has serious consequences, due to

the occurrence of stresses within the range of typical design stress. Cathodic protection of the structure and addition of corrosion inhibitors to make the environment less corrosive are some of the methods to combat stress corrosion cracking failures.

1.5.2 Corrosion Fatigue

Corrosion fatigue consists of cracking of materials under the synergistic action of fluctuating or cyclic stress and a corrosive environment. Corrosion fatigue can occur at stresses lower than the fatigue limit. The damage due to corrosion fatigue is usually greater than the sum of the damage due to corrosion and fatigue acting separately. Corrosion fatigue differs from stress corrosion cracking in the sense that it occurs in most of the aqueous media. Corrosion fatigue is affected by oxygen content, pH, temperature, and the composition of the solution. Corrosion fatigue may also be minimized by the use of corrosion inhibitors and also by the use of electrodeposited zinc, chromium, nickel, copper, and nitride coatings.

1.5.3 Fretting Corrosion

Fretting corrosion is a combination of wear and corrosion in which material is removed from contacting surfaces when the motion between the surfaces is limited to very small amplitude oscillations. The oscillatory motion between the contacting surfaces in the tangential direction results in fretting corrosion. Oxidation is the primary factor in the fretting process. In oxidizing systems, fine metal particles removed by adhesive wear are oxidized and trapped between the fretting surfaces. The oxides act as an abrasive and increase the rate

of removal of the material. Fretting corrosion may be controlled by using low viscosity, high tenacity oils and greases and phosphate coatings in conjunction with lubricants and also by hardness of one or both the parts in contact, increasing the surface hardness by shot peening or cold-working, use of lead coatings, use of gaskets, increasing the relative motion between the parts and use of laminated plastic on gold plate and cast iron with phosphate coating or rubber cement coating.

1.6 Corrosion Prevention

Corrosion prevention process depends upon inherent factors, which are within the control of the metallurgist or engineer. The three main categories considered are materials selection, design factors and life prediction analysis.

The foremost consideration is the cost of the material and its applicability in the environmental conditions so that integrity can be maintained during the lifetime of the equipment. When the material of construction is metallic in nature, the chemical composition and the mechanical properties of the metal are significant. Some of the important mechanical properties are hardness, creep, fatigue, stiffness, compression, shear, impact, tensile strength and wear.

Corrosion leads to destruction of the metals by converting them into oxides or other corrosion products. Thus, corrosion affects the global supply of pure metals by removing components or structures from services and their replacement process consumes a portion of the total supply of the earth’s material resources. Its other important impact is

on safety. This factor becomes a great concern in the minds of personnel working in the industry where metals are widely used as a raw material. The problem of metal corrosion is being ignored due to one or other reasons.

Corrosion brings about a wide range of environmental problems. The corrosion related failure of oil gas pipelines and oil tankers contributes very detrimental effect on the environmental conditions particularly in terrestrial and aquatic ecosystems. The water and air pollution are invariably the contribution of corrosion phenomenon in many instances. The pollutants developed as a result of corrosion in various forms not only affect the hygiene of the human beings but also contribute to destruction of natural fauna or flora and such loss becomes never could be replaced.

Another aspect of concern brought by corrosion is the shrinking of resources world over. A few decades ago, the term recycling was not familiar among the commons and was almost unknown. Now recycling is a household term and very familiar to every country men. Various products such as metals, paper and plastics have been subjected to recycling process all over the world. This process has widely been recognized and it also plays paramount role in conserving the resources. It has now come to a level of understanding that natural resources are limited and finite and are also on the declining trend. The conservation of these resources is to be prioritised and for which recycling process and other methods have to be opted.

The prevention and protection of metals from corrosion arrests the degradation of metals/materials thereby contributes significantly to the conservation of resources with least deleterious impact to ecosystems. Invariably a wide range of materials are prone to corrosion and the knowledge on the factors both direct and indirect responsible to bring about corrosion helps in the selection of materials resistant to corrosion. The information on the above lines plays a paramount role in the design of an engineering structure.

1.7 Measurement of corrosion

In corrosion studies, information on quantification of corrosion is essential and for which corrosion measuring techniques are practiced. Electrochemical and non electrochemical techniques are employed. Among them, non electrochemical techniques are generally preferred because of their reliability, robustness and simplicity. The limitation of these techniques is that none of them provides information regarding corrosion mechanisms.

1. 8 Corrosion control by protective coatings.

Corrosion control by coatings may be accomplished by:

- Barrier coatings which offer protection (a) by its high resistance which mitigates current transfer between anodic and cathodic sites (b) by depriving oxygen diffusion and hence impede the cathodic reaction;
- Cathodic protection as in the case of zinc-containing pigments (zinc is more anodic to iron)

- Inhibitive primers which form passive films on the metal.

1.9 Inhibitors for corrosion control.

A corrosion inhibitor is a chemical substance that, upon addition to a corrosive environment, results in reduction of corrosion rate to an acceptable level [6].Corrosion inhibitors are generally used in small concentrations. The inhibitors not only mitigate the corrosion, but also should be compatible with the environment in the sense that it should not cause any complications. A corrosion inhibitor can function in two ways. In some situations the added inhibitors can alter the corrosive environment into a non corrosive or less corrosive environment through its interaction with the corrosive species. In other cases the corrosion inhibitor interacts with the metal surface and as a consequence inhibits the corrosion of the metal. Thus, based on the mode of interaction, there are two broad classes of inhibitors.

1. Environmental modifiers

2. Adsorption inhibitors

1.9.1 Environmental Modifiers

In the case of environment modifiers the action and mechanism of inhibition is a simple interaction with the aggressive species in the environment, and thus reduce the attack of the metal by the aggressive species. This is exemplified by oxygen scavengers such as hydrazine or sodium sulphite along with cobaltous nitrate and biocides used in inhibiting microbiological corrosion. In the case of corrosion in neutral and alkaline solutions, oxygen reduction leads to cathodic reaction

which can be countered by the oxygen scavengers and thus inhibit the corrosion.

1.9.2 Adsorption Inhibitors

Inhibitors are further classified as cathodic and anodic inhibitors depending upon whether the cathodic reaction or the anodic reaction is suppressed by the added inhibitor and are as follows

1.9.2.1 Cathodic inhibitors

They prevent the hydrogen evolution in acidic solutions or reduce oxygen in neutral or alkaline solutions. It is also observed that the cathodic polarization curve is affected when a cathodic inhibitor is added to a system. Substances with high over potential for hydrogen in acidic solutions and those that form insoluble products in alkaline solutions are generally effective cathodic inhibitors. Inorganic phosphates, silicates or borates in alkaline solutions which inhibit the oxygen reduction at the cathodic sites are examples of cathodic inhibitors.

1.9.2.2 Anodic inhibitors

They are generally effective in the pH range of 6.5–10.5 (near neutral to basic). Basically, oxyanions such as chromates, molybdates, tungstates and also sodium nitrite are very effective anodic inhibitors. These oxyanions are believed to play a role of repairing the defects in the passive iron oxide film on the iron surface. In the case of chromate or dichromate, the concentration of the inhibitor used is critical.

1.9.2.3 Mixed-type inhibitors

They affect both anodic and cathodic branches of a polarization curve. The organic inhibitors adsorbed on the metal surface provide a barrier to dissolution at the anode and a barrier to oxygen reduction at the cathodic sites. The protective functional groups in the organic mixed-type inhibitors can be amino, carboxyl or phosphonate. The adsorption of inhibitors on the metal surface is governed by the residual charge on the metal and the chemical structure of the inhibitor.The two types of adsorption of an organic inhibitor on a metal surface are physical or electrostatic and chemisorption. Inhibitors involved in physisorption can be desorbed with ease while inhibitors involved in chemisorption are difficult to desorb [7].

1.9.2.4 Vapour Phase Inhibitors

Vapour phase inhibitors (VPIs) are compounds with low vapour pressures (0.0002 to 0.4 mm Hg). These inhibitors volatilize and adsorb on all surfaces located in an enclosed space. Vapour phase inhibitors are used to protect metal surfaces in storage or transport, as well as to protect electronic materials, such as circuit boards. Vapor-phase inhibitors can provide corrosion protection for periods ranging from months to years [8, 9]. Vapour phase inhibitors, in general, are effective in the prevention of corrosion in steel. The VPIs are used by impregnating wrapping paper or by placing them loosely inside a closed container [10]

1.10 Mechanism of Corrosion Inhibition

The first stage of mechanism of inhibitors in acid media involves the adsorption of the inhibitors on to the metal surface and this adsorption process is affected by the nature and surface charge of the metal, the chemical structure of the inhibitor and the type of aggressive electrolyte. Chemisorption and Physisorption (Physical adsorption) are the two types of interaction between an organic inhibitor and a metal surface.

1.10.1 Physical adsorption

It is due to electrostatic attraction between electrically charged metal surface and the inhibiting ions or dipoles. The surface on the metal is defined by the position of the free corrosion potential Ecorr of the metal with respect to its potential of zero charge, PZC. At PZC the net charge on the electrode is zero. At potentials more positive than PZC, the electrode is positively charged; at potentials more negative than PZC, the electrode is negatively charged. When Ecorr-PZC is negative, cations are adsorbed and when it is positive, negative ions are adsorbed and this adsorption process is electrostatic in nature.

1.10.2 Chemisorption

It is slow and it involves interaction forces which is stronger than the forces in physisorption. Chemisorption involves the charge transfer from the inhibitor to the metal so as to form a coordinate type of bond between metal and inhibitor. Chemisorption occurs slowly than physisorption and occurs with higher activation energy.

Considering the ill effects of corrosion on multi dimensional issues as described elsewhere, an enormous amount of research has been conducted world over to address various issues paused by corrosion. The prevention of corrosion is the best method to overcome the corrosion of metals widely used in the industries. The technology developed on this line should be reliable, consistent and also a cost effective one. Further, the newly developed technology should also able to find ways and means to solve the associated issues. Investigations carried in the past reveal that various types of inhibitors are employed in the corrosion chemistry to prevent corrosion of metals. Though the inorganic inhibitors do help to prevent corrosion on one hand and on the other side brought about many undesirable outcomes [12]. In this context, it is imperative to look for inhibitors which could answer all issues including the corrosion prevention. In recent years research thrust has been given to identify corrosion inhibitors alternate to in organic inhibitors to overcome various issues. The importance of amino acids in corrosion inhibition of metals has been reported [13]. Further, synthesis of Schiff base molecules and their corrosion prevention nature also being received the attention of chemist all over the world. The studies using amino acids and Schiff base molecules to prevent corrosion of metals largely used in industries particularly copper and silver are very meagre. It is therefore investigations have been carried out to find out the role of various amino acids viz cysteine, methionine and schiff bases synthesised from various amino acids on corrosion prevention on metals such as copper and mild steel at various time intervals and temperature gradients.

Review of Literature - Copper

Authors	Year	Reference
K. Barouni1, A. Kassale, A. Albourine, O. Jbara, B. Hammouti , L. Bazzi	2014	14
Ana T. Simonovic, Marija B. Petrovic ,	2014	15
D. Xu, Y. Li ,T. Gu	2014	16
Milosev, Jasminaka, Milan, Lesar, Antonija	2013	17
A.Zarrouk, B. Hammouti, A. Dafali, H. Zarrok	2011	18
K.F. Khaled	2010	19
Wei Luo, Yimin Xu, Qiming Wang,Peizhen Shi, Mi Yan	2010	20
Manjula Spah, Dal Chand Spah, Balraj Deshwal, Seungmoon Lee, Yoon-Keun Chae, Jin Won Park	2009	21
M.M Antonijevic , M. B. Petrovic	2008	22
K. Barouni, L. Bazzi, R. Salghi, M. Mihit, B. Hammouti , A. Albourine, S. El Issami	2008	23
K.F.Khaled	2008	24
Khaled M. Ismail	2007	25
Kumar, S. Narayanan, T.S Kumar, M. S, Manimaran	2006	26
Da-quan Zhang, Li-xin Gao, Guo-ding Zhou	2005	27
Matos, J.B. Pereira, L.P. Agostinho, S.M.L. Baricia, O.E. Cordeiro, G.G.O. Elia.	2004	28
G. Moretti, F. Guidi	2002	29
Ishtiaque Ahamad, M A Quraish	2002	30
M. Rylkina, A. Chikanova, L. Trubacheva, S. Reshetnikov	1999	31
H. Baba, T. Kodama	1999	32
G. Moretti, F. Guidi	1995	33
G. Gomma, M. Wahdan	994	34

Review of Literature – Mild Steel

Authors	Year	Reference
Qiong Deng, Hong-Wei Shi, Na-Na Ding, Bao-Qin Chen, Xiao-Peng He, Guixia Liu, Yun Tang, Yi-Tao Long, Guo-Rong Chen	2012	35
M. S. Morad	2008	36
O. Olivares-Xometl, N.V. Likhanova, M.A. Domínguez-Aguilar, E. Arce, H. Dorantes, P. Arellanes-Lozada	2008	37
M. S. Morad	2007	38
M. S. Morad	2005	39
M .Zerfaoui, H. Oudda, B. Hammouti, S. Kertit, Benkaddour	2004	40
G. Gomma	1998	41
L. Madkour, M. Ghoneim	1997	42
D. Kalota, D. Silverman	1994	43

Chapter

2

MATERIALS AND METHODS

Contents

Corrosion inhibition studies were undertaken in two widely used metals such as mild steel and copper in the industry. The corrosion behaviour of these metals in the acid medium treated with three amino acids such as cysteine, DL – methionine, alanine and five schiff bases synthesised from various amino acids were investigated. The details of materials and methodology adopted are described separately in the respective chapters.

2.1 Inhibitors

Two amino acids containing sulphur viz. Cysteine and DL – methionine and schiff bases namely HHDMP, HMMB, HMIB, HDMMA, MOAB were as inhibitors and prepared as per the standard procedures [44].

2.1.1 Synthesis of the inhibitor HHDMP

Schiff base, HHDMP was employed as inhibitor and it was synthesised by dissolving 2-hydroxy-1-naphthaldehyde (10 mmol 1.72 g) in 100 ml methanol and then added to the amino acid serine (10 mmol) solution in methanol (50 ml). The mixture was refluxed for 3 hours, the solvent was removed on a rotary evaporator and the residue was crystallized at room temperature. After a day crystals were collected and recrystallized from methanol/n-heptane and characterised by physico – chemical methods [44].

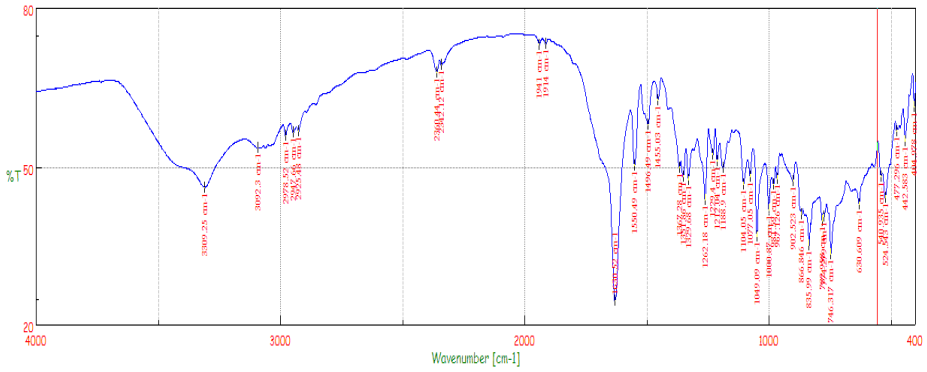

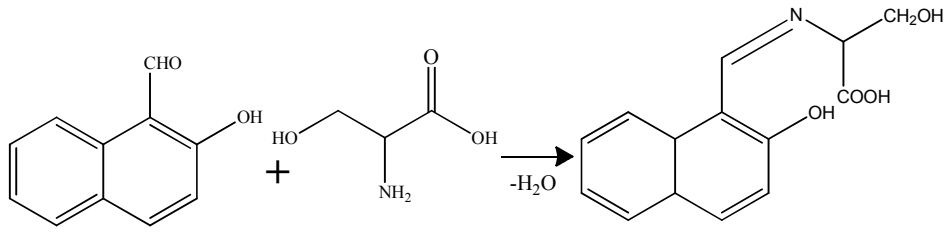

2- hydroxy 1- naphthaldehyde L - serine HHDMP

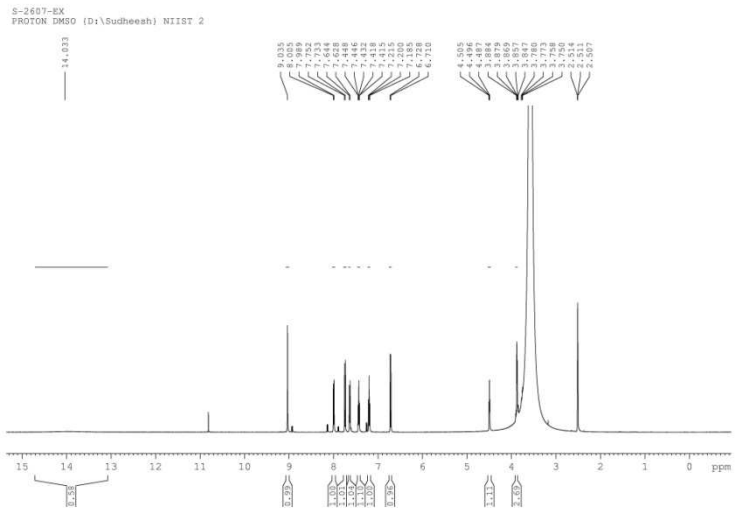

2.1.2 Synthesis of the inhibitor HMMB

Schiff base HMMB was employed as inhibitor and it was by dissolving 2-hydroxy-1-naphthaldehyde (10 mmol 1.72 g) in 100 ml methanol and then added to the amino acids , DL – methionine (10 mmol) solution in methanol (50 ml). The mixture was refluxed for 3 hours, the solvent was removed on a rotary evaporator and the residue crystallized at room temperature. After a day crystals were obtained and recrystallized from methanol/n-heptane and characterised by physico – chemical methods [44].

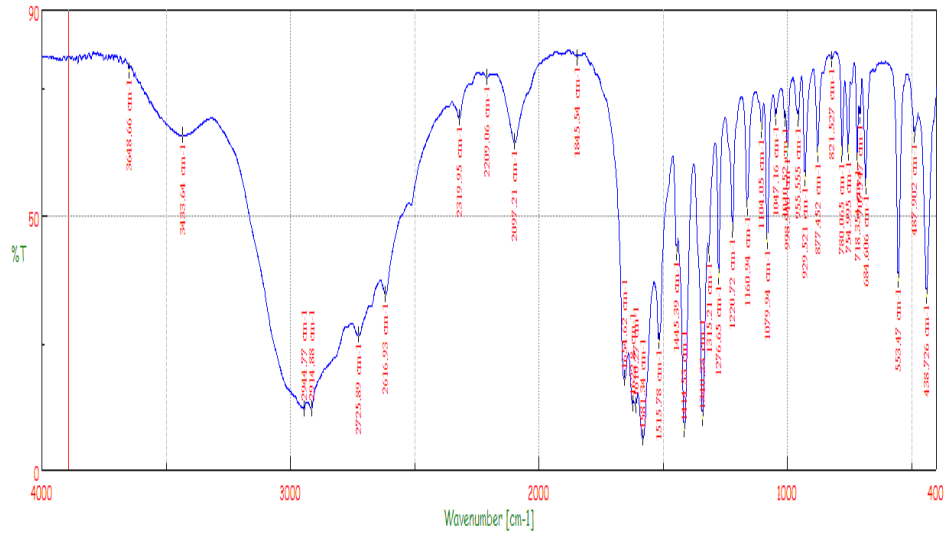
%T
Wavenumber [cm-1]
4000
3000
2000
1000
400
50
0
3048.66 cm-1
3433.64 cm-1
2944.22 cm-1
2918.38 cm-1
2725.89 cm-1
2616.93 cm-1
2319.95 cm-1
2269.86 cm-1
2095.21 cm-1
1845.54 cm-1
1515.78 cm-1
1445.39 cm-1
1315.21 cm-1
1276.65 cm-1
1230.72 cm-1
1160.94 cm-1
1101.05 cm-1
1079.94 cm-1
929.521 cm-1
877.492 cm-1
821.537 cm-1
780.065 cm-1
754.995 cm-1
684.606 cm-1
553.47 cm-1
438.726 cm-1

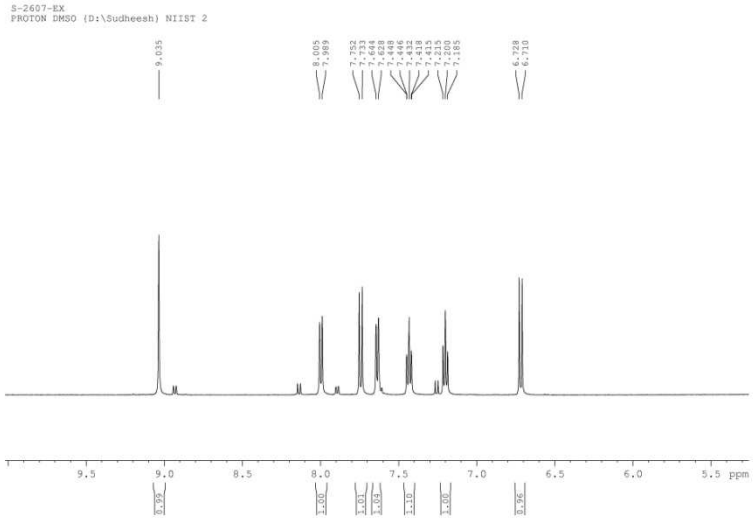
S-2607-EX
PROTON DMSO (D:\Sudheesh) NIIST 2
9.035
8.005
7.989
7.752
7.733
7.644
7.628
7.448
7.446
7.432
7.415
7.215
7.200
7.185
6.728
6.710
9.5
9.0
8.5
8.0
7.5
7.0
6.5
6.0
5.5 ppm
0.99
1.00
1.01
1.04
1.10
1.00
0.96

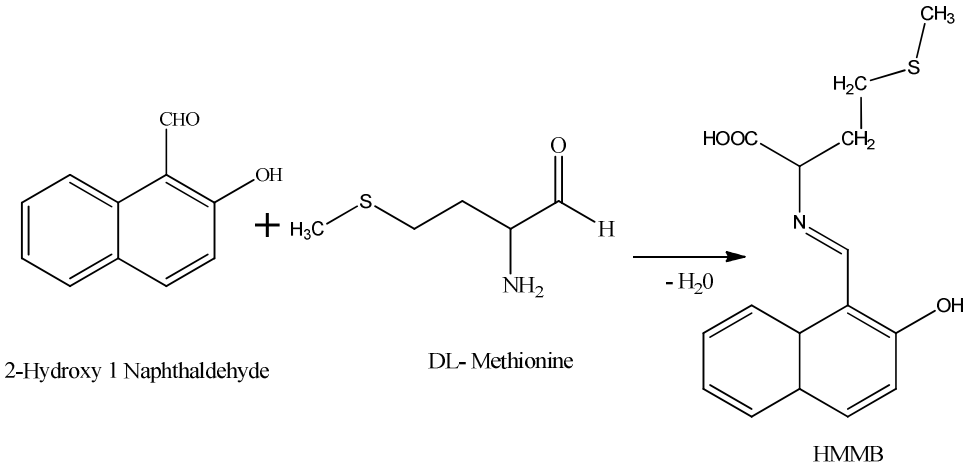

2-Hydroxy 1 Naphthaldehyde

DL- Methionine

HMMB

2.1.3 Synthesis of the inhibitor HMIB

Schiff base HMIB was employed as inhibitor and this inhibitor was prepared by dissolving 2-hydroxy-1-naphthaldehyde (10 mmol 1.72 g) in 100 ml methanol and then added to the amino acid L-histidine, (10 mmol each) solution in methanol (50 ml). The mixture was refluxed for 3 hours, the solvent was removed on a rotary evaporator and the residue crystallized at room temperature. After a day crystals were obtained and recrystallized from methanol/n-heptane and characterised by physico – chemical methods [44].

.

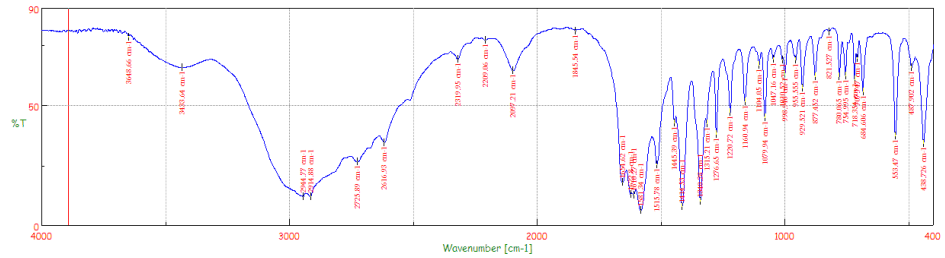

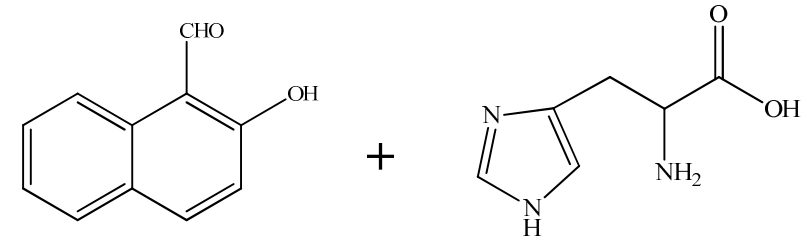

2-hydroxy 1- naphthaldehyde

L - histidine

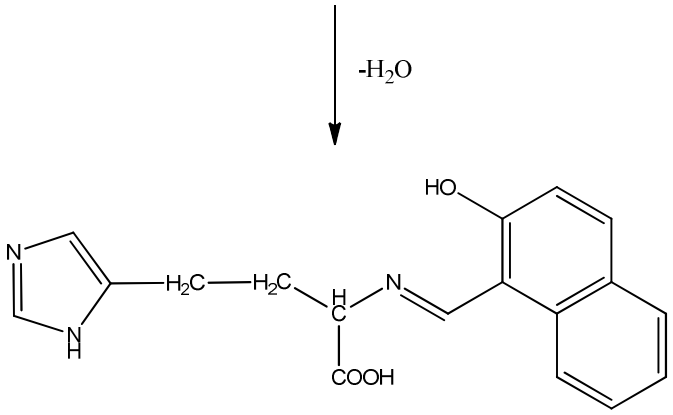

HMIB

2.1.4 Synthesis of the inhibitor MOAB

Schiff base, MOAB was used as inhibitor and it was prepared by the condensation of indoline-2, 3-dione (0.231 g; 1.57 mmole) with amino acids (0.140 - 0.321 g; 1.57 mmole) (valine) in 1:1 molar ratio using methanol (100 mL) as the reaction medium and it was refluxed for 6 - 8 hours. After this it was put on cooling at room temperature and the solid products were obtained. The excess solvent was removed on a rotary evaporator. It was dried further and then purified by recrystallization from same solvent [44].

2.1.5 Synthesis of the inhibitor HDMMA

Schiff base, HDMMA was used as inhibitor and it was prepared by dissolving 2-hydroxy-1-naphthaldehyde (10 mmol 1.72 g) in 100 ml methanol and then added to the amino acid L- cysteine (10 mmol) solution in methanol (50 ml). The mixture was refluxed for 3 hours, the solvent was removed on a rotary evaporator and the residue crystallized at room temperature. After a day crystals were obtained and recrystallized from methanol/n-heptane and characterised by physico – chemical methods [44].

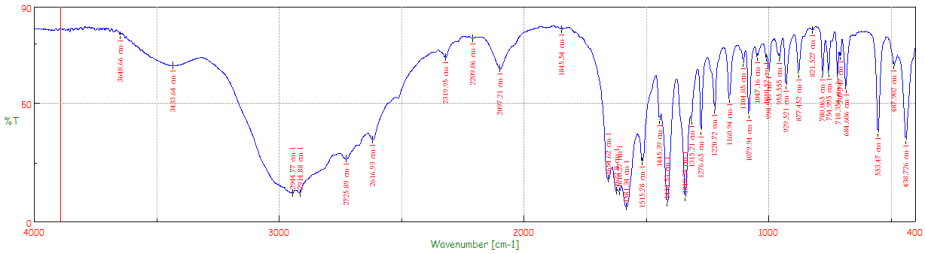

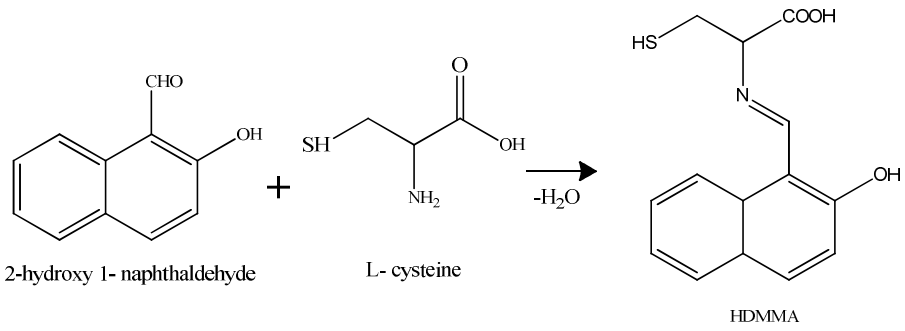

2-hydroxy 1- naphthaldehyde L- cysteine HDMMA

2.2 Materials

The metals used for corrosion studies are mild steel having a composition (atom %): C (0.2 %), Mn (1%), P (0.03 %), S (0.02 %), and Fe (98.75 %) and copper.The specimens of the metals used in the weight loss measurements were cut in to 4.8x1.9cm^2 coupons. Similar types of coupons were also used for the electrochemical studies. However, in electrochemical studies only 1cm^2 area of the specimens were exposed. Prior to recording of both the measurements, the samples were polished using different grade of emery papers followed by washing with water and acetone.

2.3 Medium:

The medium was prepared from reagent grade hydrochloric acid & sulphuric acid (E. Merck) and double distilled water. The entire tests were performed in aerated medium under standard conditions of temperature and pressure.

2.4. Methods:

2.4.1 Weight loss method

It is the most simplest and accurate method and also helps to gauge corrosion rate. The major advantage of this method is that this technique does not require any complex or sophisticated equipment or procedures. It is the most accepted method even today despite being an old one. The weight loss experiments were carried out under total immersion conditions in test solution maintained at 303K.Mild steel and copper specimens of required dimensions are first rubbed with

different grade of emery papers to remove rust particles and then subjected to the action of a buffing machine attached with a cotton wheel and a fibre wheel having buffing soap to ensure mirror bright finish. All specimens were cleaned according to ASTM standard G-1-72 procedure [45-51].The experiments were carried out in 250 ml beaker containing the solution. After the exposure period the specimens were removed, washed initially under running tap water, to remove the loosely adhering corrosion products and finally cleaned with mixture of 20% NaOH and 200g/L Zinc dust followed by acetone [56].The inhibition efficiency (%), IE was calculated using the equation

$$\% \text{ IE} = \frac{W_0 - W}{W_0} \text{ X } 100 = (\eta) \qquad (1)$$

Where W_0 and W refers to weight losses in the uninhibited and inhibited solutions respectively.

2.4.2Electrochemical methods:

Electrochemical techniques are reliable and versatile which offer high sensitivity, accuracy, and precision as well as large linear dynamic range with relatively low-cost instrumentation.

2.4.2.1 Electrochemical impedance spectroscopy (EIS)

The Electrochemical impedance spectroscopy (EIS) has gained much popularity over the last decades. This electrochemical technique is relatively non destructive (small ac voltage is applied) and can be used to study a wide variety of surfaces in situ [57]. Electrical resistance is

the ability of a circuit element to resist the flow of electrical current. Ohm's law defines resistance in terms of the ratio between voltage E and current I.

$$R = \frac{E}{I} \tag{2}$$

Ohm's law is limited to only one circuit element, i.e., the ideal resistor. Electrochemical impedance is invariably monitored by applying AC potential ($\Delta E \sin\omega t$) to an electrochemical cell and measuring the current passing through the cell and if applies a sinusoidal potential excitation, the response to this potential denote to an AC current signal ($\Delta I \sin\omega t+q$), possessing the excitation frequency and its harmonics (2ω, 3ω etc.) [53].The impedance Z has a magnitude $\frac{\Delta E}{\Delta I}$ and phase Θ and hence is a vector quantity; the EIS is generally measured using a small excitation signal. This is performed to contribute the cell's response in the pseudo-linear pattern [54]. It also expresses the impedance as a complex function. The potential is represented as

$$E(t) = E_{0\,exp}\,(j\omega t) \tag{3}$$

The current response as,

$$I(t) = I_O \exp(jo\omega - j\emptyset) \tag{4}$$

The impedance is represented as a complex number as given below,

$$Z = \frac{E}{I} = Z_o \exp(j\emptyset) = Z_0(\cos\emptyset + j\sin\emptyset) \tag{5}$$

AC impedance could provide kinetic and mechanistic information of the study of electrochemical systems, so electrochemical impedance

spectroscopy technique is applied to a great extent in corrosion processes in solution eventhough AC impedance data offer a lot of information, sophisticated techniques are required to interpret the data to derive useful inferences. In this study, a frequency response analyzer (FRA) in unison with a potentiostat allowed a cell to be stimulated with an AC signal and its response in terms of the cell potential and current was recorded [55]. The EIS data can be plotted in two ways. If the real part is plotted on the x-axis and the imaginary part on the y-axis of a chart, then it is called Nyquist plot and is shown in Fig. 2.1. On the contrary the Bode plot shown in Fig. 2.2 clearly represents frequency information. EIS data is invariably analyzed by fitting it to an equivalent electrical circuit model called Randles circuit which consists of a solution resistance, R_s in series to a parallel combination of resistor, R_{ct} and a double layer capacitor, C_{dl}. R_{ct} representing the charge transfer resistance and C_{dl} representing the electrode capacitance shown in Fig. 2.3.

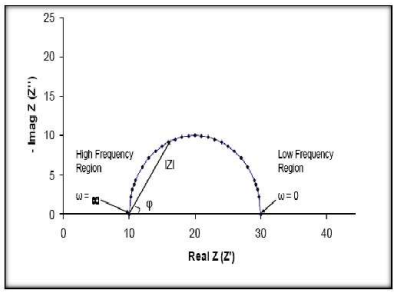

Fig. 2.1. Nyquist plot for a simple electrochemical one time constant system

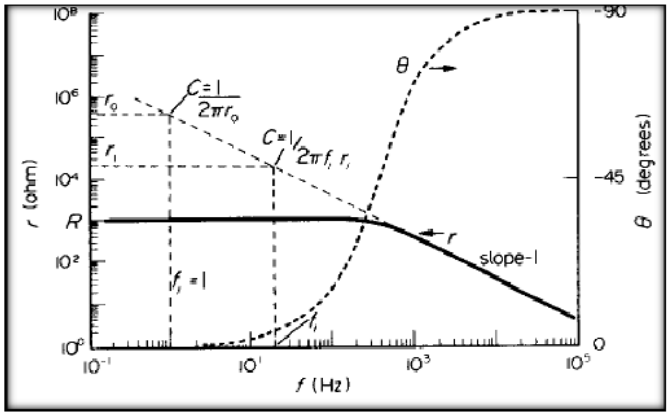

Fig. 2.2 Bode plot

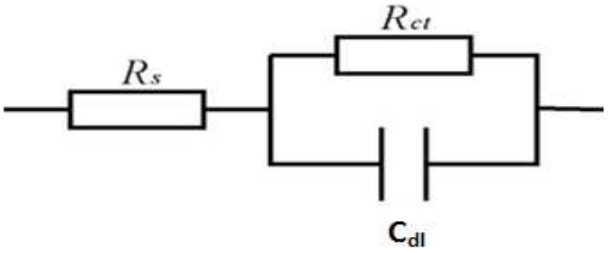

Fig. 2.3. Randles circuit

Electrochemical experiments were undertaken in a conventional three-electrode configuration with platinum sheet (1cm^2 surface area) as auxiliary electrode and saturated calomel electrode (SCE) as the reference electrode. The working electrode was initially immersed in the test solution and after establishing a steady state OCP the electrochemical measurements were made with a Gill AC computer

controlled electrochemical workstation (ACM, U.K model no: 1475). The potentiodynamic polarization curves were obtained in the potential range from –250mV to +250mV with a sweep rate of 1 mV/s. The electrochemical impedance spectroscopy (EIS) data were recorded at amplitude of 5mV ac sine wave with a frequency range of 0.1 Hz to 10000Hz.In electrochemical techniques, corrosion inhibition efficiency (η) is determined using charge transfer resistance (R_{ct}) and corrosion current densities (i_{corr}) [58].

$$\% \text{ IE } = \frac{i_{corr} - i^{*}corr}{i_{corr}} \times 100 \quad (2)$$

$$\% \text{ IE} = \frac{R_{ct^{*}} - R_{ct}}{R_{ct^{*}}} \text{ X } 100 \quad (3)$$

Where R^{*}_{ct} and R_{ct} are the charge transfer resistance and i^{*}_{corr} and i_{corr} are the corrosion current density in the inhibited and uninhibited solution.

Fig. 2.4: Electrochemical Investigation – experimental set up.

2.4.2.2 Polarization studies

In polarization method, potentiodynamic polarization was employed to assess the efficiency as the technique offers useful information

pertaining to corrosion rate and mechanism [59]. The potentiostat is used in the polarization technique. In this studies three electrodes are used and are 1) the working electrode (the metal/alloy used for investigations), the reference electrode (the potential of the WE is measured relative to WE potential) and the counter or auxiliary electrode (enable to pass current). The counter electrode helps to prevent any resistive potential drop (ohmic drop) across the reference electrode. The potential of a corroding metal (WE) is varied (polarized) from its equilibrium potential value (E_{Corr}) initially the negative and subsequently in the positive direction and recorded the current response to the applied potential [60]. The voltage/current density data pairs produced from the polarization of the WE can then be employed to plot a polarization diagram shown in Fig. 2.5.

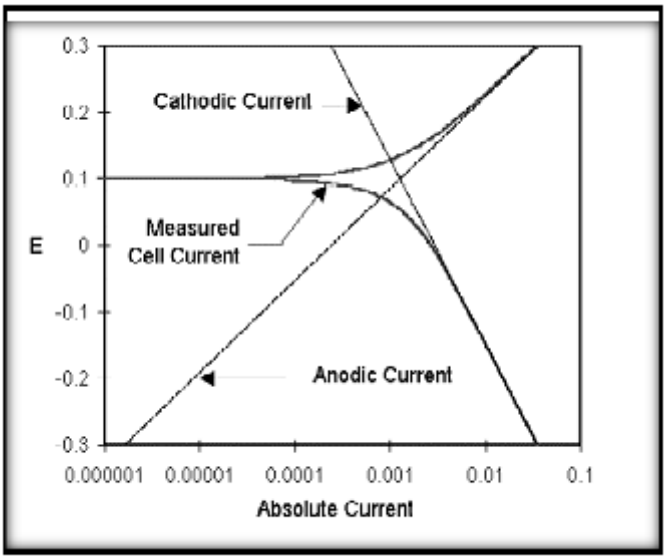

Fig. 2.5. Polarization curve

Tafel lines are overlaid in the polarization curves for the dissolution of metal. In terms of definition, at the corrosion potential (E_{Corr}) there is no net current flowing in the cell. At a high negative potential from E_{Corr}, the flow of current will be towards both the anodic and cathodic components and this makes the plot a non linear one. The experimental curves are in agreement with the linear Tafel relationships only at higher over potential (Negative or Positive) and in such cases current density (therefore the corrosion rate) could be estimated from the intersection of the two Tafel lines [61]. In a few instances one or both of the reactions may not exhibit activation polarization and this leads to cumbersome in the estimation of the corrosion current density. Whenever one reaction is under activation control, the interaction of the linear Tafel region for this reaction with the corrosion potential may be adequate to calculate the corrosion rate. In case the cathodic reaction is under complete diffusion control at $E_{corr,}$ the limiting current density will signify the corrosion current density [62]. Whenever both anodic and cathodic curves are non-linear, any arbitrary point become more positive than E_{Corr} can be used as a reference of the rate of anodic dissolution. A corrosion inhibitor is qualified to become cathodic or anodic based on its reaction phenomenon which shows retarding. However it retards both reactions, it is referred as a mixed type inhibitor and such behaviour could be identified from the polarization curves and the change of E_{Corr} value from its value in the uninhibited system [63].

2.4.3 Scanning electron microscopy (SEM):

The surface morphology of the metals mild steel and copper in the absence and presence of various inhibitors were studied by using a Digital Microscope Imaging Scanning electron microscope model SU6600 (Serial No: HI-2102-0003) with an accelerating voltage 20.0kv.Samples were attached on the top of an aluminium stopper with the support of carbon conductive adhesive tape. All micrographs of the specimens were taken at the magnification of 500X for deriving fruitful inferences.

Fig.2.2. Scanning Electron Microscope.

2.4.4 Atomic Force Microscope (AFM)

The metal strips having a size of 4.8×1.9 cm^2were immersed in 1.0 M H_2SO_4 & HCl with and without the inhibitor (150 ppm) at 303K for 24hour. The specimens were cleaned after the stipulated period with distilled water, dried, and then used for atomic force microscopic studies.

Fig.2.3. Atomic Force Microscope.

2.4.5 Computational studies:

Quantum chemical parameters of the inhibitor molecules were calculated using B3LYP, which is a version of the DFT method [30]. The B3LYP method is recognized particularly for systems containing

transition metal atoms [31-32] and hence B3LYP was used for quantum calculations. Gaussian 09 software was used to determine the geometry of the inhibitors. Various quantum chemical parameters such as energy of highest occupied molecular orbital (E_{HOMO}), energy of the lowest unoccupied molecular orbital (E_{LUMO}), energy gap (ΔE) i.e. E_{LUMO}-E_{HOMO}, ionization potential, I -E_{HOMO}, electron affinity, A–E_{LUMO}, electro negativity, χ (I+A)/2 and hardness, η (I-A)/2 of the inhibitor molecules also calculated using Gaussian 09 programme package.

The energy of HOMO is often associated with the electron donating capacity of a molecule. High value of E_{HOMO} indicates the tendency of the molecule to donate electrons to an appropriate acceptor molecule with low energy and empty molecular orbital; the energy of LUMO indicates the ability of the molecule to accept electrons [64]. As the energy of E_{LUMO} decreases, the probability of the molecule to accept electrons increases. The binding ability of the inhibitor to the metal surface improves with increasing HOMO and decreasing LUMO energy values.

The reactivity of corrosion inhibitors are to be discussed with respect chemical hardness (η) and softness (σ) parameters. These factors are often associated with the Lewis theory of acids and bases and Pearson's HSAB concept. A hard molecule has a large ΔE and therefore is less reactive; a soft molecule has a small ΔE and is therefore more reactive [65]. In the study of corrosion inhibitors and their ability to bind on the metal surface, the inhibitor is considered as

a soft base and the metal surface as a soft acid. Adsorption occurs most probably at the region of the molecule where (σ) has the highest value

$$\eta = \frac{I-A}{2}$$

$$\sigma = \frac{1}{\eta}$$

The numbers of transferred electrons (ΔN) also provide an indication of the ability of the molecule to donate electrons to bind on the metal surface [66].

$$\Delta N = \frac{\chi_m - \chi_{inh}}{2(\eta_m + \eta_{inh})}$$

Where χ_m and χ_{inh} are the absolute electro negativities of metal and inhibitor molecules. η_m and η_{inh} are the chemical hardness of the metal and inhibitor molecules, respectively. Although the no of transformed electrons (ΔN) is a calculated value and even then it serves to provide a rough estimate of the possible trend in the electron transfer among selected molecules [67]. The compound that has the highest ability to transfer electrons is considered to possess the high tendency to interact with the metal surface.

Chapter

3

ELECTROCHEMICAL STUDIES ON THE INTERACTION AND CORROSION INHIBITION BEHAVIOUR OF L – CYSTEINE WITH COPPER IN SULPHURIC ACID

Contents

3.1. General

Copper is extensively used in industrial sector particularly in electronic field due to its good thermal conductivity, mechanical properties and low electrical resistivity. It is a noble metal, however in aggressive acids and alkali it undergoes corrosion easily. In recent years, laudable efforts have been taken by the scientific community to find efficient corrosion inhibitors containing sulphur or nitrogen [68-72]. Organic inhibitors which contain nitrogen, oxygen and sulphur have been widely used in the case of corrosion of copper and its alloys [73-77]. Among the organic compounds, the most commonly used ones are benzotriazole [78-79] and benzimidazole [80]. Considering the high toxic nature of these organic compounds, amino acids were identified as an alternate, as a green corrosion inhibitors with unique chemical properties. Not much information is available on the corrosion behaviour of sulphur containing amino acid, L-cysteine on copper and

hence, investigations were undertaken to find out corrosion inhibition behaviour L-cysteine at different concentrations (50,100,150 ppm) on copper in 0.5M, 1M, and 1.5M sulphuric acid at varying temperature gradients.

3.2 Results and discussion

3.2.1. Weight loss studies

The weight loss under different intervals of time (24, 48, 72 and 96 hours) in the absence and presence of different concentrations (50ppm, 100ppm, 150ppm) of L - cysteine (Fig. 3.1) were studied. The results revealed that the inhibition efficiency is high at 24 hr in all the studied concentrations of L- cysteine and inhibition efficiency declined gradually with the advancement of time.

3.2.2 Potentiodynamic polarization studies

Potentiodynamic polarization studies of copper in 0.5M, 1M & 1.5M H_2SO_4 were carried out in the absence and presence of inhibitors at 303K, 308K and 313 K. Tafel polarization curves for copper in 0.5M, 1M, & 1.5M H_2SO_4 solution in the absence and presence of various concentrations of L-cysteine at 303K, 308K and 313 K are presented in Fig. 3.2 to 3.4. It reveals that both the anodic metal dissolution and cathodic hydrogen evolution would exhibit Tafel type behaviour. The respective values of electrochemical parameters like corrosion potential (E_{corr}), cathodic and anodic Tafel slopes (β_c & β_a) and corrosion current density (i_{corr}) are given in Table 3.1 to Table 3.3. The electrochemical parameter such as, β_a , showed relatively high value at 50 ppm compared to its high concentrations(100ppm,150ppm) at 0.5 M and 1M acid medium at a temperature of 303K and the same trend

was not observed at 1.5M acid medium. However at the same acid medium as with the increase in concentration of inhibitor, the values of electrochemical parameters like I_{corr} and corrosion rate declined. At high temperature (308K and 313 K), the response of the electrochemical parameters β_a, β_c, I_{corr}, corrosion rate etc. varied with respect to concentration of the inhibitor and acid. Results gathered from the potentiodynamic polarization studies show that L – cysteine behaves as a mixed type inhibitor. The mechanism of action involves the blocking of reaction sites by the inhibitor through adsorption and its efficiency increases by increase in the concentration of the inhibitor [81-82]. It is also evident that there is a decreasing trend in the corrosion current density and an increase in the inhibition efficiency with increase in the inhibitor concentration.

3.2.3 Electrochemical impedance spectroscopy (EIS)

EIS is an efficient technique to study organic coatings on the metal as this technique does not disturb the double layer at the metal / solution interface [83-84] and provides highly reliable results. Nyquist plots of copper in 0.5M, 1M, 1.5M H_2SO_4 at 303K, 308K and 313 K containing various concentrations of L - cysteine after 30 minutes of immersion time are presented in Fig. 3.5 to Fig. 3.7. It showed that in uninhibited solution, Nyquist plot yields a slightly depressed semi circular shape with only one time constant in Bode format. This indicated that copper has undergone corrosion in a solution without inhibitor and the process is controlled by charge transfer process [85-86]. The electrochemical parameters associated to this impedance study are given in the Table 3.4 to Table 3.6. A.C impedance data on copper revealed that an increase in inhibitor concentration leads to R_{ct} value increase at 303 K in all concentrations of the acid used in the

study. The I_{corr} value decreased with increased concentration of the inhibitor. At high temperatures (308K & 313K), R_{ct} value showed increasing trend with the inhibitor concentration in acid medium. The simplest circuit fit for these experimental data was a Randles circuit which consists of a solution resistance, R_s in series to a parallel combination of resistor, R_{ct} and a double layer capacitor, $_{Cdl}$. R_{ct} representing the charge transfer resistance and C_{dl} representing the electrode capacitance. The addition of L – cysteine to the acid solution changed the shape and size of the impedance behaviour and a depressed semicircle is obtained at the high frequency region and this is due to the charge transfer resistance and the diffuse layer resistance. It is interesting to note from the Nyquist plots that R_{ct} values increased with the inhibitor concentration, through the formation of a protective layer at the metal surface, which acts as a barrier for the mass and the charge transfers.

3.2.4 Adsorption studies

The adsorption isotherm provides information pertaining to the interaction of inhibitor with metal surface [87-88]. Adsorption parameters corresponding to the behaviour of the inhibitor on copper is presented in Table 3.7. To obtain adsorption isotherm, the surface coverage values (θ) for different concentrations of inhibitor in 0.5M, 1M, and 1.5M H_2SO_4 have been obtained from potentiodynamic polarization measurements. Using these data different graphs has been constructed to find out the most suitable adsorption isotherm. The plot of log (θ/1-θ) Vs log C yields a straight line, providing that the adsorption of the L - cysteine on copper surface obeys Langmuir adsorption isotherm and the same for copper in 0.5M, 1M &1.5M H_2SO_4 in the absence and presence of L - cysteine at 303K, 308K &

313 K is shown in Fig. 3.7. The negative value of ΔG^0_{ads} ensured the spontaneity of adsorption process and stability of the adsorbed layer on the copper surface. Generally the value of ΔG^0_{ads} around -20kJ mol^{-1} or lower are consistent with physisorption, while those around -40kJmol^{-1} or higher value involve chemisorptions [89]. Based on the calculated ΔG^0_{ads} values, it could be inferred that adsorption involved is mixed type.

3.3 Conclusions.

1. The amino acid L- cysteine may be considered as a green corrosion inhibitor for copper with relatively good efficiency.
2. As the concentration of the inhibitor increases, corrosion inhibition efficiency as well as charge transfer resistance increases whereas the corrosion rate and double layer capacitance decreases due to better adsorption of the inhibitor on metal surface.
3. The inhibitor molecule affects both the anodic and cathodic processes and hence acts as a mixed type one.
4. The adsorption of the inhibitor obeys Langmuir adsorption isotherm model.

Table 3.1: Electrochemical parameters of copper obtained from polarization curves in 0.5 M, 1 M & 1.5 M H_2SO_4 at 303K.

Sulphuric acid	L - cysteine (ppm)	E_{corr} (mV)	β_a (mV dec-1)	β_c (mV dec-1)	I_{corr} (mA cm^{-2})	CR (mils/yr)	(%IE)
0.5M	Blank	-64.49	48.14	- 217.27	3.83	33.512	------
	50	-69.04	45.53	- 98.48	2.31	22.118	39.00
	100	-56.89	26.77	- 36.70	1.80	15.764	53.00
	150	-51.23	22.64	- 24.98	1.60	14.566	58.22
1 M	Blank	-97.56	57.62	- 113.88	3.85	35.541	------
	50	-69.51	37.62	- 48.12	2.40	24.127	37.66
	100	-66.24	43.11	- 55.44	2.00	16.834	48.05
	150	-80.72	33.58	- 49.87	1.67	15.532	56.62
1.5 M	Blank	-76.69	34.89	- 237.84	3.86	36.972	-----
	50	-35.11	22.19	- 28.03	2.47	35.568	36.01
	100	-30.05	44.50	- 87.06	2.40	17.589	38.42
	150	-62.05	52.71	- 200.29	1.73	16.938	55.18

Table 3.2: Electrochemical parameters of copper obtained from polarization curves in 0.5 M, 1 M & 1.5 M H_2SO_4 at 308K.

Sulphuric acid	L - cysteine (ppm)	E_{corr} (mV)	β_a (mV dec-1)	β_c (mV dec-1)	I_{corr} (mA cm^{-2})	CR (mils/yr)	(%IE)
0.5M	Blank	- 203.05	122.22	- 70.65	3.90	34.68	------
	50	- 172.88	79.27	- 322.37	2.50	24.55	36.00
	100	- 191.29	46.01	- 90.14	1.88	23.39	51.79
	150	- 146.97	71.96	- 189.32	1.66	20.11	56.66
1 M	Blank	- 51.76	68.96	- 204.33	3.93	36.94	------
	50	- 48.54	53.00	- 311.00	2.55	26.53	35.11
	100	- 24.08	51.99	- 464.90	1.95	24.92	50.38
	150	- 33.79	51.562	- 303.67	1.90	21.93	51.65
1.5 M	Blank	- 46.89	27.69	- 15.09	3.95	38.27	-------
	50	- 96.59	36.11	- 101.77	2.60	28.32	34.17
	100	- 39.35	38.53	- 86.84	2.13	25.20	45.56
	150	- 31.13	34.08	- 55.61	1.98	23.49	49.87

Table 3.3: Electrochemical parameters of copper obtained from polarization curves in 0.5M, 1 M & 1.5 M H2SO4 at 313K

sulphuric acid	L-cysteine (ppm)	E_{corr} (mV)	β_a (mV dec-1)	β_c (mV dec-1)	I_{corr} (mA cm^{-2})	CR (mils/yr)	(%IE)
	Blank	- 180.31	66.27	- 173.92	3.95	35.88	-------
	50	- 181.14	59.71	- 173.56	2.55	27.73	35.44
0.5 M	100	- 185.35	45.34	- 100.59	2.50	25.87	36.70
	150	- 188.01	57.85	- 258.11	2.00	24.25	49.36
	Blank	- 27.20	46.20	- 354.33	3.97	37.10	-------
	50	- 33.47	47.77	- 173.55	2.59	29.44	34.76
1 M	100	- 69.75	38.39	- 132.82	2.57	26.05	35.26
	150	- 62.07	71.26	- 382.50	2.54	25.48	36.02
	Blank	- 84.61	35.73	- 74.88	3.99	38.65	-------
1.5 M	50	- 96.31	39.95	- 46.25	2.70	30.52	32.33
	100	- 84.61	31.87	- 63.22	2.65	28.13	33.58
	150	-39.13	42.13	- 130.93	2.60	26.25	34.83

Table 3.4: AC impedance data on copper with L – cysteine in 0.5 M, 1 M & 1.5 M H_2SO_4 at 303K.

sulphuric acid	L - cysteine (ppm)	R_{ct} (Ω cm^2)	C_{dl} (μF cm^{-2})	I_{corr} (μA cm^2)	C.R (mils/yr)	(%IE)
	Blank	598	409.10	2.90	26.59	------
	50	1820	315.30	1.43	13.13	67.14
0.5M	100	1904	261.60	1.37	12.55	68.59
	150	3024	234.00	1.28	11.80	70.13
	Blank	540	1440.00	3.15	28.93	------
	50	1539	173.00	1.69	15.52	64.91
1M	100	1700	107.80	1.51	13.85	68.23
	150	1802	76.00	1.49	13.21	70.00
	Blank	514	1205.00	3.21	32.50	------
	50	1010	358.37	1.76	17.53	57.16
1.5 M	100	1504	64.31	1.87	15.21	65.82
	150	1704	37.21	1.53	14.20	68.01

Table 3.5: AC impedance data on copper with L – cysteine in 0.5 M, 1 M & 1.5 M H_2SO_4 at 308K.

Sulphuric acid	L - cysteine (ppm)	R_{ct} (Ω cm^2)	C_{dl} (μF cm^{-2})	I_{corr} (mA cm^{-2})	C.R (mils/yr)	(%IE)
	Blank	101	4936.00	3.25	34.58	--------
	50	158	1006.00	1.78	19.09	36.00
0.5M	100	164	821.00	1.70	16.57	38.00
	150	325	223.70	1.57	15.00	68.92
	Blank	93	1275.00	3.29	36.40	--------
	50	130	803.20	1.83	21.20	28.46
1M	100	149	552.60	1.75	17.90	37.30
	150	290	206.30	1.63	16.21	67.93
	Blank	74	2298.00	3.53	38.90	-------
	50	87	1401.00	1.86	25.07	14.49
1.5M	100	115	674.30	1.79	20.90	35.60
	150	215	513.00	1.67	18.94	65.58

Table 3.6: AC impedance data on copper with L – cysteine in 0.5 M, 1 M & 1.5 M H_2SO_4 at 313K.

Sulphuric acid	L - cysteine (ppm)	R_{ct} (Ωcm^2)	C_{dl} (μF cm^{-2})	I_{corr} (mA cm^{-2})	C.R (mils/yr)	(%IE)
	Blank	124	511.90	3.57	40.53	----
	50	172	434.00	1.89	27.54	27.70
0.5M	100	173	297.50	1.85	23.49	28.48
	150	350	189.80	1.77	21.25	64.57
	Blank	100	3088.00	3.62	42.05	-------
	50	120	2973.00	1.93	29.67	16.66
1M	100	138	1464.00	1.88	25.84	27.50
	150	280	1154.00	1.81	23.85	64.28
	Blank	47	1491.00	3.70	43.65	------
	50	54	811.00	1.96	30.18	11.62
1.5M	100	65	607.00	1.93	28.99	26.71
	150	116	303.00	1.86	25.21	58.74

Table 3.7: Adsorption parameters of inhibitor (L – cysteine) for corrosion of copper at various temperatures and concentration of sulphuric acid.

Sulphuric acid	Temperature (K)	ΔG^{o}_{ads} (kJ mol^{-1}) & K_{ads} (mol^{-1}) L - cysteine (ppm)					
		50		100		150	
	303	-29.86	1046	-28.25	1337	-27.6	2536
0.5 M	308	-28.78	756	-27.26	1371	-32.15	5116
	313	-28.15	900	- 26.51	479	-30.68	2371
	303	-29.40	977	-28.25	1335	-27.46	2109
1 M	308	-25.81	429	-27.15	724	-30.46	2638
	313	-28.03	456	-26.39	856	-30.03	1854
	303	-29.26	800	-27.85	1139	-26.86	1195
1.5 M	308	-25.61	396	-26.93	664	-30.96	2500
	313	-25.29	300	-26.21	426	-28.79	1150

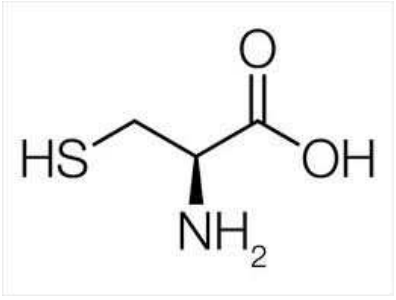

Figure 3.1: Structure of L- cysteine

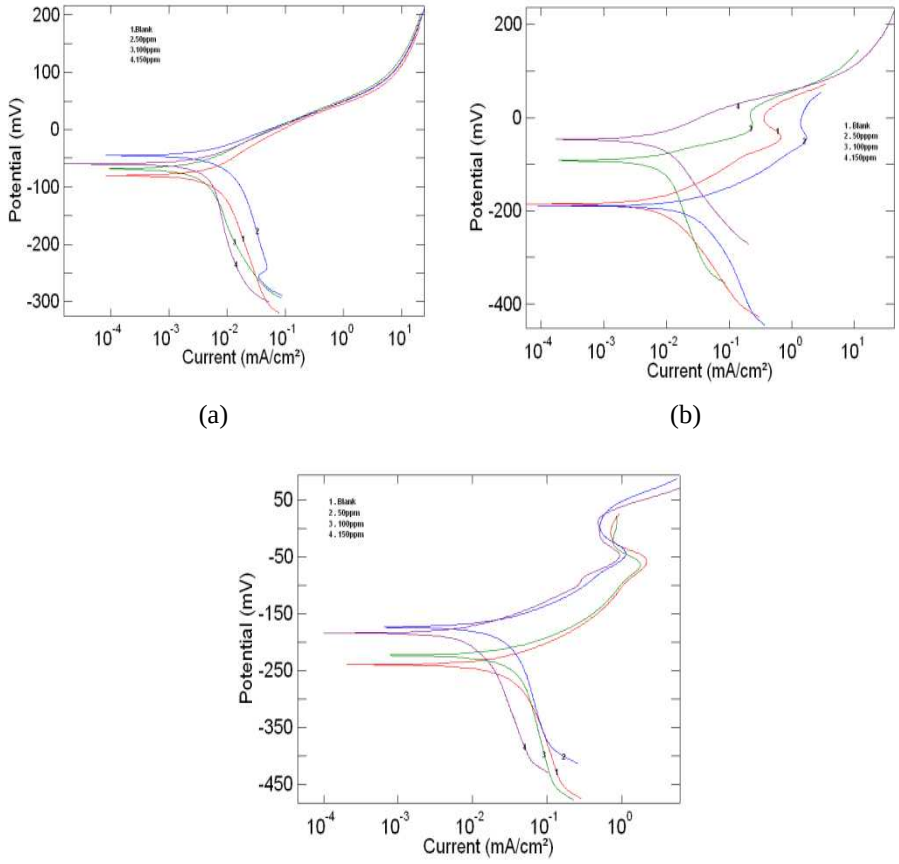

Figure 3.2: Polarization curves of copper in 0.5M H_2SO_4 in different concentrations of L – cysteine at (a) 303K (b) 308K (c) 313K.

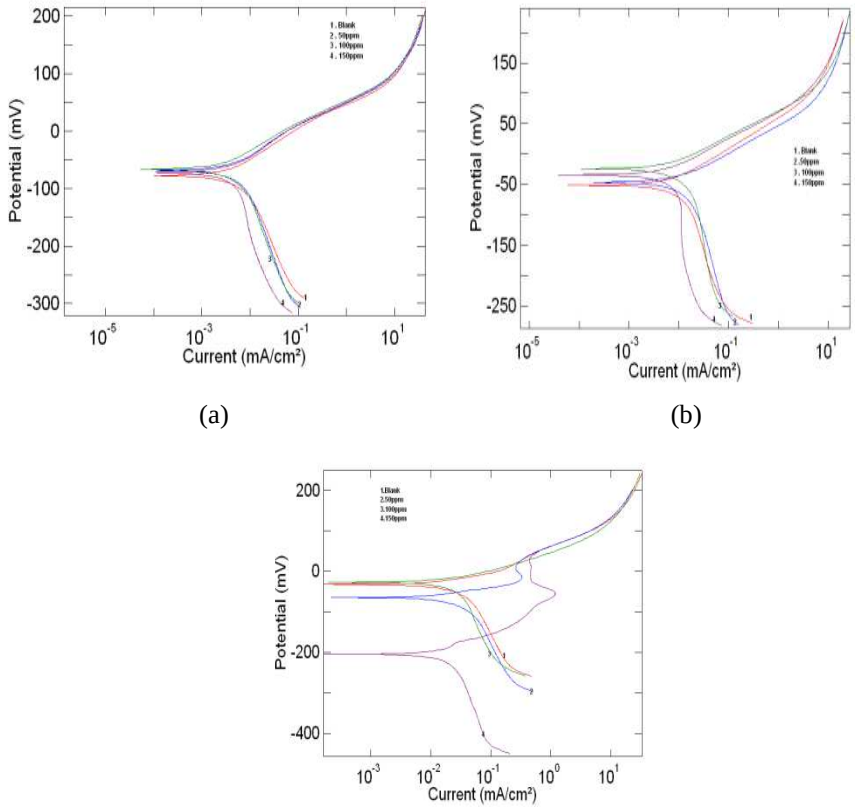

Figure 3.3: Polarization curves of copper in 1M H_2SO_4 in different concentrations of L – cysteine at (a) 303K (b) 308K (c) 313K.

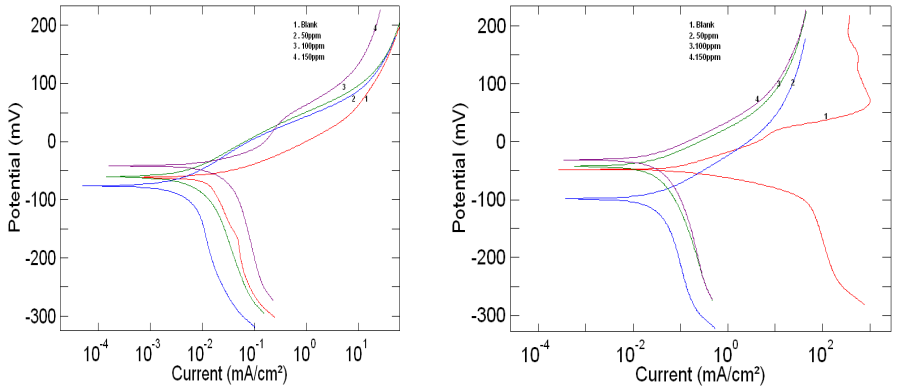

(a) (b)

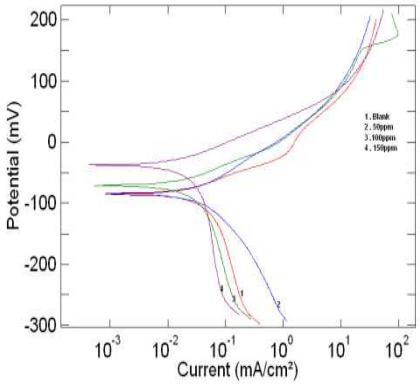

(c)

Figure 3.4: Polarization curves of copper in 1.5 M H_2SO_4 in different concentrations of L – cysteine at (a) 303K (b) 308K (c) 313K.

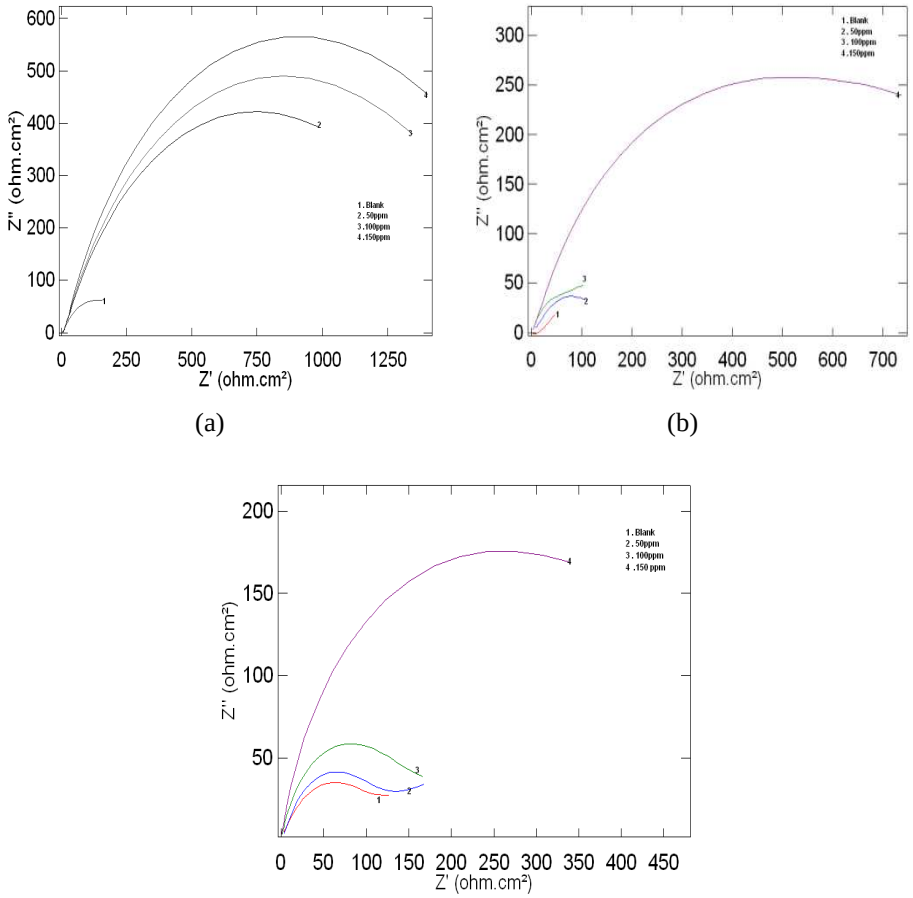

Figure 3.5: Nyquist plots of copper in 0.5 M H_2SO_4 in different concentrations of L- cysteine at (a) 303K (b) 308K (c) 313K.

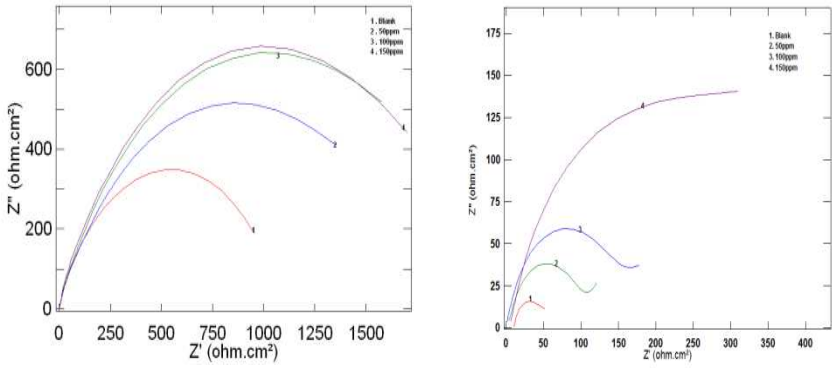

(a) (b)

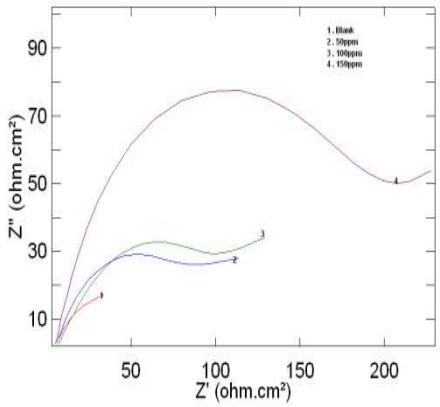

(c)

Figure 3.6: Nyquist plots of copper in 1M H_2SO_4 in different concentrations of L- cysteine at (a) 303K (b) 308K (c) 313K.

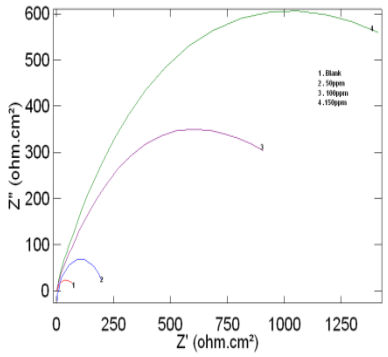

(a)

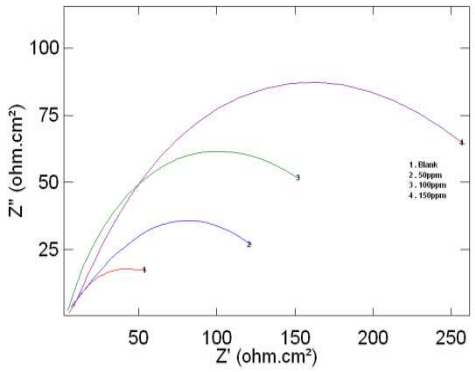

(b)

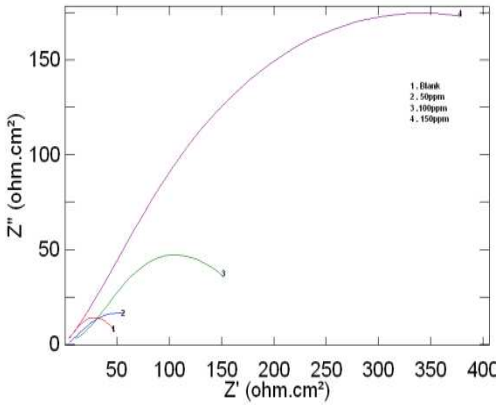

(c)

Figure 3.7: Nyquist plots of copper in 1.5M H_2SO_4 in different concentrations of L – cysteine at (a) 303K (b) 308K (c) 313K.

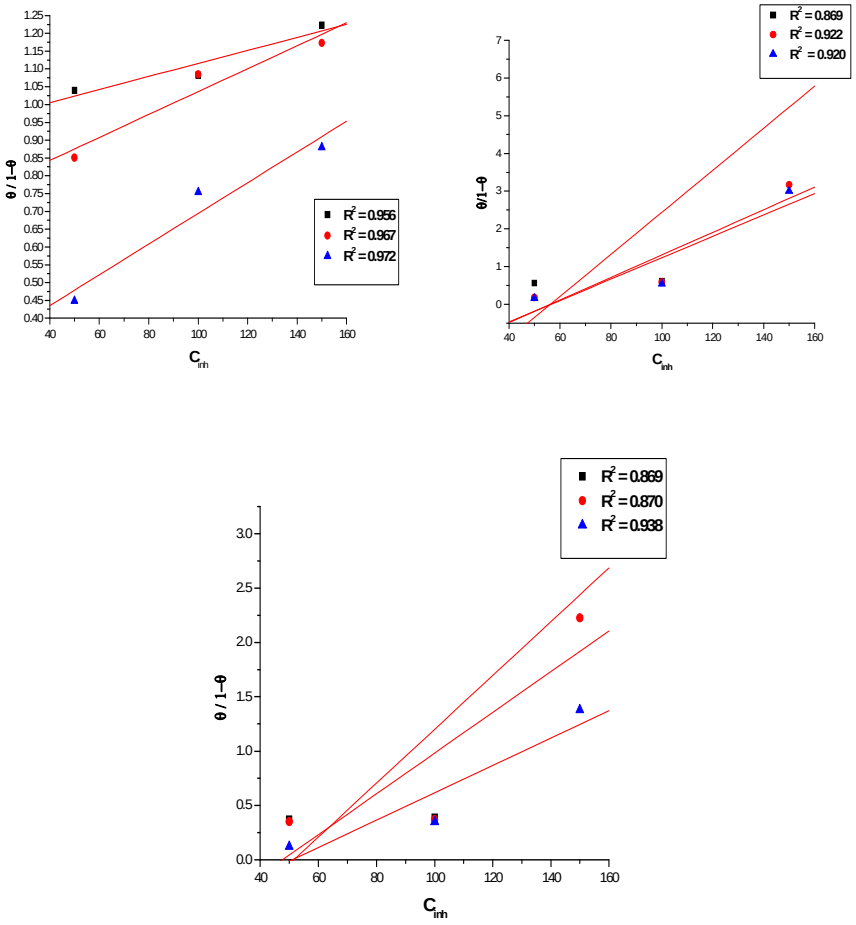

Figure 3.8: Langmuir adsorption isotherm for copper in 0.5M, 1M & 1.5M H_2SO_4 in L - cysteine inhibitor at (a) 303K (b) 308K (c) 313 K.

Chapter

4

ELECTRO CHEMICAL INTERACTIONS OF HHDMP, A L-SERINE BASED SCHIFF BASE, WITH COPPER IN SULPHURIC ACID

Contents

4.1 Results and Discussion

4.1.1. Weight loss studies

The weight loss recorded on the sample specimen reflects on the inhibition efficiency. The weight loss under different intervals of time (24, 48, 72 and 96 hours) in 1M sulphuric acid at different concentrations of inhibitor HHDMP (Fig.4.1) was studied. Results revealed that the inhibition efficiency is high at 24 hour interval irrespective of concentrations of the inhibitors and subsequently the efficiency declined. The inhibition efficiency increased with the increased concentrations of the inhibitor, however with the advancement of time interval inhibition efficiency decreased irrespective of the inhibitor concentrations.

4.1.2 Potentiodynamic polarization studies

Potentiodynamic polarization behaviour of copper in 1M sulphuric acid in the absence and presence of inhibitor HHDMP at 303K, 308K and 313K were presented in Table 4.1. Results indicated that the electrochemical parameters vary with the inhibitor concentration and temperature. Tafel polarization curves for copper in 0.5M, 1M & 1.5M sulphuric acid in the absence and presence of different concentrations of HHDMP at 303K are presented in Fig.4.2. The polarization results indicated that increase in the inhibitor concentration reduces both the cathodic and anodic current and there is no definite trend in the shift of E_{corr} values. The displacement in E_{corr} between in the absence and presence of the inhibitor was less than 85 mV which conforms the mixed type behaviour of the inhibitor. Therefore it is also clear that the values of electrochemical parameters like I_{corr} and corrosion rate decreased with the increase in concentration of the inhibitor. The decreasing trend of I_{corr} with the increase in inhibitor concentration in all the acid concentration is shown in Fig.4.3.

4.1.3. Electrochemical impedance spectroscopy (EIS)

Electrochemical impedance spectroscopy (EIS) is an efficient technique to study organic coatings on the metal as this technique does not disturb the double layer at the metal / solution interface and thus provides highly reliable results. The electrochemical parameters associated to impedance study at varying temperatures (303K, 308K, 313K) were presented in Table 4.2. Results revealed that I_{corr} value showed decreasing trend with increase in concentration of the

inhibitor. Nyquist plots of copper in 1M sulphuric acid solution at 303K, 308K & 313K containing various concentrations of HHDMP after 30 minutes of immersion are presented in Fig.4.4. The plot of concentration of the inhibitor against efficiency is depicted in Fig.4.5. The efficiency is found to be high at 150ppm of inhibitor HHDMP. It further reveals that in uninhibited solution, Nyquist plot yields a slightly depressed semi circles and it amply explains that the corrosion of the copper in the absence of inhibitor is mainly controlled by a charge transfer process. [85-86]. The simplest circuit fit for these experimental data was a Randles circuit consists of a solution resistance, R_s in series to a parallel combination of resistor, R_{ct} and a double layer capacitor, C_{dl}. R_{ct} representing the charge transfer resistance and C_{dl} representing the electrode capacitance. It may be noted from Nyquist plots that R_{ct} values increased with inhibitor concentration, which can be attributed to the formation of a protective layer at the metal surface and this layer acts as a barrier for the mass and the charge transfers.

4.1.4 Adsorption studies

The adsorption isotherm provides information pertaining to the interaction of inhibitor with metal surface [87-88]. Adsorption behaviour of the HHDMP in copper corrosion is presented in Table 4.3. Results revealed that corrosion behaviour varies with inhibitor concentrations. The surface coverage values (θ) for different concentrations of inhibitor in 1M sulphuric acid obtained from, electrochemical measurements were used for the construction of adsorption isotherm. Using these data, different isotherms have been

plotted to find out the most suitable adsorption isotherm. The plot C/ θ Vs C shows a straight line, providing that the adsorption of HHDMP on copper surface obeys Langmuir adsorption isotherm and the same at 303K, 308K & 313K are shown in Fig.4.6.

The values of K_{ads} and ΔG^0_{ads} of inhibitor HHDMP is given in Table 4.4. The negative value of ΔG^0_{ads} indicates the spontaneity of adsorption process and stability of the adsorbed layer on the copper surface. Generally the value of ΔG^0_{ads} around -20kJ mol^{-1} or lower are consistent with physisorption, while those around -40kJmol^{-1} or higher value involve chemisorptions [89]. In this case mode of adsorption involved is physisorption

4.1.5 Computational studies

Computational calculations of various quantum chemical parameters like energy of highest occupied molecular orbital (E_{HOMO}), energy of the lowest unoccupied molecular orbital (E_{LUMO}), energy gap (ΔE) i.e. E_{HOMO}-E_{LUMO}, ionization potential, I which is -E_{HOMO}, electron affinity, A which is –E_{LUMO}, electro negativity, χ which is (I+A)/2 and hardness, η which is (I-A)/2 were calculated and optimized the geometry of the molecule using Gaussian 09 program package. The calculated values of quantum chemical parameters are E_{HOMO} (eV), ELUMO (eV), ΔE (eV), I (eV), A (eV), χ(eV), η (eV) which are found to be -5.72, -1.62, 4.03, 5.72, 1.62, 3.67, 2.05 respectively. The optimized geometry of HHDMP is presented in Fig. 4.7. HOMO and LUMO of HHDMP are given in Fig.4.8. It is generally stated that the efficiency of inhibitors increase with decrease in energy gap, ΔE, increase in E_{HOMO} and

decrease in E_{LUMO}. Higher E_{HOMO} value enhances the adsorption of inhibitor and thereby increasing the inhibition efficiency. Smaller the E_{LUMO} value greater will be the probability of molecules to accept electrons. Higher the ionization energy, easier will be the removal of electrons from the molecule.

4.1.6 Scanning electron microscopy

The SEM images of a bare polished copper, copper after immersion in 1M sulphuric acid without inhibitor & with inhibitor for a period of 24 hours were given in Fig.4. 9 a-c respectively. It also revealed that the metal surface was smooth and free from depressions in the case of copper immersed in sulphuric acid containing HHDMP where as the surface is damaged in the case of copper immersed in sulphuric acid without inhibitor.

4.1.7 Atomic force microscope (AFM)

The three dimensional AFM images are shown in the Fig.4.10 (a–c). It is evident from the Fig 4.10 c, there is much less damage on the surface of copper in the presence of HHDMP. The average roughness of polished copper (Fig. 4.10 a) and copper exposed in 1M H_2SO_4 without inhibitor (Fig.4.10b) was calculated to be 6.84nm and 84 nm, respectively. The copper surface in the free acid solution is getting cracked due to the acid attack (Figure.4.10 b). However, in the presence of 150ppm of inhibitor, the average roughness was reduced to 33.72.

4.2 Conclusions.

1) The amino acid schiff base HHDMP is a green corrosion inhibitor with fairly good efficiency

2) As the concentration of the inhibitor increases, corrosion inhibition efficiency as well as charge transfer resistance increases.

3) The corrosion rate and double layer capacitance decreased due to increased adsorption of the inhibitor.

4) The inhibitor molecule affects both the anodic and cathodic processes and hence acts as a mixed type inhibitor.

5) The adsorption of the inhibitor obeys Langmuir adsorption isotherm model.

6) HHDMP inhibits copper corrosion in 1M H_2SO_4 even at fairly high temperature also.

Table 4. 1: Data on Electrochemical parameters of copper obtained from polarisation curves in 1M H_2SO_4.

Temp (K)	HHDMP (ppm)	E_{corr} (mV)	β_a (mV dec-1)	β_c (mV dec-1)	I_{corr} (mA cm^{-2})	CR (mils/yr)	(%IE)
	Blank	-39.52	61.15	-184.44	0.0110	10.30	------
	50	-79.20	57.76	- 110.72	0.0032	3.010	71.42
303K	100	-72.60	54.32	- 62.13	0.0021	2.560	75.89
	150	-110.32	37.12	- 56.45	0.0020	2.100	80.35
	Blank	-52.20	43.77	- 275.60	0.0090	11.26	------
	50	-80.65	56.29	- 90.64	0.0032	3.25	68.68
308K	100	-110.25	45.97	- 68.57	0.0024	2.60	71.74
	150	-84.87	64.45	- 99.30	0.0025	2.23	74.74
	Blank	-53.21	47.32	- 396.42	0.0126	11.57	-----
313K	50	-78.63	58.67	- 144.30	0.0040	3.73	66.66
	100	-39.56	36.93	- 50.42	0.0038	3.49	69.84
	150	-80.47	58.20	- 92.04	0.0034	3.11	73.01

Table 4.2: AC impedance data on copper with HHDMP in 1 M H_2SO_4 at 303K, 308K & 313K.

Temp (K)	HHDMP (ppm)	R_{ct} (Ω cm^2)	C_{dl} (μF cm^{-2})	I_{corr} (mA cm^{-2})	C.R (mils/yr)	(%IE)
	Blank	493	409.10	0.052	48.38	------
	50	1533	315.30	0.017	15.58	68.84
303K	100	2588	261.60	0.010	9.23	80.95
	150	3273	234.00	0.008	7.52	85.98
	Blank	442	14430.00	0.058	54.02	------
	50	1311	173.00	0.019	18.15	67.28
308K	100	1772	107.80	0.014	13.48	75.05
	150	2715	76.00	0.009	8.79	83.72
	Blank	438	1105.00	0.060	54.96	------
	50	1298	318.20	0.020	19.36	66.00
313K	100	1715	54.22	0.015	13.93	74.40
	150	2512	29.13	0.010	9.51	82.50

Table 4.3: Adsorption parameters of inhibitor (HHDMP) for corrosion of 1 M H_2SO_4 at 303K, 308K & 313K.

Temperature (K)	ΔG^o_{ads} (kJ mol^{-1})& K_{ads} x 10^4(mol^{-1}) HHDMP (ppm)					
	50		100		150	
303K	-16.18	11.00	-16.19	11.12	-16.08	10.68
308K	-16.06	10.59	-15.30	7.83	-15.50	8.49
313K	-15.95	10.13	-15.17	7.42	-15.33	7.91

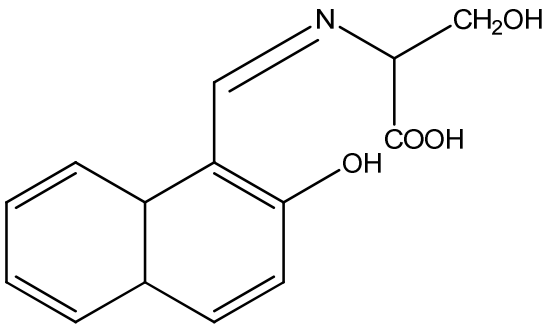

Figure 4.1: Structure of HHDMP.

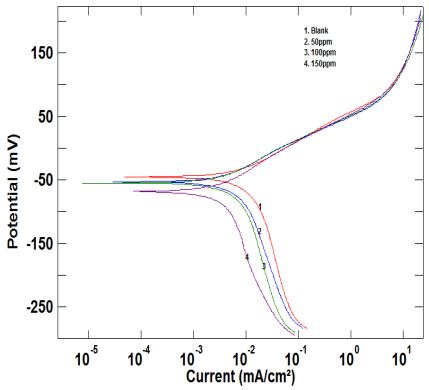

(a)

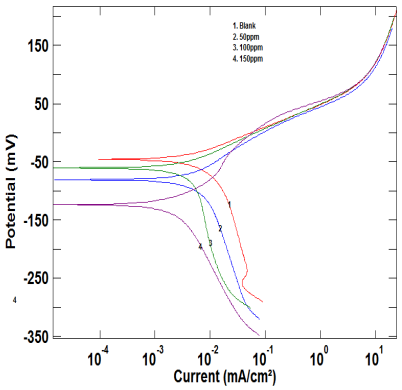

(b)

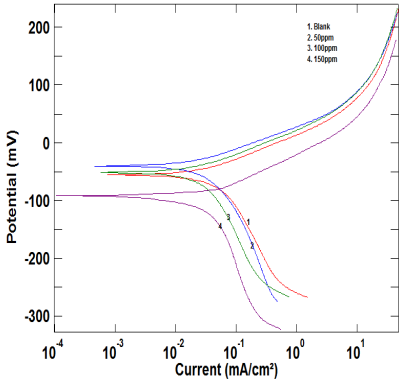

(c)

Figure 4.2: Polarization curves for copper in 1M sulphuric acid at 303K, 308K & 313K respectively.

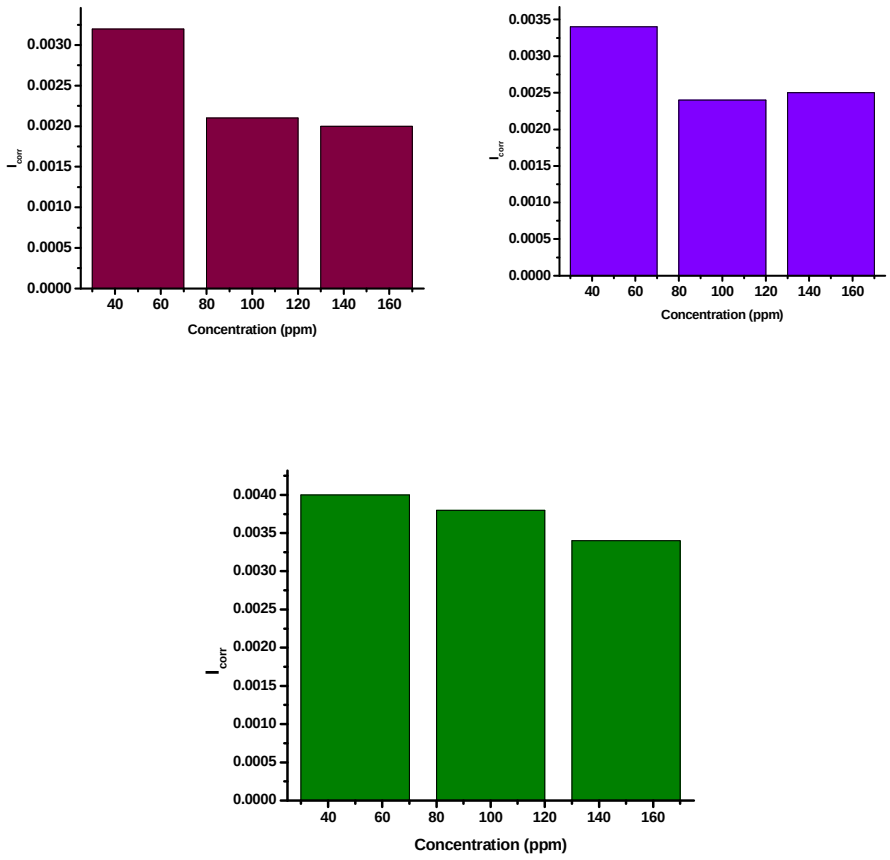

Figure 4.3: Plot of I_{corr} against inhibitor concentration in 1M sulphuric acid at a) 303K b) 308K c) 313K.

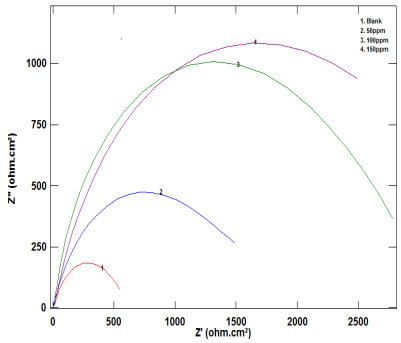

(a)

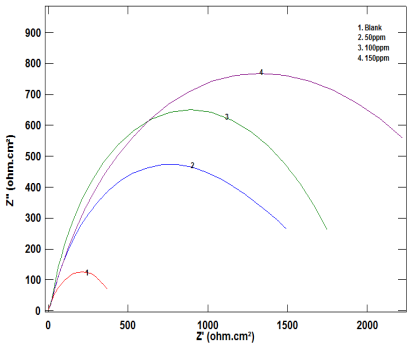

(b)

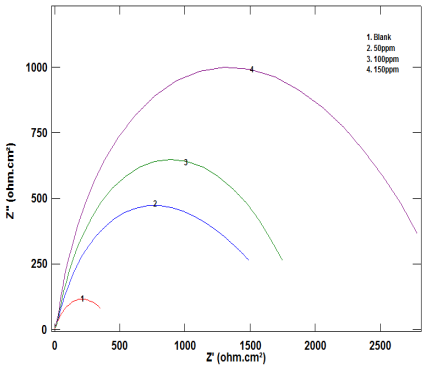

(c)

Figure 4.4: Nyquist plots of copper in 1M sulphuric acid solution at (a) 303K (b) 308K (c) 313K.

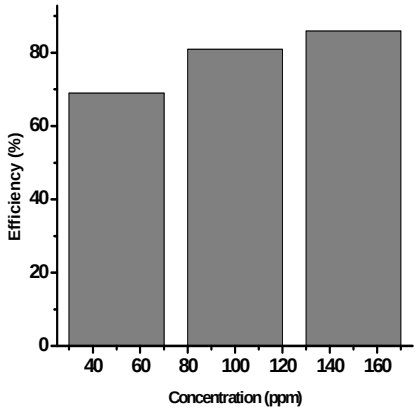

(a)

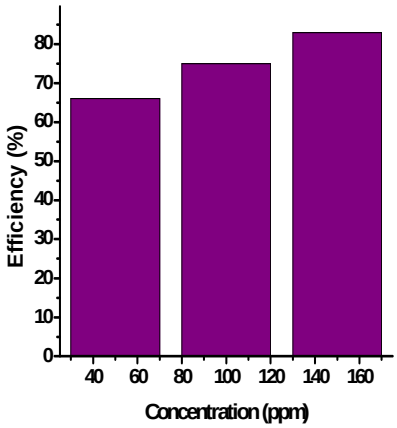

(b)

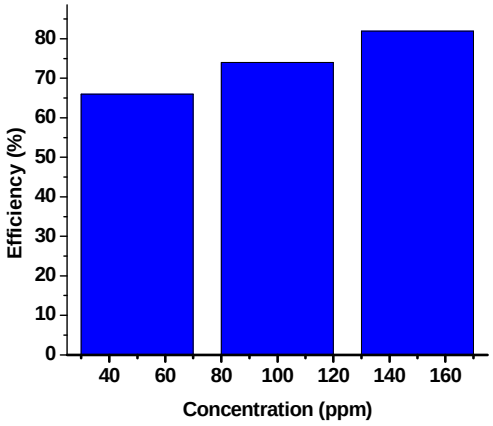

(c)

Figure 4.5: Plot of efficiency against concentration of the inhibitor in 1M H_2SO_4 at (a) 303K (b) 308K (c) 313K.

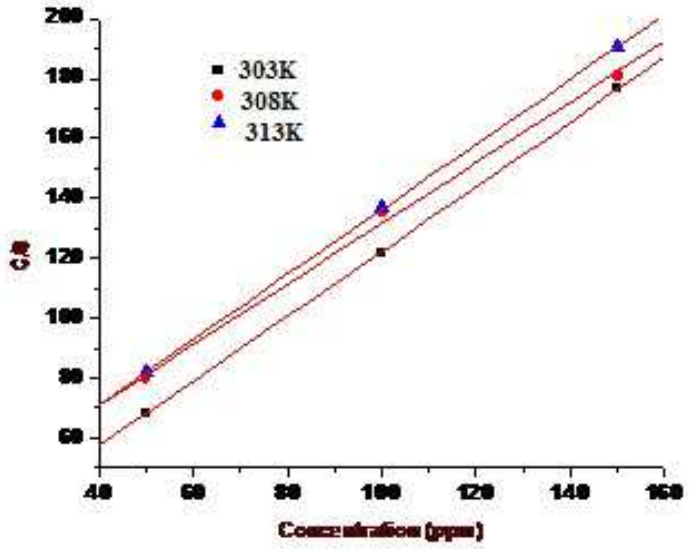

Figure 4. 6: Langmuir adsorption isotherm

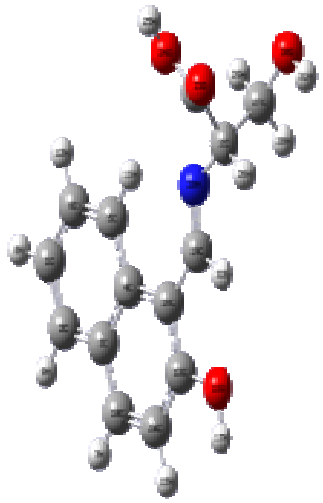

Figure 4.7: Optimized geometry of HHDMP

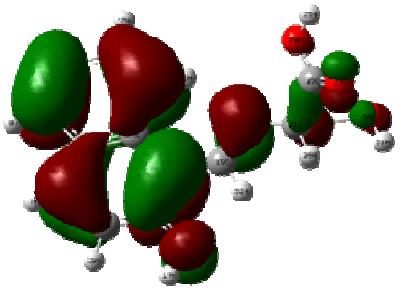

(a) HOMO

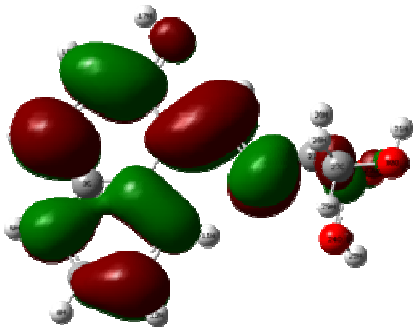

(b) LUMO

Figure 4.8: (a) HOMO (b) LUMO of HHDMP.

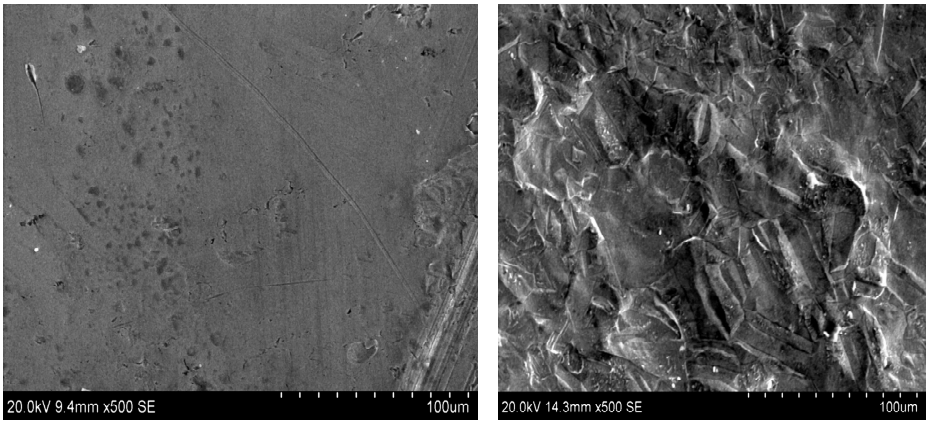

(a) (b)

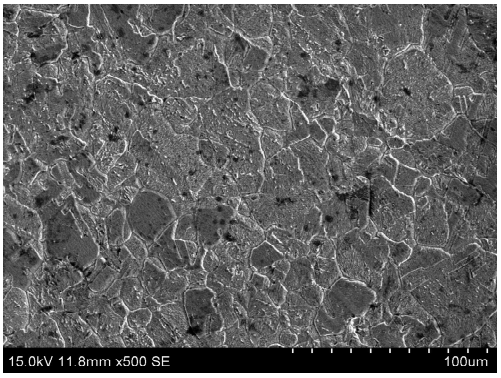

(c)

Figure 4. 9: The SEM images of (a) bare polished copper (b) copper after immersion in 1M sulphuric acid medium without inhibitor (c) With HHDMP

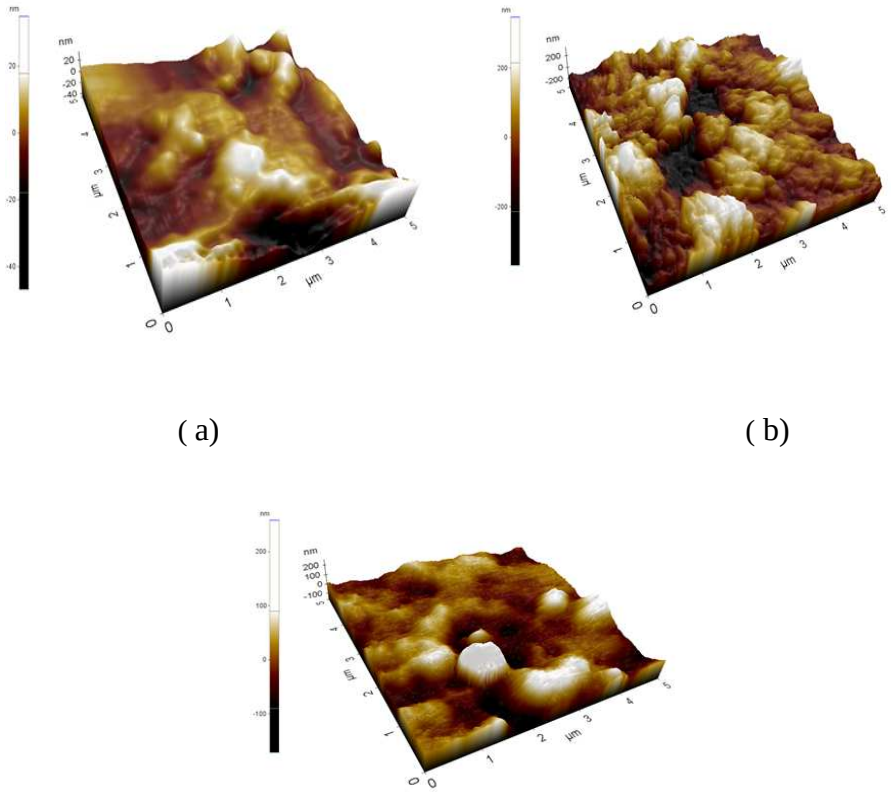

(a) (b)

(c)

Figure 4.10: AFM images of (a) copper (b) copper in 1M H_2SO_4 without inhibitor (c) copper in the presence of 150 ppm of HHDMP after 24 hr exposure.

Chapter

5

ELECTROCHEMICAL INTERACTIONS OF HDMMA,A CYSTEINE BASED SCHIFF BASE, WITH COPPER IN HYDROCHLORIC ACID

Contents

5.1 Results and Discussion

5.1.1 Weight loss studies

The weight loss under different intervals of time (24, 48, 72 and 96 hours) in the absence and presence of different concentrations (50ppm, 100ppm, 150ppm) of inhibitor HDMMA (Fig.5.1) were studied. Results revealed that the inhibition efficiency became high upto 24 hour interval irrespective of concentration of the inhibitor and subsequently the efficiency declined. The inhibition efficiency increased with the increased concentrations of the inhibitor. With the advancement of time interval, inhibition efficiency decreased irrespective of the inhibitor concentration.

5.1.2 Potentiodynamic polarization studies

Potentiodynamic polarization behaviour of copper in hydrochloric acid in the absence and presence of inhibitor HDMMA at 303K, 308K & 313K are presented in the Table 5.1. Tafel polarization curves for copper in 1M hydrochloric acid in the absence and presence of various concentrations of HDMMA at 303K, 308K & 313K are presented in Fig.5.2. It revealed that both the anodic metal dissolution and cathodic hydrogen evolution would exhibit Tafel type behaviour. The results emanating from these studies revealed that HDMMA can act as a mixed type inhibitor. It is also evident that corrosion rate decreased with the increase in concentration of the inhibitor in all temperature regimes and is represented in the Fig.5.3. The mechanism of corrosion inhibition involves the blocking of reaction sites by the inhibitor due to the adsorption of inhibitor molecule on the metal surfaces and the surface adsorption increases by increase in the concentration of inhibitor [81-82].The formation of a coating on the surface of the metal as a result of adsorption of the inhibitor molecule gives a considerable protection against corrosion.

5.1.3 Electrochemical impedance spectroscopy (EIS)

Electrochemical impedance spectroscopy (EIS) is an efficient technique to study organic coatings on the metal as this technique does not disturb the double layer at the metal / solution interface and hence the technique provides highly reliable and consistent results. The electrochemical parameters associated to impedance study at various temperature gradients (303K, 308K &313K) are presented in Table 5.2. Results revealed that I_{corr} value showed a decreasing trend with increased concentration of the

inhibitor. It is interesting to note that in all the varied acid medium devoid of inhibitor registered high values of $I_{corr.}$ Nyquist plots of copper in 1M hydrochloric acid solution at 303K, 308K & 313K containing various concentrations of HDMMA after 30 minutes of immersion are presented in Fig.5.4. The efficiency is found to be high at 150ppm of inhibitor HDMMA in all temperature regimes and the graphical representation of this relationship is presented in the Fig.5.5. It also revealed that in uninhibited solution, Nyquist plot yields a slightly depressed semi circles and it amply explains that the corrosion of the copper in the absence of inhibitor is mainly controlled by a charge transfer process [85-86]. The simplest circuit fit for these experimental data was a Randles circuit which consists of a solution resistance, R_s in series to a parallel combination of resistor, R_{ct} and a double layer capacitor, C_{dl}. R_{ct} representing the charge transfer resistance and C_{dl} representing the electrode capacitance. It may be noted from Nyquist plots that R_{ct} values increased with inhibitor concentration, which can be attributed to the formation of a protective layer at the metal surface and this layer acts as a barrier for the mass and the charge transfers.

5.1.4 Adsorption studies

The adsorption isotherm provides information pertaining to the interaction of inhibitor with metal surface. Adsorption behaviour of HDMMA on copper metal presented in the Table 5.3. Results revealed that corrosion behaviour varies with inhibitor concentration in the acid medium. The surface coverage values (θ) for different concentrations of inhibitor in 1M hydrochloric acid obtained from electrochemical measurements were used for adsorption studies. Using these data, different graphs have been

constructed to find out the most suitable adsorption isotherm. The plot C/ θ Vs C shows a straight line, providing that the adsorption of the Schiff base HDMMA on copper surface obeys Langmuir adsorption isotherm and the same is given in Fig.5.6. The values of K_{ads} and ΔG^{0}_{ads} of HDMMA is given in Table 5.3. The negative value of ΔG^{0}_{ads} ensures the spontaneity of adsorption process and stability of the adsorbed layer on the copper surface. Generally the value of ΔG^{0}_{ads} around -20kJ mol^{-1} or lower are consistent with physisorption, while those around -40kJmol^{-1} or higher value involve chemisorptions [89]. Based on the calculated ΔG^{0}_{ads} values, it could be concluded that adsorption involved is physisorption.

5.1.5 Computational studies

Computational studies indicated that various quantum chemical parameters like energy of highest occupied molecular orbital (E_{HOMO}), energy of the lowest unoccupied molecular orbital (E_{LUMO}), energy gap (ΔE) i.e. E_{HOMO}-E_{LUMO}, ionization potential, I which is -E_{HOMO}, electron affinity, A which is –E_{LUMO}, electro negativity, χ which is (I+A)/2 and hardness, η which is (I-A)/2 were calculated and optimized the geometry of the molecule using Gaussian 09 program package.. The calculated values of quantum chemical parameters are E_{HOMO} (eV), E_{LUMO} (eV), ΔE (eV), I (eV), A (eV), χ (eV), η (eV) which are found to be -6.10, -2.11, 3.99, 6.10, 2.11, 4.10, 1.99 respectively. The optimized geometry of the inhibitor HDMMA is presented in Fig.5.7. HOMO and LUMO of HDMMA are given in Fig.5.8.It is generally believed that the efficiency of inhibitor increase with decrease in energy gap, ΔE, increase in E_{HOMO} and decrease in E_{LUMO}. Higher E_{HOMO} value enhances the adsorption of inhibitor thereby increasing the inhibition efficiency. Smaller the E_{LUMO}

value greater will be the probability of molecules to accept electrons. Higher the ionization energy, easier will be the removal of electrons from the molecule.

5.1.6 Scanning electron microscopy

SEM studies enable to understand the effect of inhibitor molecules on the surface of copper. The SEM images of a bare polished copper, the status of the copper samples after immersion in 1M hydrochloric acid medium without inhibitor & with inhibitor HDMMA, are given in the Figure.5.9. It also revealed that the metal surface was smooth and free from depressions in the case of copper immersed in hydrochloric acid which contains HDMMA where as the surface is damaged in the case of copper which is immersed in hydrochloric acid free from the inhibitor.

5.2 Conclusions.

1. The HDMMA shows effective inhibition efficiency for copper in HCl
2. The corrosion rate and double layer capacitance decreased due to adsorption of the inhibitor. The adsorption of the inhibitor obeys Langmuir adsorption isotherm model.
3. Polarization studies reveal that HDMMA acts as a mixed type inhibitor.
4. The inhibitor molecules adsorb on the copper surface and block the reaction sites. The surface area available for the attack of the corrosive species decreases with the increase in the inhibitor concentration.

Table 5.1: Data on Electrochemical parameters of copper obtained from polarization curves in 1 M HCl at 303K, 308K & 313K.

Temp (K)	HDMMA (ppm)	E_{corr} (mV)	β_a (mV dec-1)	β_c (mV dec-1)	I_{corr} (mA cm^{-2})	CR (mils/yr)	(%IE)
303	Blank	-96.11	118.01	355.86	0.0166	15.243	--------
	50	-88.20	86.93	182.72	0.0041	3.789	75.30
	100	-109.05	72.85	162.03	0.0032	2.993	80.72
	150	-190.26	101.15	183.11	0.0030	2.875	82.00
308	Blank	-59.50	79.53	361.61	0.0185	17.800	-------
	50	-26.25	42.51	53.17	0.0047	4.125	74.59
	100	-83.52	81.16	227.28	0.0055	5.048	70.27
	150	-109.25	78.33	239.83	0.0045	4.2103	75.67
313	Blank	-60.523	80.259	401.27	0.0186	18.250	------
	50	-26.52	53.17	152.21	0.0048	4.938	74.19
	100	-84.26	82.26	227.28	0.0056	5.126	69.00
	150	-110.25	79.25	239.83	0.0046	4.317	75.26

Table.5. 2. AC impedance data on copper with HDMMA Schiff base in 1M HCl at 303K, 308K & 313K.

Temp (K)	HDMMA (ppm)	R_{ct} (Ω cm^2)	C_{dl} (μF cm^{-2})	I_{corr} (mA cm^{-2})	C.R (mils/yr)	(%IE)
	Blank	609.20	95.5	0.0428	39.32	-----
	50	2010	74.15	0.01298	11.89	69.70
303	100	4890	59.07	0.005335	4.85	87.54
	150	6600	41.98	0.00395	3.620	90.77
	Blank	502.5	121.3	0.0560	47.54	-----
	50	1471	57.51	0.0177	16.24	65.87
308	100	2776	70.97	0.0093	8.60	81.89
	150	4610	53.81	0.0056	5.18	89.11
	Blank	465	243.4	0.0591	51.36	------
313	50	1310	47.68	0.0199	18.24	64.50
	100	2303	59.24	0.0113	10.237	79.80
	150	4016	42.52	0.0063	5.784	88.42

Table 5. 3. Adsorption parameters of HDMMA for corrosion of copper in 1M HCl at 303 K, 308K & 313K.

Temperature (K)	ΔG^{o}_{ads} (kJ mol^{-1})& K_{ads} x 10^{4}(mol^{-1}) HDMMA (ppm)					
	50		100		150	
303K	-18.23	12.09	-18.15	12.33	-18.25	11.25
308K	-18.27	11.35	-17.35	11.25	-17.23	10.83
313K	-18.04	11.26	-17.25	11.13	-17.17	10.26

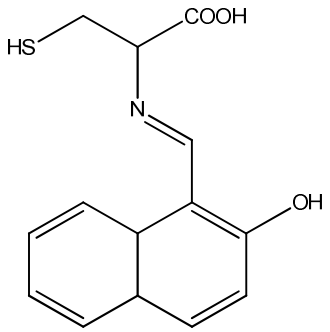

Fig. 5.1: Structure of the inhibitor

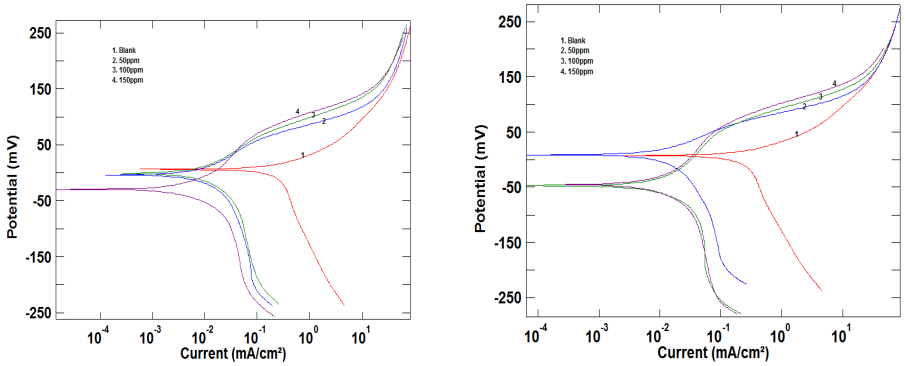

(a) (b)

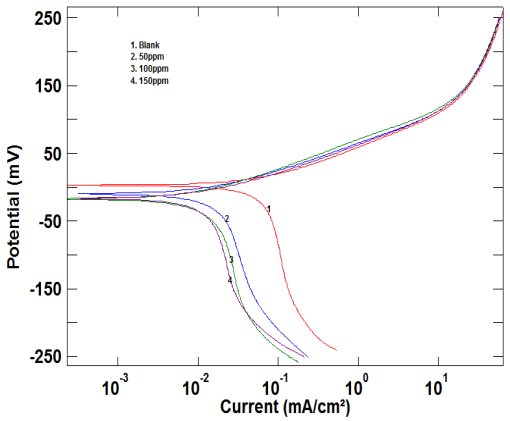

(c)

Fig. 5.2: Polarization curves of copper in 1 M HCl in the absence and presence of different concentrations of HDMMA at 303K, 308K & 313K respectively.

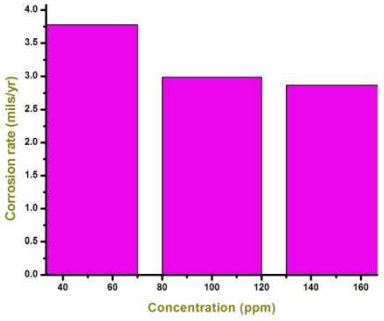

(a)

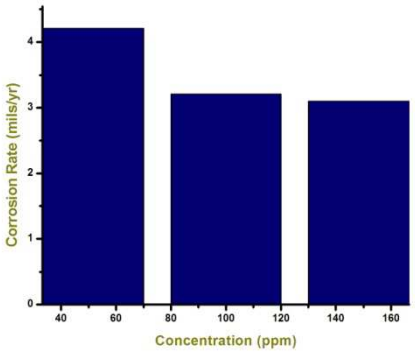

(b)

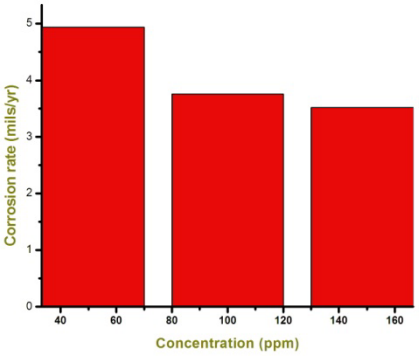

(c)

Fig. 5.3: Variation of corrosion rate Vs concentration of inhibitor

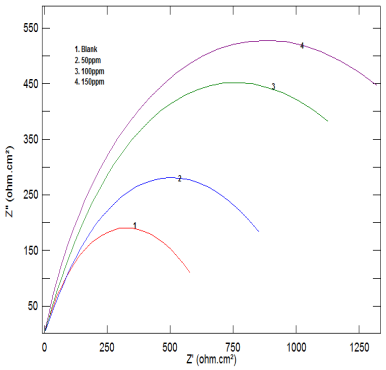

(a)

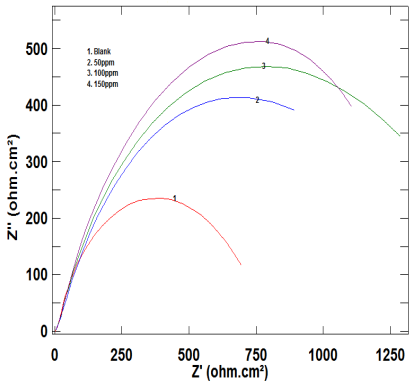

(b)

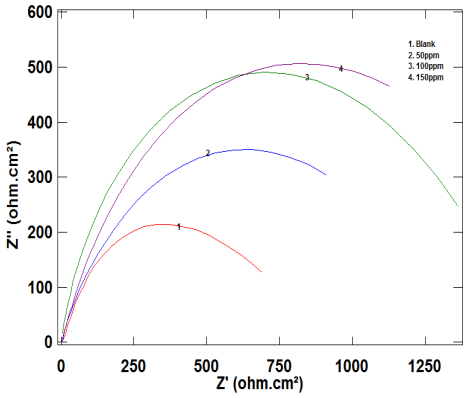

(c)

Fig.5.4 Nyquist plots of copper in 1M HCl in the absence and presence of different concentrations of HDMMA at 303K, 308K & 313K respectively.

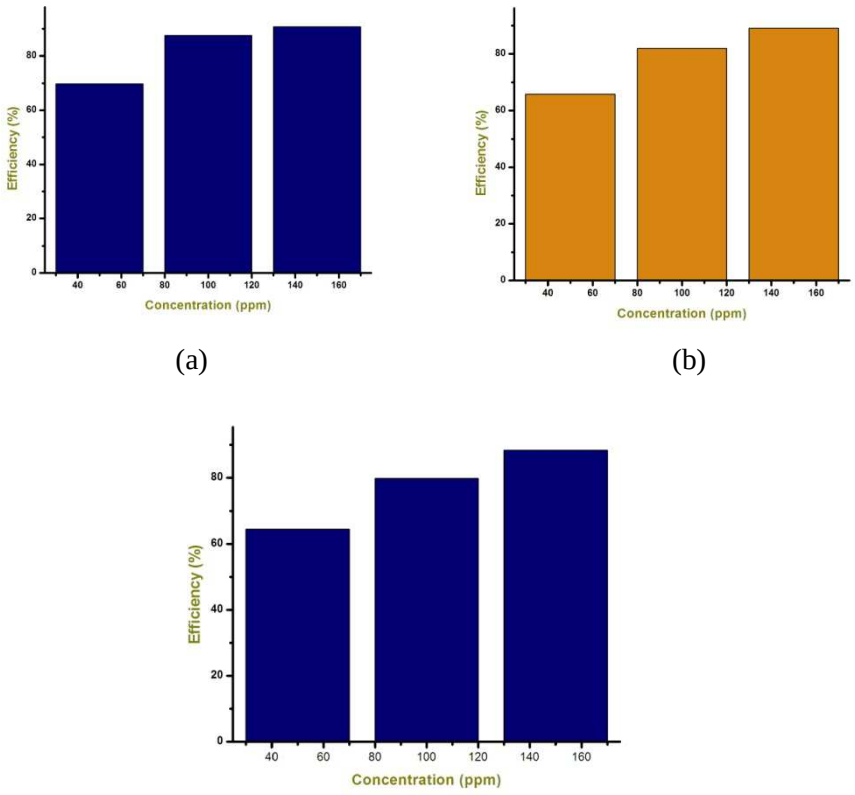

Fig. 5.5: Variation of inhibition efficiency vs concentration of the inhibitor at (a) 303K (b) 308K (c) 313K.

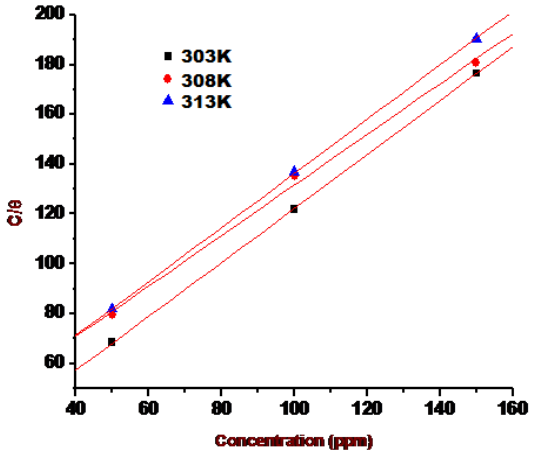

Fig .5.6: Langmuir adsorption isotherm for copper in 1M HCl different concentrations of HDMMA at 303K, 308K &313K respectively.

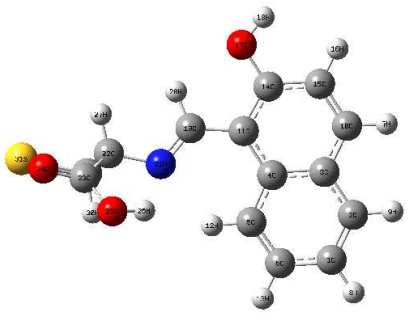

Fig.5.7: Optimized geometry of inhibitor HDMMA

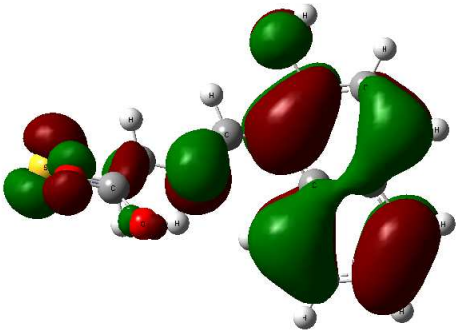

(a) HOMO

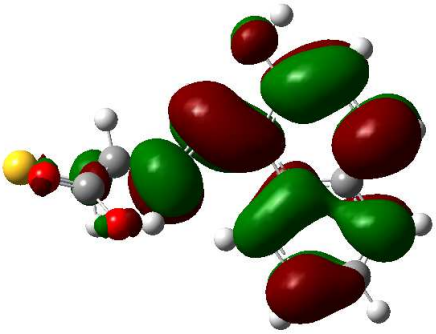

(b) LUMO

Fig.5. 8. HOMO and LUMO of the inhibitor HDMMA

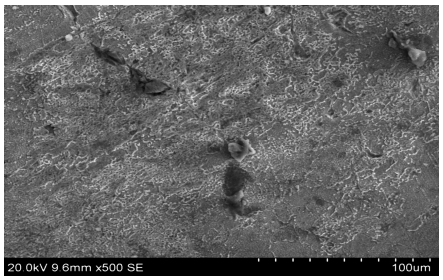

(a)

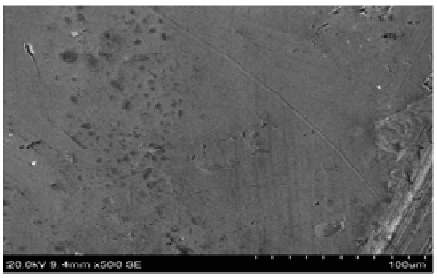

(b)

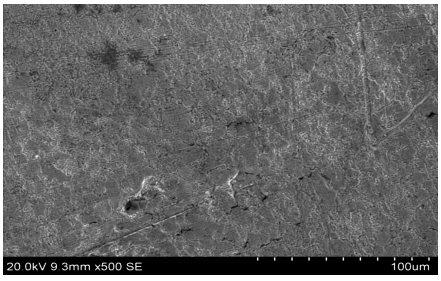

(c)

Fig.5.9. SEM images of (a) copper (b) copper in 1M HCl without inhibitor (c) copper in the presence of 150 ppm of HDMMA after 24 hour.

Chapter

6

ELECTROCHEMICAL STUDIES ON THE INTERACTION AND CORROSION INHIBITION BEHAVIOUR OF CYSTEINE/ALANINE PAIR ON COPPER IN SULPHURIC ACID

Contents

6.1 Results and Discussion

6.1.1. Weight loss studies

The weight loss under different intervals of time (24, 48, 72 and 96 hours) in 1 M sulphuric acid in a combination of inhibitors cysteine and alanine (Fig. 6.1 a & b) were studied. Results revealed that the inhibition efficiency is maximum upto 24 hour. The inhibition efficiency increased with the increased concentrations of the inhibitors and the maximum efficiency of the inhibitor was found in the presence of 150ppm of cysteine and 50 ppm of alanine.

6.1.2. Electrochemical Impedance Spectroscopy (EIS)

Electrochemical impedance spectroscopy (EIS) is an efficient and a reliable technique to study the nature of organic coatings on the metal without disturbing the double layer at the metal / solution interface [83-84]. The electrochemical parameters associated to impedance spectroscopy using the combination of inhibitors cysteine and alanine at 303K, 308K and 313K in sulphuric acid are presented in Table 6.1. Results indicated that I_{corr} value showed decreasing trend with increased concentration of the inhibitors in all temperature regimes taken for study. Nyquist plots of copper in 1M H_2SO_4 at 303K, 308K and 313K at various concentrations of inhibitor after 30 minutes of immersion are presented in Fig 6.2. It is evidenced that as the concentration of the inhibitor increases, inhibition efficiency also increases and reaches to maximum at a combination of cysteine 150ppm and alanine 50ppm and this trend was not observed with increase in temperature regimes. The variation of inhibition efficiency at 303K, 308K & 313K is given in Fig. 6.3. Corrosion is mainly controlled by a charge transfer process and is represented by a circuit fit called Randle's circuit which consists of a solution resistance, R_s in series to a parallel combination of resistor, R_{ct} and a double layer capacitor, C_{dl}. R_{ct} representing the charge transfer resistance and C_{dl} representing the electrode capacitance. It may be noted from Nyquist plots that R_{ct} values increased with inhibitor concentration, which can be attributed to the formation of a protective layer at the metal surface and this layer acts as a barrier for the mass and the charge transfer. The increase in the R_{ct} value with the increase in concentration of the

inhibitor is observed in all temperature regimes and the plot of R_{ct} Vs concentration of the inhibitor in 1M H_2SO_4 at 303K, 308K and 313K is depicted in Fig 6.4.

6.1.3. Potentiodynamic polarization studies

Potentiodynamic polarization behaviour of copper in 1M sulphuric acid in the absence and presence of combination of inhibitors at 303K, 308K and 313K is presented in Table 6.2. Results indicated that the electrochemical parameters vary with the concentration of inhibitor and temperature gradients. Tafel polarization curves for copper in 1M H_2SO_4 in the absence and presence of different concentrations of inhibitor at 303K, 308K and 313K are presented in Fig. 6.5. Inhibitors are classified into cathodic or anodic type when the displacement in corrosion potential is more than 85 mV with respect to corrosion potential of the blank. In the presence of the inhibitors, cysteine, alanine separately and in a combination of these two, the change in corrosion potential was found to be less than 85 mV. Thus it can be concluded that the combination acts as mixed type inhibitor.

6.1.4. Adsorption studies

The adsorption isotherm provides information pertaining to interaction of inhibitor with metal surface [87-88]. Adsorption behaviour of inhibitors for corrosion of copper is presented in Table 6.3. Results revealed that the extent of corrosion inhibition varies with inhibitor concentration under varied temperature conditions in sulphuric acid. The surface coverage values (θ) obtained from electrochemical measurements were used in adsorption isotherm.

Using these data different isotherms has been constructed to find out the most suitable one. The plot C/ θ Vs C gives a straight line, shows that the adsorption of the inhibitor on copper surface obeys Langmuir adsorption isotherm and is shown in Fig 6.6. The values of K_{ads} and ΔG^{0}_{ads} are given in the Table 6.3. The negative value of ΔG^{0}_{ads} ensures the spontaneity of adsorption process and stability of the adsorbed layer on the metal surface. Generally the value of ΔG^{0}_{ads} around -20kJ mol^{-1} or lower are consistent with physisorption, while those around -40kJmol^{-1} or higher value involve chemisorption [89]. Based on the calculated ΔG^{0}_{ads} values, it could be concluded that the adsorption process mainly involve physisorption.

6.1.5 Computational studies

Computational studies indicate that various quantum chemical parameters like energy of highest occupied molecular orbital (E_{HOMO}), energy of the lowest unoccupied molecular orbital (E_{LUMO}), energy gap (ΔE) i.e. E_{LUMO}-E_{HOMO}, ionization potential, I -E_{HOMO}, electron affinity, A–E_{LUMO}, electro negativity, χ (I+A)/2 and hardness, η (I-A)/2 were calculated and the geometry of the molecule optimized using Gaussian 09 program package. The number of transferred electrons (ΔN) was also calculated depending up on the quantum chemical method as in the following equation,

$$\Delta N = \frac{\chi_{Cu} - \chi_{inh}}{2\,(\eta_{Cu} + \eta_{inh})}$$

Where χ_{Cu} and χ_{inh} denote the absolute electro negativity of copper and the inhibitor molecules respectively. η_{Cu} and η_{inh} denotes the absolute hardness of copper and the inhibitor molecules respectively. The calculated values of quantum chemical parameters are recorded in Table 6.4 and presented the optimized geometry of the inhibitor in Fig. 6.7, HOMO and LUMO of the inhibitors in Fig. 6.8. It is evident that in the combined form of inhibitor molecules, the HOMO is mainly distributed on the alanine and LUMO is mainly distributed on the cysteine. This indicates that electrons are transferred from the orbitals of alanine to the metal and electrons in the occupied orbitals of metal are transferred to the LUMO of the cysteine molecule. It is generally believed that the efficiency of inhibitors increase with decrease in energy gap, ΔE, and increase in E_{HOMO} and decrease in E_{LUMO}. Higher E_{HOMO} value enhances the adsorption of inhibitor and thereby increasing the inhibition efficiency. Smaller the E_{LUMO} value greater will be the probability of molecules to accept electrons. Higher the ionization energy, easier will be the removal of electrons from the molecule. The $E_{HOMO,}$ $E_{LUMO,}$ energy gap, ΔE value are schematically represented in Fig 6.9. On comparison of cysteine with alanine, cysteine has relatively high ionization potential and electron affinity than alanine and this findings support that cysteine is a more efficient inhibitor than alanine. For cysteine alanine cluster the HOMO –LUMO gap (HLG) is 6.15 ev which is due to the stabilization of LUMO compared to cysteine and alanine and this attributes to the high efficiency of the inhibitors in the combined form which is in accordance with the electrochemical studies. The local reactivity of inhibitors can be analyzed by means of the condensed Fukui function.

The condensed Fukui functions and condensed local softness indices allow us to distinguish each part of the molecule on the basis of its distinct chemical behaviour due to the different substituent functional groups. Thus, the site for nucleophilic attack will be the place where the value of $\int^{+}$ is a maximum. In turn, the sight for electrophilic attack is controlled by the value of $\int^{-}$. The values of the Fukui functions for nucleophilic and electrophilic attack in the combined form are given in Table 6.5. From the table, it is clear that the most reactive site for the electrophilic attack are C (3) in cysteine and C (6) in alanine and C(3) in cysteine + alanine system. Similarly, the sites for nucleophilic attack are the S (9) in cysteine and N (1) in alanine and N (15) in cysteine + alanine system.

6.1.6. Synergism

Synergism is an important phenomenon in corrosion inhibition process and it serves as a base for many corrosion inhibition processes. Synergism parameter S_θ is calculated to study the synergic interaction between cysteine and alanine by the following equation [32]

$$S_\theta = \frac{1-\theta_1-\theta_2+(\theta_1\,\theta_2)}{1-\theta_{1+2}}$$

where θ_1 and θ_2 are the surface coverage of the individual inhibitors and θ_{1+2} is the surface coverage of the inhibitor in the cluster form. Synergism parameter S_θ approaches one when there is no interaction exists between the inhibitor molecules and $S_\theta > 1$ indicates a synergistic effect. In the case of $S_\theta < 1$, antagonistic behavior prevails

which may be attributed to competitive adsorption. Synergism parameter S_θ was calculated from electrochemical data and is given in Table 6.6. It is clear that the values of S_θ were greater than unity only at high temperature. The variation in the synergism parameter with temperature highlights the interaction between inhibitor molecules at high temperature (Fig 6.10). At low temperature, $S_\theta < 1$, imply that antagonistic behaviour of inhibitor molecules. Therefore, the increased inhibition efficiency of the inhibitor molecule is explained by co-adsorption mechanism, which may be either competitive or co-operative [33]. For competitive adsorption, the inhibitor molecules were adsorbed at different sites on the metal surface separately. This type of adsorption occurs at lower temperature. In co-operative adsorption, one of the inhibitor molecules is chemisorbed on the metal surface and another type is adsorbed on a layer of the first type.

6.1.7. Scanning electron microscopy

Scanning electron microscopy studies were carried out to understand nature of interaction of the inhibitor molecules on the metal surface. The SEM images of bare copper, copper after immersion in 1M H_2SO_4 without inhibitor and with the inhibitor were given in Fig. 6.11. SEM studies revealed that the metal surface was smooth and free from major depressions in the case of copper immersed in H_2SO_4 containing the inhibitor whereas the surface is more damaged when immersed in H_2SO_4 containing no inhibitor.

6.2. Conclusions.

1. Cysteine and alanine are effective inhibitors for the corrosion protection of copper in 1M H_2SO_4. Inhibition efficiency highly enhanced when these inhibitors are used in the combination.

2. Higher inhibition efficiency is shown by a combination of 150 ppm cysteine and 50 ppm alanine.

3. Potentiodynamic studies reveal that the inhibitor combination acts as mixed type. The adsorption of the inhibitor obeys Langmuir adsorption isotherm model.

4. Synergism was more pronounced at higher temperature. Synergism parameter explains the inhibition property of combined form of alanine and cysteine inhibitors through co-adsorption mechanism.

Table.6.1: AC impedance data on copper in 1M H_2SO_4

Temperature (K)	Inhibitor Concentration (ppm)		R_{ct} Ωcm^{-2}	C_{dl} mA/cm^{2}	IE (%)
	cysteine	alanine			
	Blank	Blank	121	3211	-----
	0	200	688	772	82.4
	50	150	2565	113.60	95.28
303	100	100	2725	109.70	95.55
	150	50	2745	39.18	95.59
	200	0	787	556.60	84.60
	Blank	Blank	108		-----
	0	200	274.4	1377	60.50
	50	150	1668	193.3	93.50
308	100	100	1793	145.4	93.90
	150	50	2146	35.06	94.90
	200	0	396	614.20	72.70
	Blank	Blank	54.50	494.8	-----
	0	200	123.6	590	56.09
	50	150	776	157.3	92.70
313	100	100	893	148.20	93.72
	150	50	903	57.39	93.79
	200	0	150	406.50	64.00

Table 6. 2: Data on Electrochemical parameters of copper obtained from polarisation curves in 1M H_2SO_4

Temperature (K)	Inhibitor Concentration (ppm)		E_{corr} Ωcm^{-2}	i_{corr} $mAcm^{-2}$	IE (%)
	cysteine	alanine			
	Blank	Blank	-46.33	0.0187	-----
	0	200	-46.15	0.0029	84.50
	50	150	-55.70	0.0021	88.77
303	100	100	-70.06	0.0019	89.57
	150	50	-59.42	0.0017	91.00
	200	0	-54.85	0.0027	85.50
	Blank	Blank	-47.17	0.0216	----
	0	200	-54.68	0.0041	81.01
	50	150	-100.18	0.0030	86.11
308	100	100	-59.42	0.0025	88.42
	150	50	-123.12	0.0020	90.60
	200	0	-79.33	0.0034	84.25
	Blank	Blank	-39.14	0.0229	----
	0	200	-52.96	0.0054	76.41
	50	150	-78.42	0.0034	85.15
313	100	100	-110.59	0.0027	88.20
	150	50	-110.29	0.0025	89.08
	200	0	-72.67	0.0048	79.03

Table 6.3: Adsorption parameters for corrosion of copper at various temperatures in acid medium.

Inhibitors	cysteine (ppm)	alanine (ppm)	Temperature					
			303K		308K		313K	
			K	$-\Delta G^0_{ads}$ (kJ mol^{-1})	K	$-\Delta G^0_{ads}$ (kJ mol^{-1})	K	$-\Delta G^0_{ads}$ (kJ mol^{-1})
Cysteine + Alanine	200	0	5512	-14.420	17851	-11.99	18585	-12.06
	50	150	18093	-17.39	15099	-17.23	16443	-17.74
	100	100	20209	-17.693	16159	-17.41	19956	-18.24
	150	50	20641	-17.74	19533	-17.89	33601	-19.60

Table 6.4: Calculated quantum chemical properties for Inhibitor

Inhibitor	E_{HOMO} (eV)	E_{LUMO} (eV)	ΔE (eV)	I (eV)	A (eV)	χ (eV)	η (eV)	ΔN
cysteine	-6.58	-0.30	6.28	6.58	0.30	3.44	3.14	0.547
alanine	-6.47	-0.17	6.30	6.47	0.17	3.32	3.15	0.526
cysteine + alanine	-6.57	-0.42	6.15	6.57	0.42	3.49	3.07	0.567

Table 6. 5: Fukui functions for cations and anions for cysteine, cysteine + alanine

cysteine			alanine			cysteine + alanine		
Atom	f^-	f^+	Atom	f^-	f^+	Atom	f^-	f^+
N1	-0.01376	0.27109	N1	-0.00839	0.49276	N1	0.01334	0.16292
H2	-0.01842	0.03416	H2	-0.01735	0.04368	H2	0.01188	0.02216
C3	0.01789	-0.02514	C3	0.02213	-0.04326	C3	-0.01322	-0.01667
H4	-0.05255	0.04575	H4	-0.07479	0.06816	H4	0.03761	0.02861
C5	-0.03906	-0.03442	C5	0.00497	0.01759	C5	0.02049	-0.02314
C6	-0.20581	-0.011	C6	-0.35463	-0.01283	C6	0.1517	-0.00496
H7	-0.0402	0.04661	H7	-0.03047	0.03686	H7	0.02386	0.02842
H8	-0.0333	0.05495	H8	-0.02919	0.0662	H8	0.01969	0.03257
S9	-0.28377	0.4051	H9	-0.11013	0.04214	S9	0.18527	0.25617
O10	-0.14438	0.0973	O10	-81972.4	0.1356	O10	0.08361	0.02938
H11	-0.0654	0.02121	H11	-0.0452	0.061	H11	0.03849	0.01402
O12	-0.05389	0.03319	O12	-0.08436	0.05233	O12	0.05506	0.02032
H13	-0.04523	0.03443	H13	-0.05905	0.03979	H13	0.00897	0.007
						H14	0.02036	0.0185
						N15	0.00277	0.24581
						H16	0.00512	0.02382
						C17	-0.00986	-0.02523
						H18	0.02835	0.03322
						C19	-0.00392	0.0054
						C20	0.13575	-0.00493
						H21	0.00985	0.01634
						H22	0.00912	0.0304
						H23	0.03811	0.02226
						O24	0.05803	0.01507
						H25	0.02442	0.03232
						O26	0.04821	0.02031
						H27	0.00231	0.00454

Table 6 .6: Values of synergism parameter.

Inhibitor	cysteine (ppm)	alanine (ppm)	synergism parameter S_θ		
			303K	308K	313K
cysteine + alanine	50	150	0.567	1.72	1.98
	100	100	0.602	1.83	2.51
	150	50	0.614	2.19	2.55

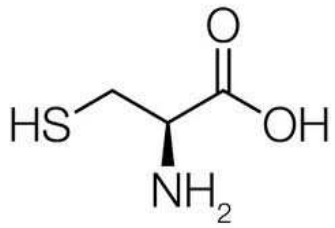

(a)

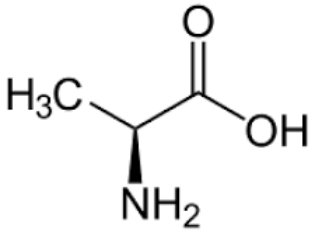

(b)

Fig. 6.1: Structure of the inhibitor molecules (a) cysteine (b) alanine

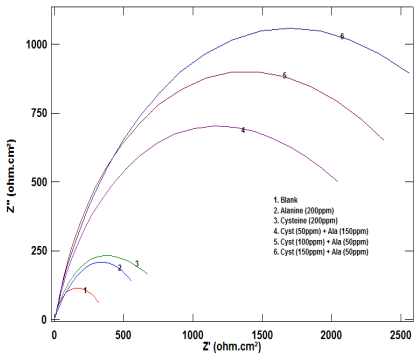

(a)

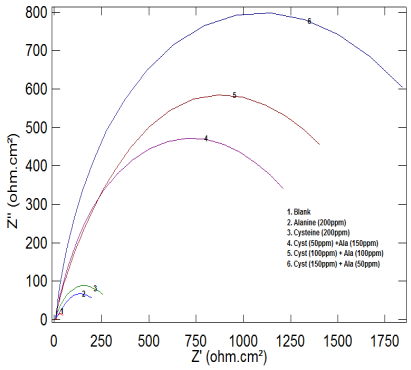

(b)

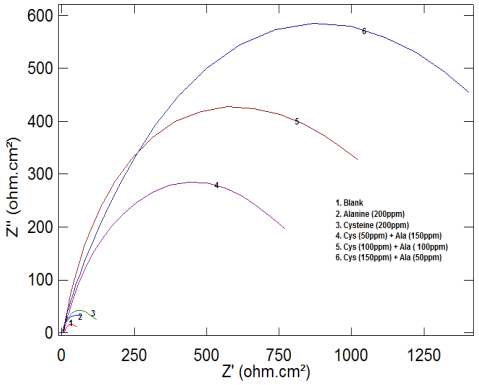

(c)

Fig. 6.2: Nyquist plots of copper in 1 M H_2SO_4 in the absence and presence of different concentrations of cysteine and alanine at 303K,308K and313K.

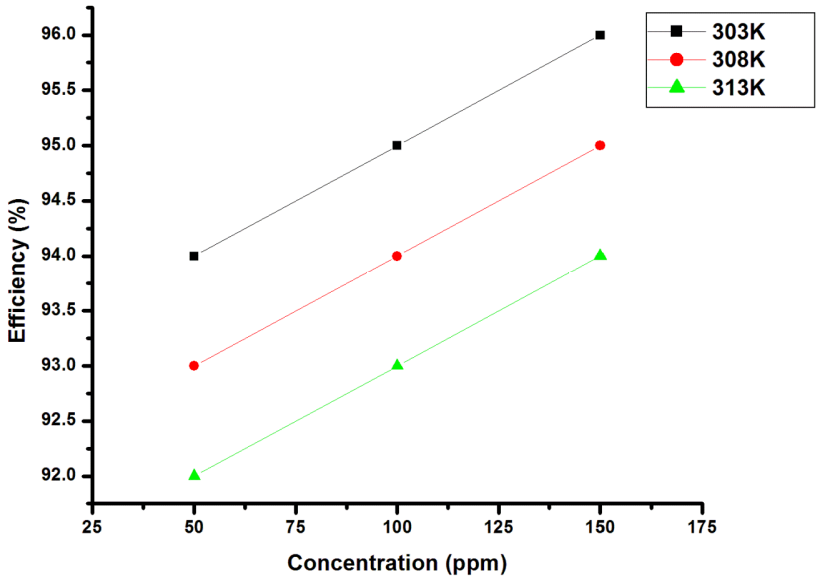

Fig. 6.3: Plot of variation in inhibition efficiency with increase in temperature a)303K b) 308K c)313K

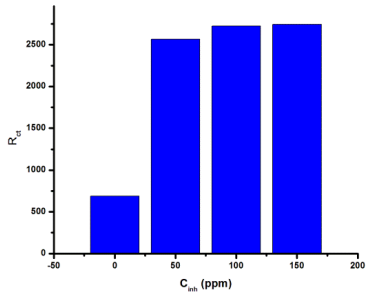

(a)

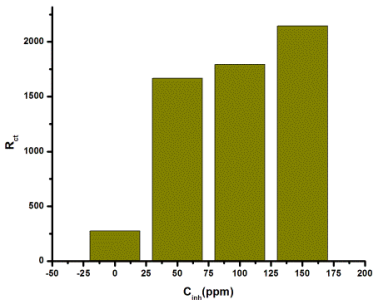

(b)

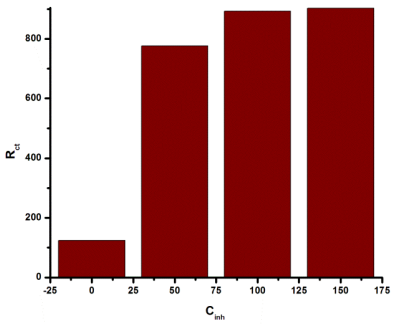

(c)

Fig.6.4: Plot of R_{ct} vs concentration of the inhibitor in 1M concentration of the acid at (a) 303K (b)308K (c) 313K .

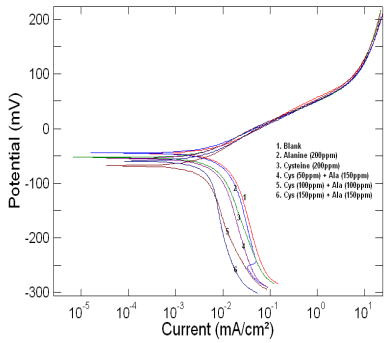

(a)

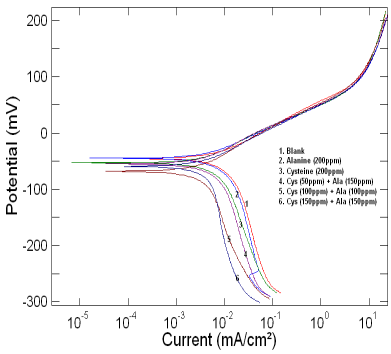

(b)

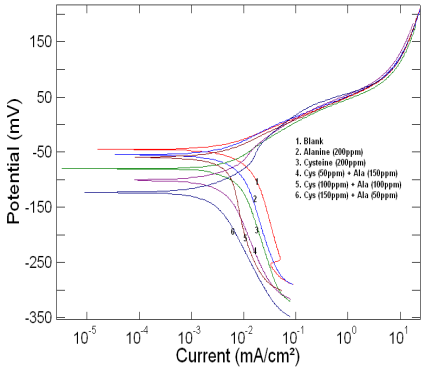

(c)

Fig. 6.5: Polarization curve of copper in 1 M H_2SO_4 in the absence and presence of different concentrations of inhibitor cysteine and alanine at (a) 303 K (b) 308K (c) 313K

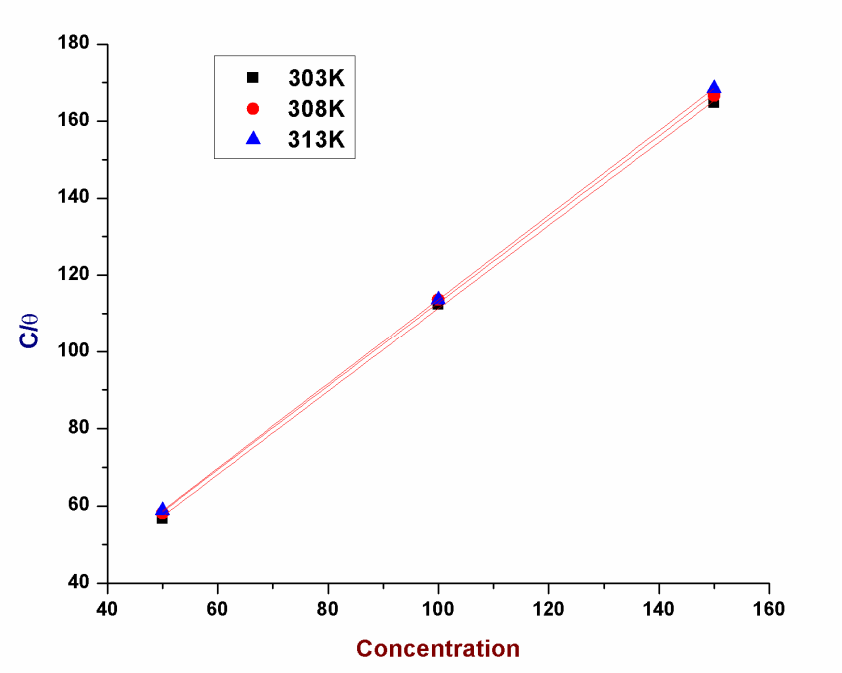

Fig. 6.6: Langmuir adsorption isotherm for copper in 1M H_2SO_4 at 303K, 308K and 313K

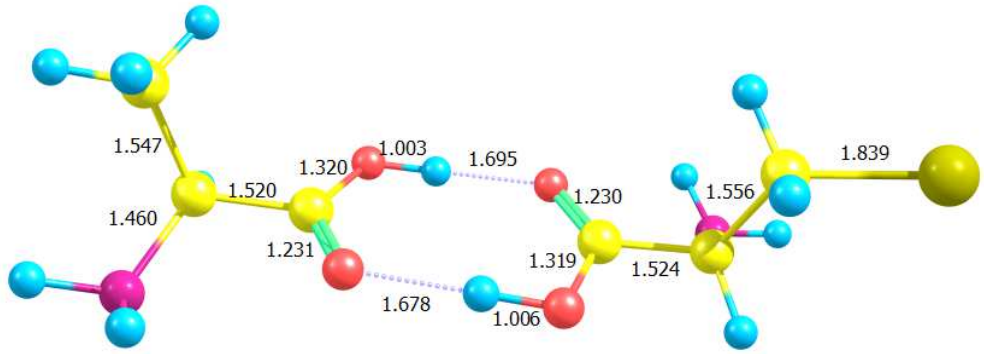

Fig. 6.7: Optimized geometry of cysteine – alanine Cluster.

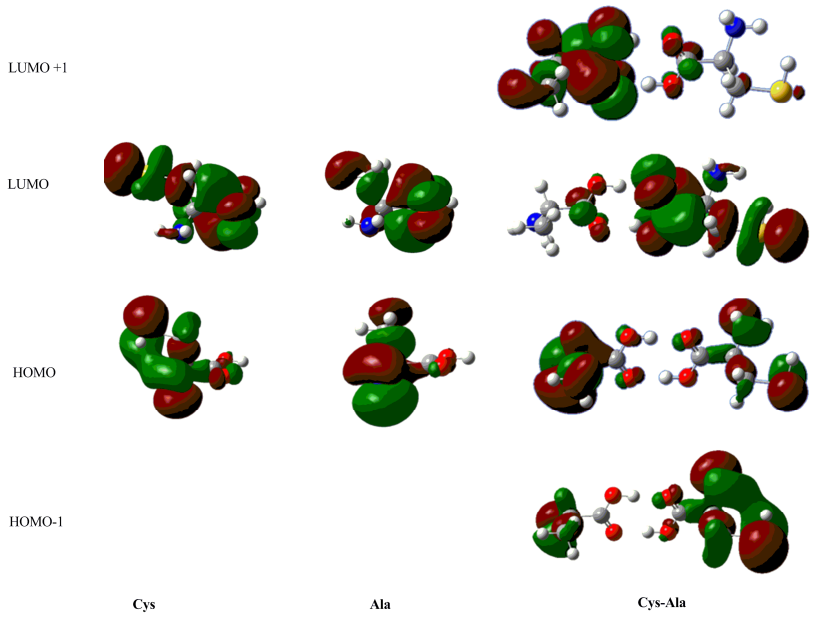

Fig. 6.8: HOMO and LUMO of cysteine, alanine and cysteine – alanine cluster.

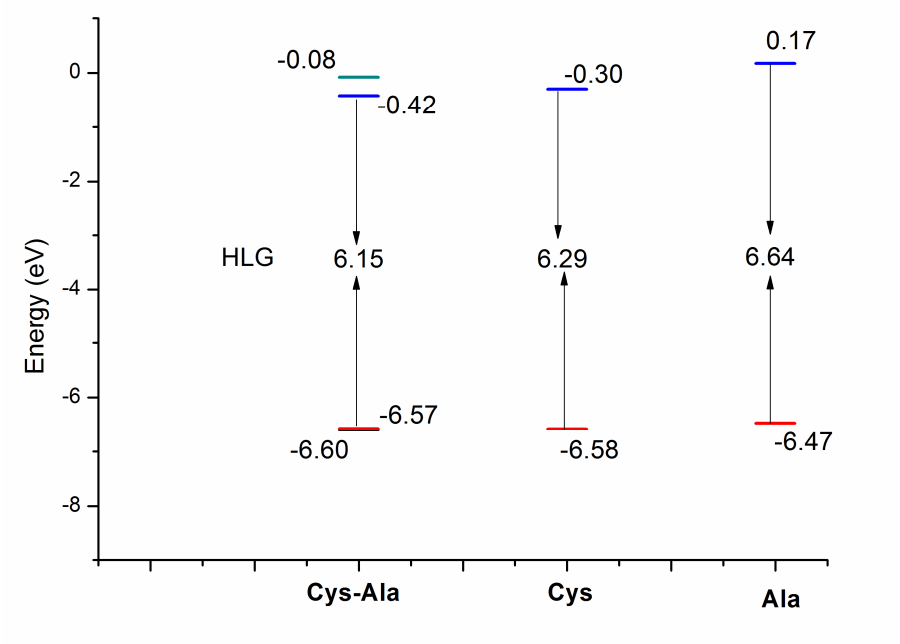

Fig. 6.9: Schematic representation of $E_{HOMO,}$ $E_{LUMO,}$ and energy gap, ΔE.

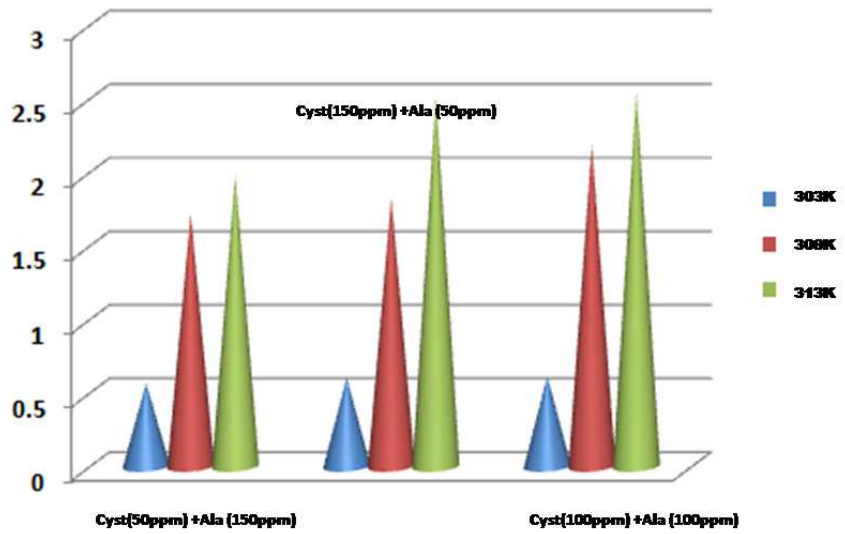

Fig. 6.10: The variation in the synergism parameter with temperature

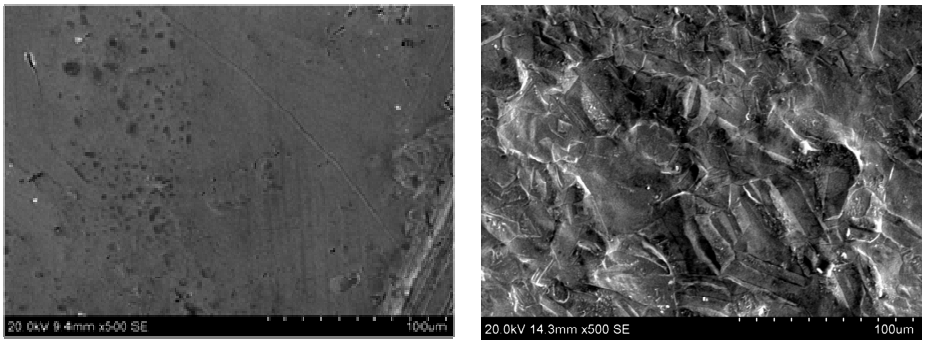

(a) (b)

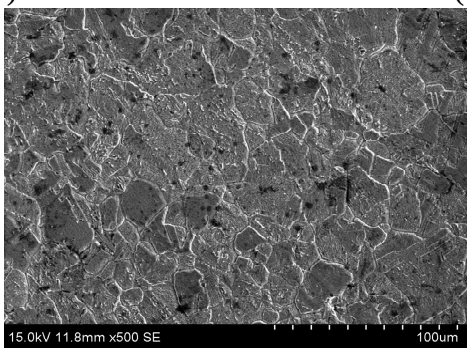

(c)

Fig. 6.11: SEM images of (a) copper (b) copper in 1M H_2SO_4 without inhibitor (c) copper in the presence of inhibitor after 24 Hour

Chapter

7 ELECTROCHEMICAL STUDIES ON THE INTERACTION AND CORROSION INHIBITION BEHAVIOUR OF MOAB, A VALINE BASED SCHIFF BASE, WITH COPPER IN SULPHURIC ACID

Contents

7.1 Results and Discussion

7.1.1. Weight loss studies

Weight loss under different intervals of time (24, 48, 72 and 96 hours) in 1.0 M sulphuric acid at different concentrations of MOAB (Fig.7.1) was studied. Results revealed that the inhibition efficiency is high at 24 hour. The inhibition efficiency increased with the increased concentrations of the inhibitor. With the advancement of time interval, inhibition efficiency decreased irrespective of the inhibitor concentrations.

7.1.2 Potentiodynamic polarization studies

Polarization measurements have been carried out to gather information concerning the kinetics of anodic and cathodic reactions. The values of electrochemical kinetic parameter, corrosion potential (E_{corr}), corrosion

current density (i_{corr}) and tafel slopes (β_a and β_c) determined from these experiments by extrapolation method are listed in Table.7.1. Results indicated that the electrochemical parameters vary with the inhibitor and acid concentrations. Tafel polarization curves for copper in 1M sulphuric acid in the absence and presence of various concentrations of MOAB at 303K, 308K and 313K are presented in Fig.7.2. The inhibitor molecule first adsorbs on the copper surface and then blocks available reaction sites. The formation of surface inhibitor film on the metal surface provides considerable protection to copper against corrosion. This film reduces the active surface area exposed to the corrosive medium and delays the hydrogen evolution and copper dissolution. The polarization results show that increasing the inhibitor concentration reduces both the cathodic and the anodic current, and there is no definite trend in the shift of E_{corr} values. The displacement in E_{corr} between in the absence and presence of the inhibitors, were less than 85 mV. Therefore, the inhibitor was defined as mixed type. It was found that with the increase in concentration of inhibitor, the values of electrochemical parameters like I_{corr} and corrosion rate declined. The mechanism of corrosion inhibition involves the blocking of reaction sites by the inhibitor due to its adsorption on the metal surfaces and the surface adsorption increases with increase in the concentration of inhibitor [90-91].

7.1.3. Electrochemical impedance spectroscopy (EIS)

Electrochemical Impedance Spectroscopy (EIS) is an efficient technique to study organic coatings on the metal as this technique does not disturb the double layer at the metal / solution interface and thus

provides highly reliable results. The electrochemical parameters associated to impedance study at 303K were presented in Table.7.2. Results revealed that I_{corr} value showed decreasing trend with increased concentration of the inhibitor. Nyquist plots of copper in 1M sulphuric acid at 303K, 308K & 313K containing various concentrations of MOAB after 30 minutes of immersion are presented in Fig.7.3. It was found that the inhibitor concentration is associated with corrosion efficiency performance. The efficiency is found to be high at 150ppm of MOAB. It also reveals that in uninhibited solution, Nyquist plot yields a slightly depressed semi circles and it amply explains that the corrosion of the copper in the absence of inhibitor is mainly controlled by a charge transfer process [85-86]. The simplest circuit fit for these experimental data was a Randles circuit which consists of a solution resistance, R_s in series to a parallel combination of resistor, R_{ct} and a double layer capacitor, C_{dl}. R_{ct} representing the charge transfer resistance and C_{dl} representing the electrode capacitance. It may be noted from Nyquist plots that R_{ct} values increased with inhibitor concentration, which can be attributed to the formation of a protective layer at the metal surface and this layer acts as a barrier for the mass and the charge transfers. The above impedance diagrams (Nyquist) contain depressed semicircles with the centre under real axis. Such behavior are characteristic of solid electrode and often referred to frequency dispersion could be attributed to different physical phenomenon such as roughness, inhomoginities of the solid surfaces, impurities, grain boundaries, and distribution of surface active sites. In this case, the constant phase element CPE is introduced in the circuit

instead of a pure double layer capacitor to give a more accurate fit [92-94]. The impedance function of a CPE has the following equation.

$$Z_{CPE} = \mathbf{A}^{-1}(\mathbf{CW})^{-\mathbf{n}}$$

Where A is the CPE constant (in $\Omega^{-1}S^{n}cm^{-2}$), W is the sine wave modulation angular frequency (rad^{-1}), $i^2 = -1$ is the imaginary number and α, is an empirical exponent ($0 \leq n \leq 1$), which measures the deviation from whole concentration range, it can be supposed that a protective layer covers the whole surface of the electrode [95-98]. The double layer between charged metal surface and the solution is considered as an electrical double capacitor**.** The decrease in this capacity with increase in concentration of the inhibitor may be attributed to the formation of a protective film on the electrode surface [99-100**].** The thickness of this protective layer also increases with increase in inhibitor concentration as more inhibitors electrostatically adsorbed on the electrode surface, resulting in a noticeable decrease in C_{dl}. This trend is in accordance with Helmholtz model given by the equation

$$\mathbf{C_{dl}} = \frac{\Sigma\Sigma_0\mathbf{A}}{\mathbf{d}}$$

Where d is the thickness of the protective layer, Σ is the dielectric constant of the medium, Σ_0 is the vacuum permitivity and A is the surface area of the electrode.

7.1.4 Adsorption studies

The adsorption isotherm provides information pertaining to the interaction of inhibitor with metal surface [14]. Adsorption behaviour of MOAB for corrosion of copper is presented in Table7.3. Results revealed that corrosion behaviour varies with inhibitor concentrations in the acid medium. The surface coverage values (θ) for different concentrations of inhibitor in 1M sulphuric acid obtained from electrochemical measurements were used in adsorption isotherm. Using these data, different graphs have been constructed to find out the most suitable adsorption isotherm. The plot C/ θ Vs C shows a straight line, providing that the adsorption of the Schiff base MOAB on copper surface obeys Langmuir adsorption isotherm and the Langmuir adsorption isotherm for copper in 1M sulphuric acid in the absence and presence of MOAB at 303K, 308K & 313K are shown in Fig.7.4. The values of K_{ads} and ΔG^{0}_{ads} of MOAB is given in Table 7.4. The negative value of ΔG^{0}_{ads} ensures the spontaneity of adsorption process and stability of the adsorbed layer on the copper surface. Generally the value of ΔG^{0}_{ads} around -20kJ mol^{-1} or lower are consistent with physisorption, while those around -40kJmol^{-1} or higher value involve chemisorptions [15]. Based on the calculated ΔG^{0}_{ads} values, it could be derived that adsorption involved is physisorption.

7.1.5 Computational studies

Computational studies indicated that various quantum chemical parameters like energy of highest occupied molecular orbital (E_{HOMO}), energy of the lowest unoccupied molecular orbital (E_{LUMO}), energy gap

(ΔE) i.e. E_{HOMO}-E_{LUMO}, ionization potential, I which is -E_{HOMO}, electron affinity, A which is –E_{LUMO}, electro negativity, χ which is (I+A)/2 and hardness, η which is (I-A)/2 were calculated and optimized the geometry of the molecule using Gaussian 09 program package. The calculated values of quantum chemical parameters are E_{HOMO} (eV), E_{LUMO} (eV), ΔE (eV), I (eV), A (eV), χ (eV), η (eV) which are found to be -5.86, -1.32, 4.54, 5.86, 1.32, 3.59, 2.27 respectively. The optimized geometry of the inhibitor MOAB is presented in Fig.7.5. HOMO and LUMO of the inhibitor MOAB are given in Fig.7.6 .It is generally said that the efficiency of inhibitor increase with decrease in energy gap, ΔE, increase in E_{HOMO} and decrease in E_{LUMO}. Higher E_{HOMO} value enhances the adsorption of inhibitors thereby increasing the inhibition efficiency. Smaller the E_{LUMO} value greater will be the probability of molecules to accept electrons. Higher the ionization energy, easier will be the removal of electrons from the molecule.

7.1.6 Scanning Electron Microscopy

SEM studies enabled to understand the effect of inhibitor molecules on the surface of copper. The SEM images of a bare polished copper, copper after immersion in 1M sulphuric acid medium without inhibitor & with inhibitor for a period of 24 hours were given in Fig 7.7 (a), (b), (c) respectively. It also revealed that the metal surface was smooth and free from depressions in the case of copper immersed in sulphuric acid which contains the inhibitor MOAB where as the surface is damaged in the case of copper which is immersed in sulphuric acid which is kept free from the inhibitors.

7.1.7 Atomic Force microscope (AFM)

The three dimensional AFM images are shown in Fig.7.8 (a–c). It is evident from the Fig 7.8c, there is least damage on the surface of copper in the presence of MOAB. The average roughness of polished copper (Fig. 7.8 a) and copper in 1.0 M H_2SO_4 without inhibitor (Fig7.8b) was found to be 6.84nm and 84 nm, respectively. The copper surface in the free acid solution is getting cracked due to the acid attack on the surface (Figure.7.8 c). However, in the presence of 150ppm of, the average roughness was reduced to 33.72.

7.2 Conclusions.

1) MOAB shows relatively good inhibition efficiency for copper in 1M HCl.

2) The inhibition efficiency increases with increase in concentration and decreases with exposure time and temperature.

3) The adsorption of MOAB on copper follows Langmuir adsorption isotherm.

4) Polarization studies reveal that MOAB act as a mixed type inhibitor.

5) Quantum chemical parameters calculated by DFT method are in good agreement with electrochemical results.

Table 7. 1: Data on Electrochemical parameters of copper obtained from polarisation curves in 1M H_2SO_4 medium.

Temp (K)	MOAB (ppm)	E_{corr} (mV)	β_a (mV dec-1)	β_c (mV dec-1)	I_{corr} (mA cm^{-2})	CR (mils/yr)	(%IE)
	Blank	- 67.33	83.39	286.7	0.0185	16.98	-------
	50	-73.15	65.95	235.42	0.0065	5.954	66.60
303	100	-99.65	82.89	172.10	0.0041	3.822	77.70
	150	-96.21	71.65	184.88	0.0035	3.261	80.60
	Blank	-71.69	80.97	292.64	0.0209	19.160	-------
	50	-90.09	86.36	105.60	0.0083	7.664	60.00
308	100	-98.63	87.87	155.61	0.0065	5.059	67.50
	150	-98.28	76.73	217.09	0.0060	4.530	71.29
	Blank	-79.82	81.89	597.63	0.0230	20.184	------
313	50	-66.32	74.73	217.43	0.0095	9.384	58.69
	100	-73.15	69.12	631.36	0.0088	7.642	61.73
	150	-98.28	80.74	213.53	0.0080	6.805	65.21

Table.7. 2. AC impedance data on copper with MOAB schiff base in 1M H_2SO_4 at 303K, 308K & 313K.

Temp (K)	MOAB (ppm)	R_{ct} (Ω cm^2)	C_{dl} (μF cm^{-2})	I_{corr} (mA cm^{-2})	C.R (mils/yr)	(%IE)
	Blank	324	267.9	0.0705	73.73	------
	50	933.6	350.10	0.0279	25.59	65.27
303	100	1415	64.43	0.0184	16.88	77.10
	150	1815	90.95	0.0143	13.16	82.14
	Blank	321.0	264.50	0.0811	74.28	------
	50	906.0	338.7	0.0287	26.36	64
308	100	1237	52.51	0.0210	19.31	74.05
	150	1641	80.18	0.0150	14.56	80.43
	Blank	292	209.6	0.0893	81.84	------
	50	613	204.30	0.0425	38.95	52.50
313	100	834.50	292.20	0.0292	28.63	65.12
	150	909.5	295.9	0.0286	26.27	67.98

Table 7. 4. Adsorption parameters of inhibitor (MOAB) for corrosion of copper at in 1M H_2SO_4 medium at 303K,308K &313K.

Temperature (K)	ΔG^{o}_{ads} (kJ mol^{-1}) & K_{ads} x 10^4 MOAB (ppm)					
	50		100		150	
303K	16.18	11.09	16.19	11.12	16.08	10.68
308K	16.06	10.59	15.30	7.83	15.50	8.49
313K	15.95	10.13	15.17	7.42	15.33	7.91

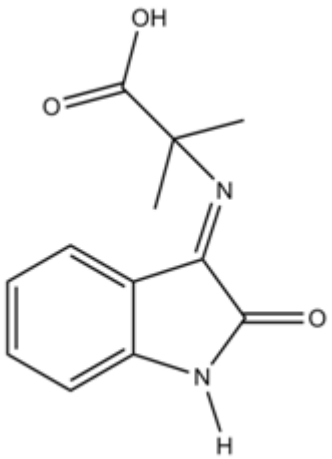

Figure. 7.1: Structure of the inhibitor

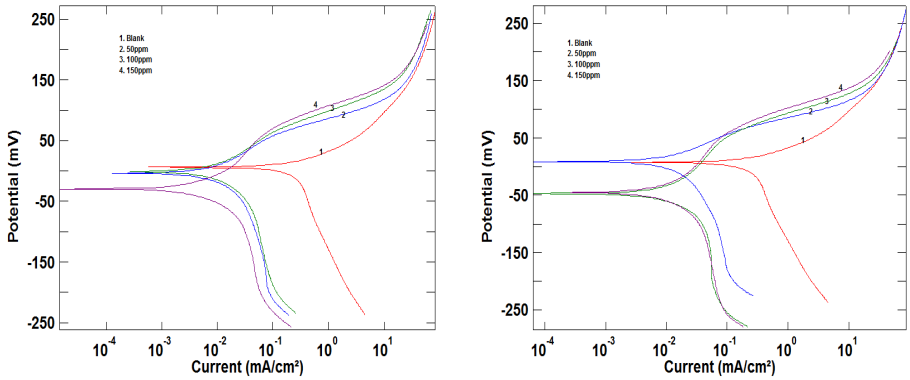

(a) (b)

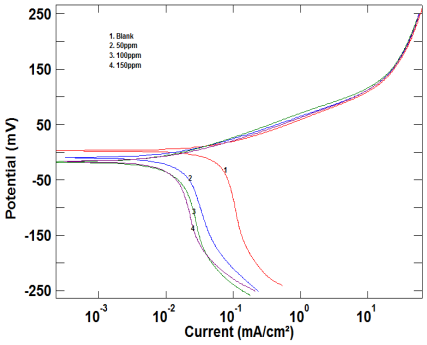

(c)

Figure 7.2: Polarization curves of copper in 1M H_2SO_4 in the absence and presence of different concentrations of MOAB at 303K, 308K &313K respectively.

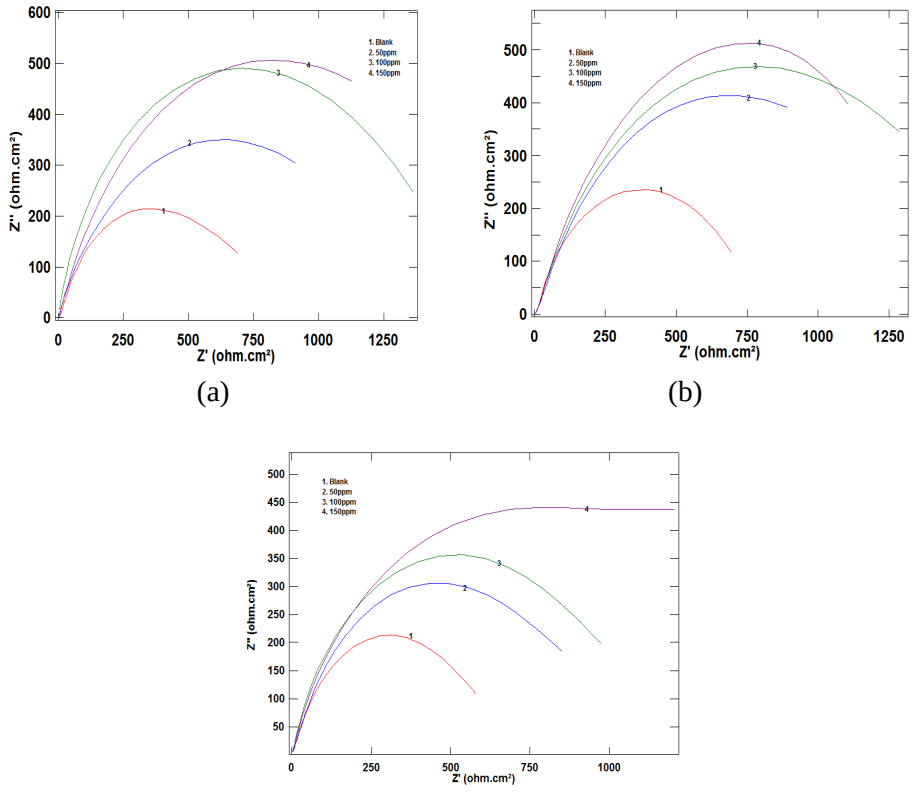

Figure. 7.3: Nyquist plots of copper in 1M H_2SO_4 in the absence and presence of different concentrations of MOAB at 303K, 308K & 313K respectively.

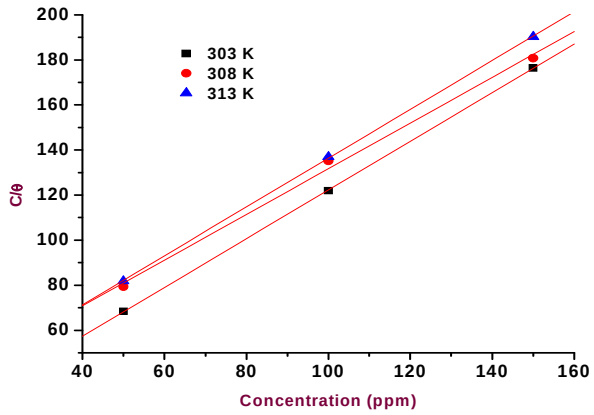

Figure 7.4: Langmuir adsorption isotherm for copper in 1M H_2SO_4 different concentrations of MOAB at 303K, 308K &313K respectively.

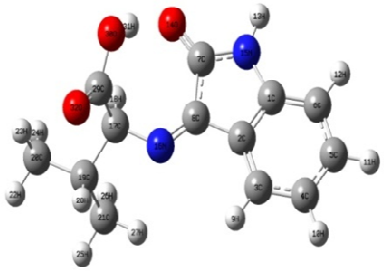

Figure. 7.5: Optimized geometry of inhibitor MOAB

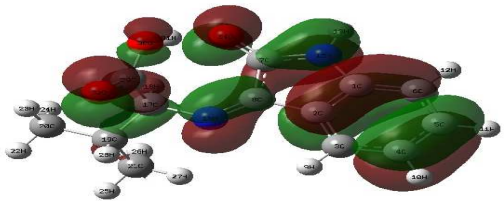

(a) HOMO

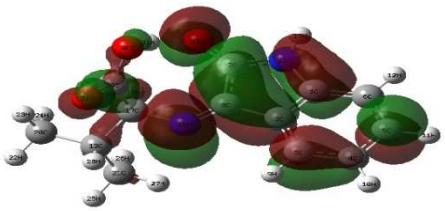

(b) LUMO

Figure. 7.6 : HOMO and LUMO of the inhibitor MOAB

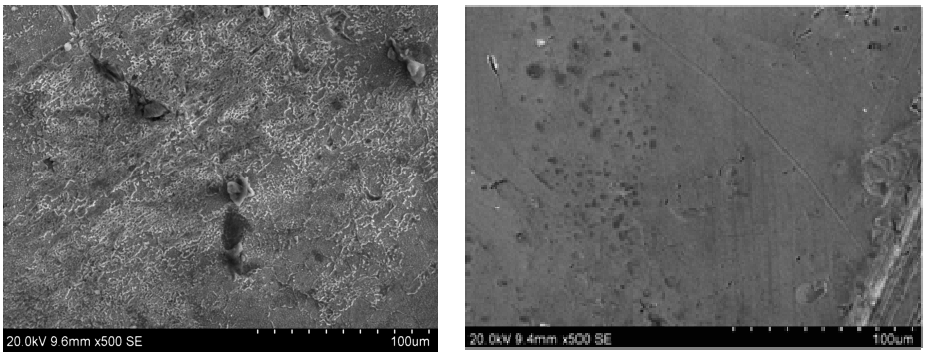

(a) (b)

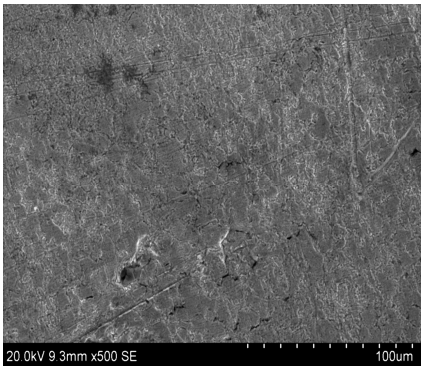

(c)

Figure 7.7: SEM images of (a) copper (b) copper in 1M H_2SO_4 without inhibitor and (c) copper in the presence of 150 ppm of MOAB after 24 Hour

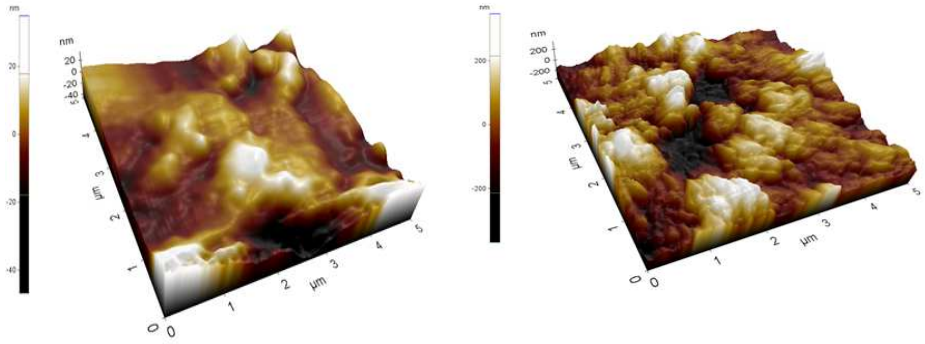

(a) (b)

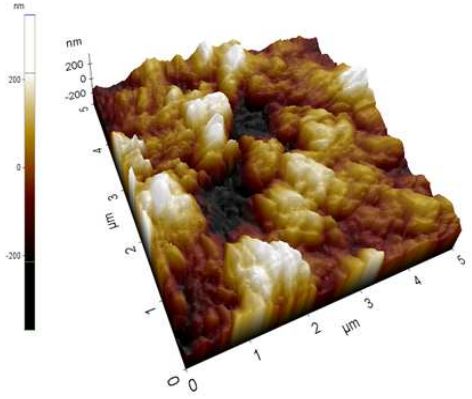

(c)

Figure 7.8: AFM images of (a) copper, (b) copper in 1M H_2SO_4without inhibitor and (c) copper in the presence of 150 ppm of MOAB after 24 hr exposure.

Chapter

8

ELECTROCHEMICAL STUDIES ON THE INTERACTION AND CORROSION INHIBITION OF SCHIFF BASE HMMB WITH MILD STEEL IN HYDROCHLORIC ACID

Contents

8.1Results and Discussion

8.1.1 Weight loss studies

Weight loss under different intervals of time (24, 48, 72 and 96 hours) in the absence and presence of inhibitor HMMB (Figure 8.1) were studied. Results revealed that the inhibition efficiency is high at 24 hour interval irrespective of concentrations of the inhibitor and subsequently the efficiency declined.

8.1.2 Potentiodynamic polarization studies

Potentiodynamic polarization behaviour of mild steel in acid medium at various concentration (0.5M, 1.0M & 1.5M) in the absence and presence of inhibitor HMMB at 303K, 308K & 313K were presented in Tables 8.1 to 8.3. Results indicated that the electrochemical parameters vary

with the inhibitor as well as acid concentration. With the variation in temperature, potentiodynamic polarization behaviour also varied. Tafel polarization curves for mild steel in 0.5M, 1M, & 1.5M HCl medium in the absence and presence of various concentration of HMMB at 303K, 308K &313K are presented in Figure 8.2 to 8.4 respectively. It reveals that both the anodic metal dissolution and cathodic hydrogen evolution would exhibit Tafel type behaviour. The results emanating from these studies revealed that HMMB can act as a mixed type inhibitor. The mechanism of corrosion inhibition involves the blocking of reaction sites by the inhibitor due to the adsorption of inhibitor molecule on the metal surfaces and the surface adsorption increases by increase in the concentration of inhibitor [81-82]. The formation of a coating on the surface of the metal as a result of adsorption of the inhibitor molecule provides a considerable protection against corrosion.

8.1.3 Electrochemical impedance spectroscopy (EIS)

The electrochemical parameters associated with impedance study using HMMB at303K, 308K, 313K were presented in Tables 8.4 to 8.6. Results revealed that I_{corr} value showed decreasing trend with increased concentration of the inhibitor in all the concentrations of the acid. The same trend was observed in all the temperature conditions. It is worth to mention that in all the varied acid concentration devoid of inhibitor, registered high values of I_{corr}. Nyquist plots of mild steel in 0.5M, 1M and 1.5MHCl solution at 303K, 308K, & 313Kcontaining various concentrations of HMMB after 30 minutes of immersion are presented in Figures.8.5 to 8.7. The efficiency is found to be high at 150ppm of inhibitor HMMB but the efficiency showed decreasing trend with the

increase of acid concentration. (Figure.8.8) .It reveals that in uninhibited solution, Nyquist plot yields a slightly depressed semi circles. This clearly explains that the corrosion of the mild steel in the absence of inhibitor is mainly controlled by a charge transfer process [85-86]. The simplest circuit fit for these experimental data was a Randles circuit which consists of a solution resistance, R_s in series to a parallel combination of resistor, R_{ct} and a double layer capacitor, C_{dl}. R_{ct} representing the charge transfer resistance and C_{dl} representing the electrode capacitance. It may be noted from Nyquist plots that R_{ct} values increased with inhibitor concentration, which can be attributed to the formation of a protective layer at the metal surface and this layer acts as a barrier for the mass and the charge transfers.

8.1.4 Adsorption studies

The adsorption isotherm provides information pertaining to the interaction of inhibitor with metal surface [87]. Adsorption behaviour of Inhibitor HMMB for corrosion of mild steel is presented in Table 8.7. A perusal of the results revealed that corrosion behaviour varies with inhibitor concentration under varied temperature in the acid medium. The surface coverage values (θ) for different concentration of inhibitor at 0.5M, 1M, and 1.5M HCl obtained from electrochemical measurements were used for the construction of adsorption isotherm. Using these data, different graphs have been constructed to find out the most suitable adsorption isotherm. The plot C/ θ Vs C shows a straight line, providing that the adsorption of the Schiff base HMMB on mild steel surface obeys Langmuir adsorption isotherm and the Langmuir adsorption isotherm for mild steel in 0.5M, 1M &1.5M HCl in the absence and presence of HMMB at 303K, is shown in Figure8.9. The

values of K_{ads} and ΔG^{0}_{ads} of inhibitor HMMB is given in Table 8.8. The negative value of ΔG^{0}_{ads} ensures the spontaneity of adsorption process and stability of the adsorbed layer on the mild steel surface. Generally the value of ΔG^{0}_{ads} around -20kJ mol^{-1} or lower are consistent with physisorption, while those around -40kJmol^{-1} or higher value involve chemisorptions [89].Based on the calculated ΔG^{0}_{ads} values, it could be derived that adsorption involved is physisorption.

8.1.5 Computational studies

Computational studies indicated that various quantum chemical parameters like energy of highest occupied molecular orbital (E_{HOMO}), energy of the lowest unoccupied molecular orbital (E_{LUMO}), energy gap (ΔE) i.e. E_{HOMO}-E_{LUMO}, ionization potential, I which is -E_{HOMO}, electron affinity, A which is –E_{LUMO}, electro negativity, χ which is (I+A)/2 and hardness, η which is (I-A)/2 were calculated and optimized the geometry of the molecule using Gaussian 09 program package.. The calculated values of quantum chemical parameters are given in the Table 8.9. The optimized geometry of the inhibitor HMMB is presented in Figure 8.10. HOMO and LUMO of the inhibitor HMMB are given in Figure 8.11.It is generally said that the efficiency of inhibitors increase with decrease in energy gap, ΔE, increase in E_{HOMO} and decrease in E_{LUMO}. Higher E_{HOMO} value enhances the adsorption of inhibitors thereby increasing the inhibition efficiency. Smaller the E_{LUMO} value greater will be the probability of molecules to accept electrons. Higher the ionization energy, easier will be the removal of electrons from the molecule.

8.1.6 Scanning Electron Microscopy

A SEM study enables to understand the effect of inhibitor molecules on the surface of mild steel. The SEM images of a bare polished mild steel, mild steel after immersion in 1M HCl medium without inhibitor & with inhibitor, for a period of 24 hours were given in Figure 8.12. It also revealed that the metal surface was smooth and free from depressions in the case of mild steel immersed in HCl which contains the inhibitor where as the surface is damaged in the case of mild steel which is immersed in HCl which is kept free from the inhibitor.

8.2. Conclusions.

Based on the electrochemical studies including EIS and polarization studies to find out the inhibitory effect of HMMB on mild steel in HCl it can be concluded that

1) HMMB is an effective inhibitor for the corrosion of mild steel in HCl. The efficiency of the inhibitor increased with inhibitor concentration and decreased with the increase in temperature. The maximum efficiency was obtained at 150ppm of the inhibitor at room temperature.

2) Based on the polarization studies it can be concluded that inhibitor behaves as a mixed type and adsorption of the inhibitor obeys Langmuir adsorption isotherm model.

3) Quantum chemical parameters calculated after the geometry optimization also support good inhibition efficiency of the inhibitor.

Table 8. 1: Data on Electrochemical parameters of mild steel obtained from polarisation curves in 0.5 M, 1 M &1.5 M HCl at 303K.

HCl	HMMB (ppm)	E_{corr} (mV)	β_a (mV dec-1)	β_c (mV dec-1)	I_{corr} (mA cm^{-2})	CR (mils/yr)	(%IE)
	Blank	-483	76.29	181.66	0.062	197.31	--------
0.5M	50	-468.9	63.11	94.26	0.031	118.3	50.00
	100	-472.14	50.62	56.68	0.024	94.141	61.29
	150	-484	29.45	46.90	0.016	59.25	74.19
	Blank	-486	85.35	120.98	0.483	220.83	-------
	50	-489.99	77.10	114.93	0.253	115.67	47
1.0 M	100	-459.81	77.10	114.93	0.197	90.22	59.21
	150	-486.86	18.25	42.68	0.126	57.67	73.90
	Blank	-463	85.95	100.13	0.562	256.48	------
1.5M	50	-452	96.48	173.43	0.309	136.76	45.81
	100	-441	95.80	114.52	0.244	111.49	57
	150	-474	45.38	65.99	0.181	83.68	67.43

Table 8.2: Data on Electrochemical parameters of mild steel obtained from polarisation curves in 0.5 M, 1 M &1.5 M HCl at 308K

HCl	HMMB (ppm)	E_{corr} (mV)	β_a (mV dec-1)	β_c (mV dec-1)	I_{corr} (mA cm^{-2})	CR (mils/yr)	(%IE)
	Blank	-446.44	104.02	129.2	0.442	197.31	--------
0.5M	50	-439.00	78.40	118.28	0.245	118.3	44.5
	100	-458.77	104.66	149.45	0.197	94.141	55.40
	150	-460.00	71.899	140.23	0.129	59.25	71
	Blank	-457.70	102.38	144.82	0.500	228.55	-------
	50	-444.48	85.08	155.57	0.294	134.46	41.20
1.0 M	100	-450.97	101.35	182.96	0.241	110.4	52
	150	-443.01	93.187	166.95	0.164	75.09	68
	Blank	-519.00	119.06	193.36	0.573	261.67	-----
1.5M	50	-465.00	106.93	175.22	0.349	159.48	40.35
	100	-456.81	102.53	172.65	0.275	125.58	52.36
	150	-439.74	90.63	187.25	0.206	94.26	64

Table 8. 3: Data on Electrochemical parameters of mild steel obtained from polarisation curves in 0.5 M, 1 M & 1.5 M HCl at 313K

HCl	HMMB (ppm)	E_{corr} (mV)	β_a (mV dec-1)	β_c (mV dec-1)	I_{corr} (mA cm^{-2})	CR (mils/yr)	(%IE)
	Blank	-439.28	89.50	93.93	0.480	219.07	------
	50	-444.62	82.43	140.22	0.283	129.33	41.66
0.5M	100	-448.00	77.70	125.25	0.243	111.17	50.00
	150	-453.00	71.54	107.28	1.90	74.95	66.66
	Blank	-443.22	63.96	76.21	0.554	253.13	------
	50	-450.53	99.86	141.78	0.332	151.61	40.00
1M	100	-456.08	104.32	180.02	0.303	138.56	45.00
	150	-461.78	84.92	166.94	0.223	102.17	60.00
	Blank	-469.80	57.38	123.31	0.705	321.8	------
1.5M	50	-513.00	54.31	62.66	0.476	217.35	32.80
	100	-502.00	47.59	67.25	0.447	204.08	37.00
	150	-509.00	3.77	51.49	82.75	152.48	52.00

Table 8.4: AC impedance data on mild steel with HMMB in 0.5 M, 1 M & 1.5 M HCl at 303K.

HCl	HMMB (ppm)	R_{ct} (Ω cm^2)	C_{dl} (μF cm^{-2})	i_{corr} (mA cm^{-2})	C.R (mils/yr)	(%IE)
	Blank	192	67	0.135	61.96	------
	50	777.5	52	0.035	15.31	75.28
	100	1301	32	0.020	9.14	85.24
0.5M	150	1553	40	0.016	7.66	88.00
	Blank	204	71	0.136	59.82	-------
	50	623	124	0.041	19.09	67.28
	100	1054	46	0.025	11.0	81.61
1M	150	1292	59	0.021	9.75	84.55
	Blank	197	205	0.132	60.58	---------
	50	584	82	0.043	20	66.00
1.5M	100	980	77	0.026	12.05	79.80
	150	1123	44	0.022	10.51	82.00

Table 8. 5: AC impedance data on mild steel with HMMB in 0.5 M, 1 M, & 1.5 M HCl at 308K.

HCl	HMMB (ppm)	R_{ct} (Ω cm^2)	C_{dl} (μF cm^{-2})	i_{corr} (mA cm^{-2})	C.R (mils/yr)	(%IE)
0.5M	Blank	205	69	0.127	57.9	--------
	50	700	46	0.037	18.0	70.71
	100	883	36	0.029	16.9	76.70
	150	1172	26	0.022	10.1	82.50
1M	Blank	152	126	0.170	78.8	------
	50	399	54	0.060	31.3	62.00
	100	543	72	0.050	23.0	72.00
	150	765	46	0.030	15.8	80.10
1.5M	Blank	149	120	0.170	79.1	------
	50	365	60	0.070	32.2	59.17
	100	493	55	0.050	24.3	70.20
	150	683	47	0.030	17.0	78.18

Table 8.6: AC impedance data on mild steel with HMMB in 0.5 M, 1 M, & 1.5 M HCl at 313K.

HCl	HMMB (ppm)	R_{ct} (Ω cm^2)	C_{dl} (μF cm^{-2})	i_{corr} (mA cm^{-2})	C.R (mils/yr)	(%IE)
0.5M	Blank	195	178	0.133	61	------
	50	575	92	0.453	20	66.0
	100	801	55	0.032	14	75.3
	150	998	41	0.258	11	80.4
1M	Blank	188	168	0.130	81	------
	50	459	40	0.050	34	59.04
	100	650	67	0.030	28	71.0
	150	845	49	0.031	18	77.75
1.5M	Blank	181	74	0.143	84	-------
	50	403	64	0.064	36	55.08
	100	612	73	0.040	30	69.49
	150	745	51	0.034	21	75.70

Table 8.7: Adsorption parameters of inhibitor (HMMB) for corrosion of mild steel at various temperatures and concentration.

HCl	Temperature (K)	ΔG^{o}_{ads} (kJ mol^{-1})& K_{ads} x 10^{4}(mol^{-1}) HMMB (ppm)					
		50		100		150	
	303	-17.44	18.32	-17.30	17.28	-19.93	49.16
0.5M	308	-17.08	14.20	-16.09	9.67	-19.04	30.51
	313	-16.88	11.84	-16.20	19.16	-19.01	26.82
	303	-16.46	12.40	-16.58	13.02	-19.09	35.21
1M	308	-16.17	9.95	-15.56	7.84	-18.21	26.82
	313	-16.09	8.73	-15.68	7.45	-18.54	22.39
	303	-16.34	11.85	-16.27	11.85	-18.74	30.71
1.5M	308	-15.83	8.73	-15.30	17.11	-13.52	23.74
	313	-15.68	7.45	-15.56	7.10	-18.40	21.19

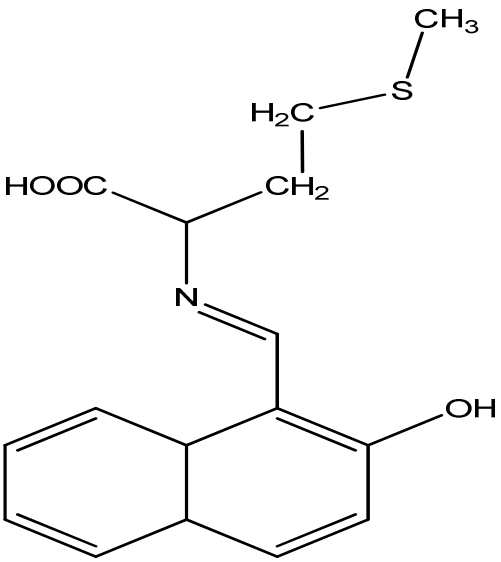

Figure 8.1: Structure of the inhibitor

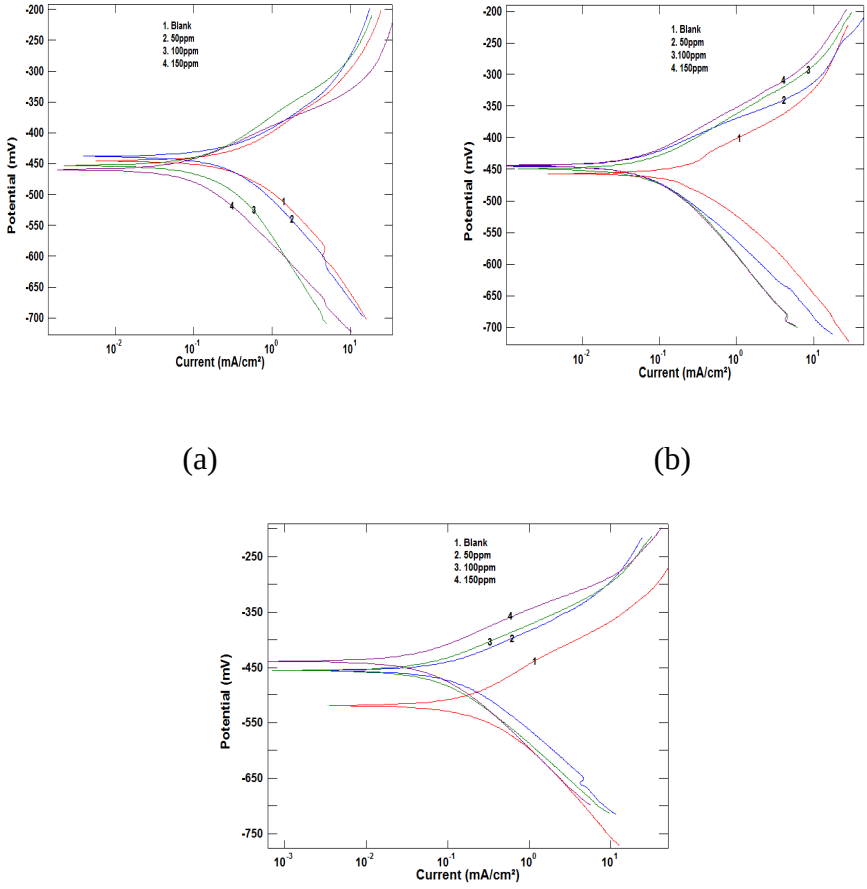

Figure 8.2: Polarization curves of mild steel in different concentrations of HCl (0.5,1.0,1.5M) and HMMB (50,100,150ppm) at 303K.

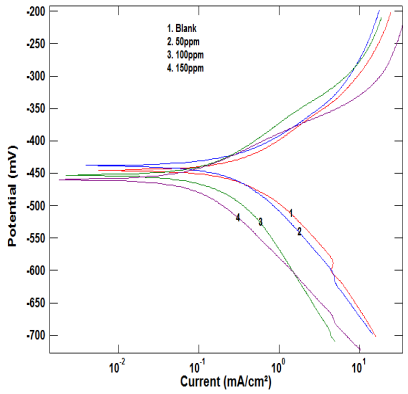

(a)

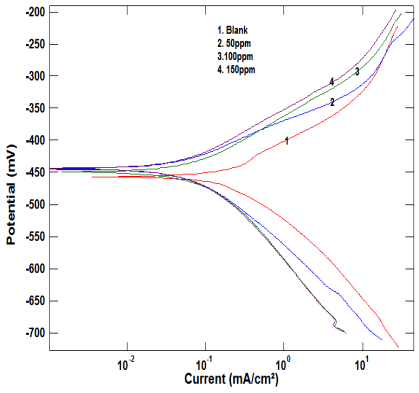

(b)

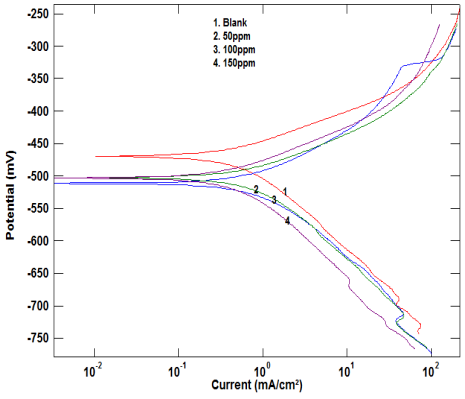

(c)

Figure 8.3: Polarization curve of mild steel in different concentrations of HCl (0.5,1.0,1.5M) and HMMB (50,100,150ppm) at 308K.

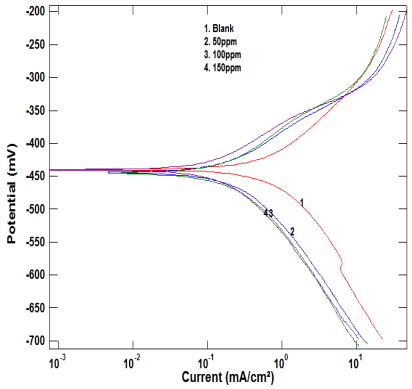

(a)

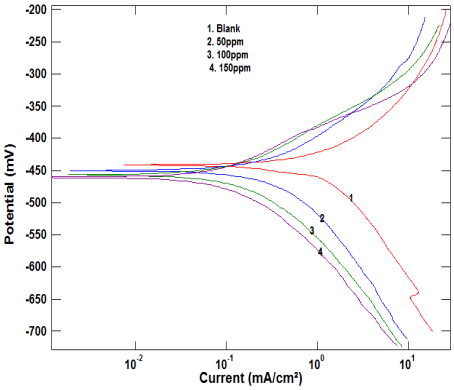

(b)

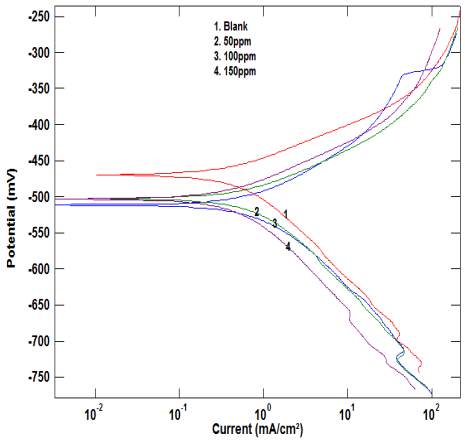

(c)

Figure 8.4: Polarization curve of mild steel in different concentrations of HCl (0.5,1.0,1.5M) and HMMB (50,100,150ppm) at 313 K.

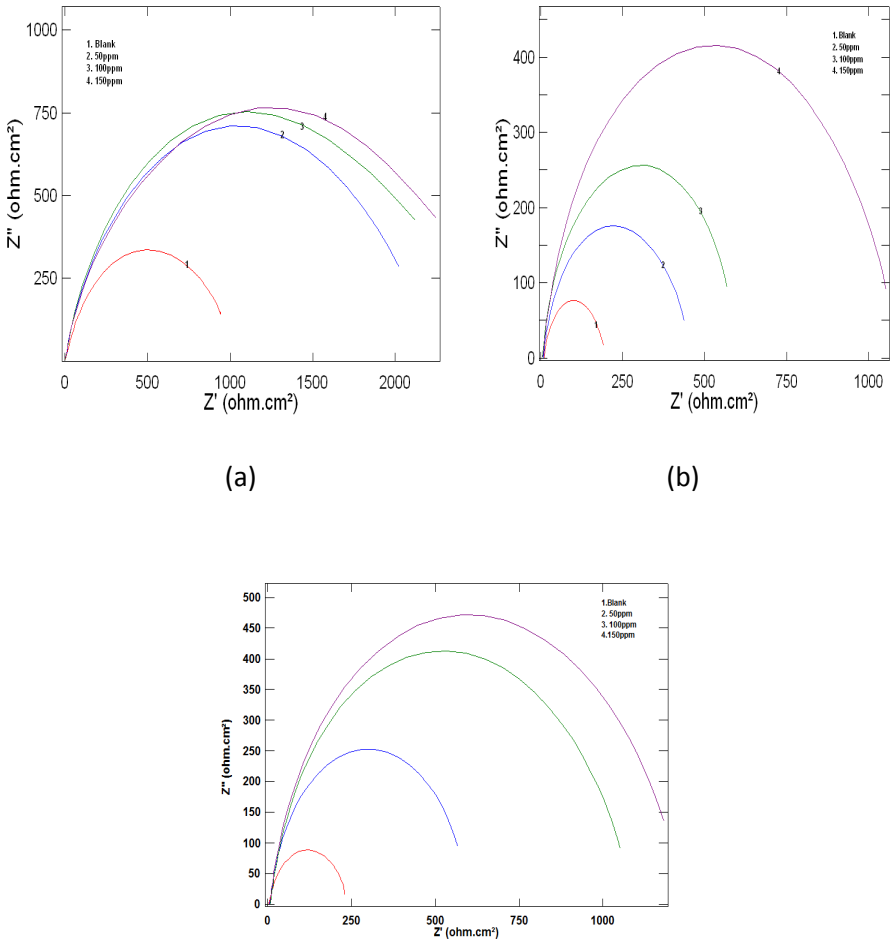

Figure 8. 5: Nyquist plots of mild steel in different concentrations of HCl (0.5,1.0,1.5M) and HMMB (50,100,150ppm) at 303K.

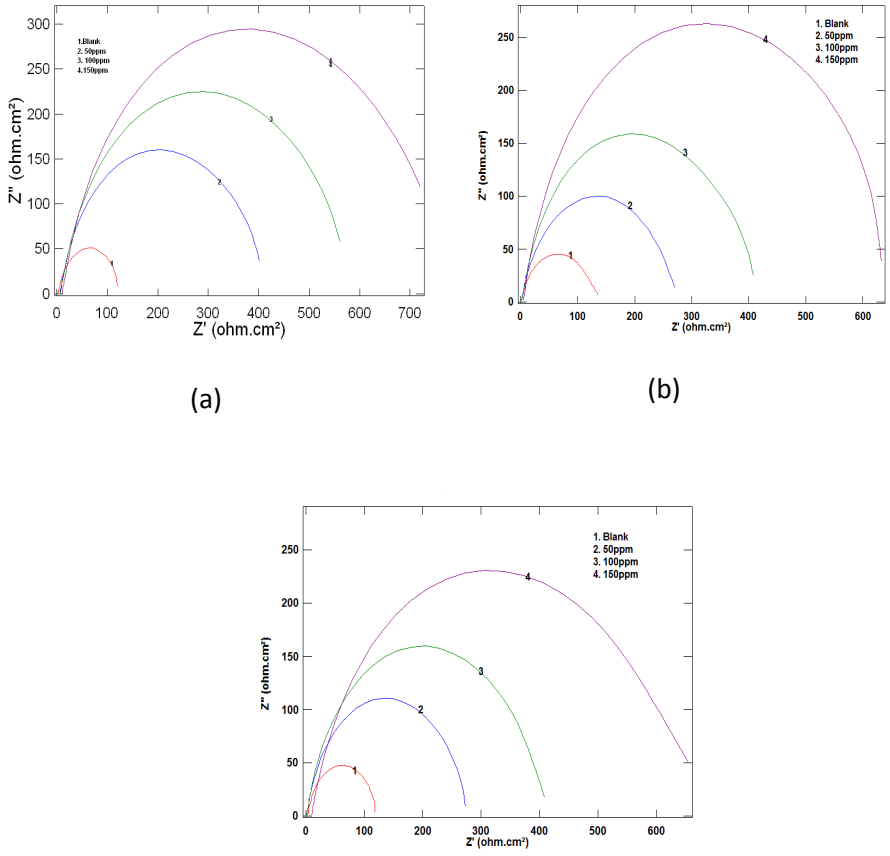

(a)

(b)

(c)

Figure 8.6: Nyquist plots of mild steel in different concentrations of HCl (0.5,1.0,1.5M) and HMMB (50,100,150ppm) at 308K.

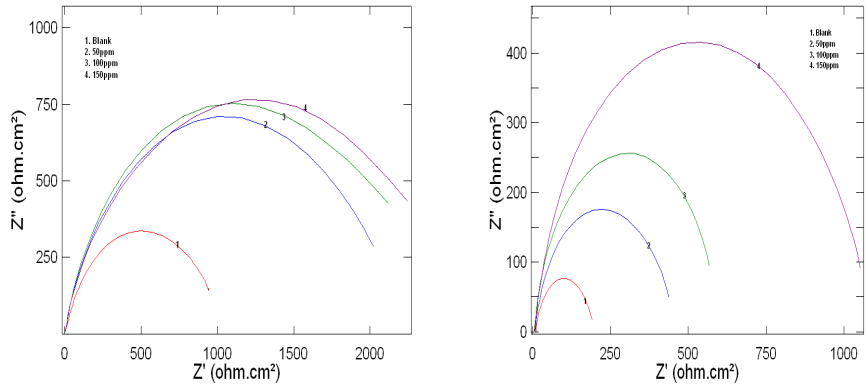

(a)

(b)

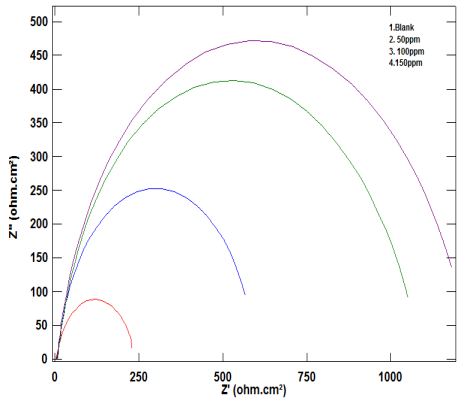

(c)

Figure 8.7: Nyquist plots of mild steel in different concentrations of HCl (0.5,1.0,1.5M) and HMMB (50,100,150ppm) at 313K.

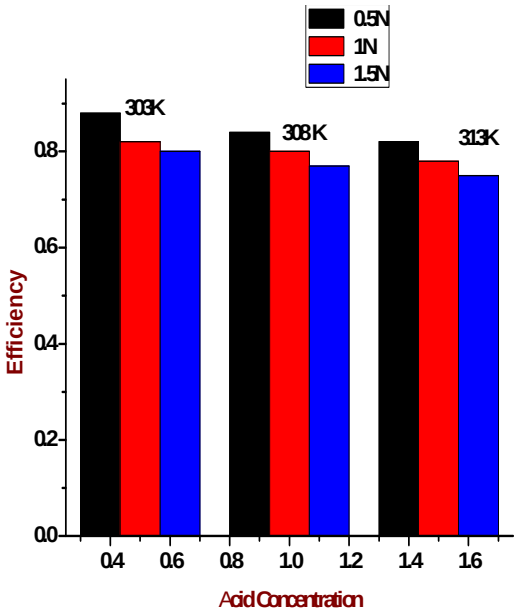

Figure 8.8 : Plot of acid concentration Vs Efficiency at 150 ppm of HMMB

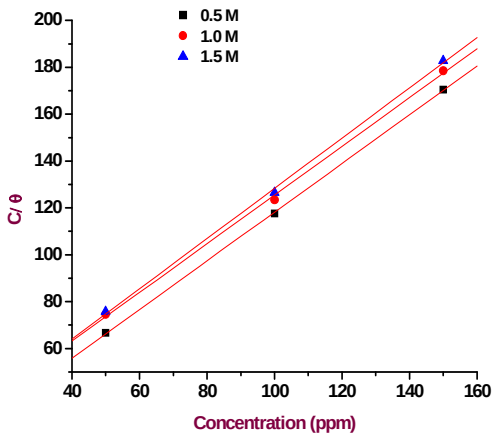

Figure 8.9: Langmuir adsorption isotherm for mild steel in 0.5M, 1M & 1.5M HCl in inhibitor HMMB at 303K.

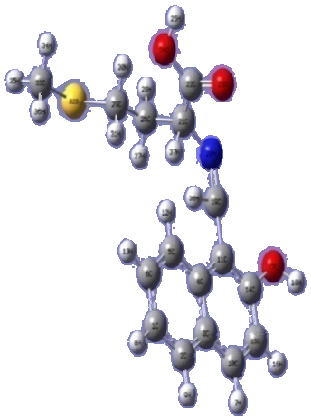

Figure 8.10: Optimized geometry of inhibitor HMMB

Figure 8.11 : HOMO and LUMO of the inhibitor HMMB

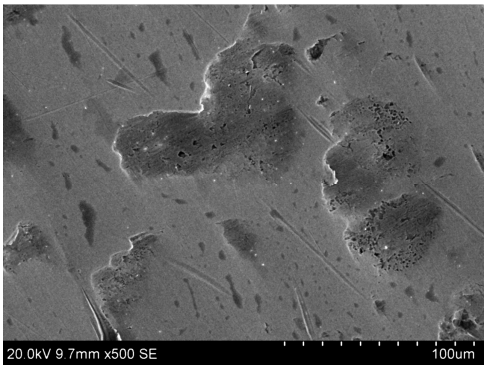

(a)

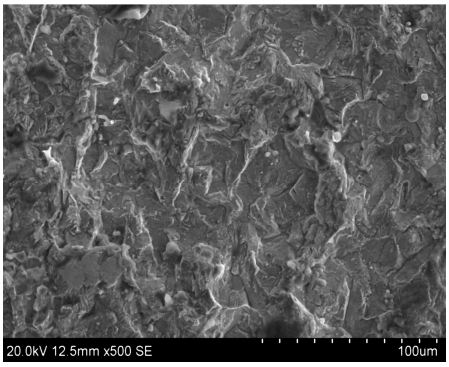

(b)

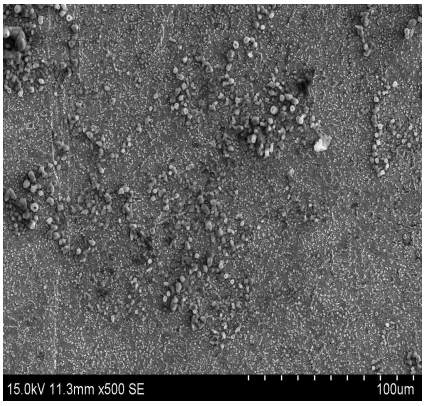

(c)

Fig.8. 12 : SEM images of (a) mild steel, (b) mild steel in 1M HCl without inhibitor (c) mild steel in the presence of 150 ppm of HMMB after 24 Hour

Chapter

9

ELECTROCHEMICAL STUDIES ON THE INTERACTION AND CORROSION INHIBITION OF MILD STEEL WITH HMIB IN HYDROCHLORIC ACID

Contents

9.1 Results and Discussion

9.1.1 Weight loss studies

Weight loss under different intervals of time (24, 48, 72 and 96 hours) in the absence and presence of inhibitor HMIB (Fig.9.1) were studied. Results revealed that the inhibition efficiency is high at 24 hour interval irrespective of concentrations of the inhibitor and subsequently the efficiency declined. The inhibition efficiency increased with the increased concentrations of the inhibitor, however with the advancement of time interval, inhibition efficiency decreased irrespective of the inhibitor concentrations.

9.1.2 Potentiodynamic polarization studies

Potentiodynamic polarization behaviour of mild steel in acid medium at various concentrations (0.5M, 1.0M, & 1.5M) in the absence and

presence of HMIB at 303K, 308K & 313K are presented in Table 9.1 to Table 9.3. Results indicated that the electrochemical parameters vary with the inhibitor as well as acid concentrations. Tafel polarization curves for mild steel in 0.5M, 1M, & 1.5M HCl medium in the absence and presence of various concentrations of HMIB at 303K, 308K & 313K are presented in Fig. 9.2 to Fig. 9.4. It revealed that both the anodic metal dissolution and cathodic hydrogen evolution would exhibit Tafel type behaviour. The result emanating from these studies reveals that HMIB can act as a mixed type inhibitor. The mechanism of corrosion inhibition involves the blocking of reaction sites by the inhibitor due to the adsorption of inhibitor molecule on the metal surfaces and the surface adsorption increases by increase in the concentration of inhibitor [81-82]. The formation of a coating on the surface of the metal as a result of adsorption of the inhibitor molecule gives a considerable protection against corrosion.

9.1.3 Electrochemical impedance spectroscopy (EIS)

Electrochemical impedance spectroscopy (EIS) is an novel technique extensively used to study organic coatings on the metal as this technique does not disturb the double layer at the metal / solution interface [83-84].The electrochemical parameters associated to impedance study using inhibitor HMIB at303K, 308K, 313K are recorded in Table 9.4 to Table 9.6. Results revealed that I_{corr} value showed decreasing trend with increased concentration of the inhibitor in all the concentrations of the acid. The same trend was observed in all the temperature conditions. It is worth to mention that in all the varied acid medium devoid of inhibitor, registered high values of I_{corr}.

Nyquist plots of mild steel in 0.5M, 1M, and 1.5M HCl solution at 303K, 308K, & 313K containing various concentrations of HMIB after 30 minutes of immersion are presented in Figures 9.5 to9.7. It was found that as the concentration of the inhibitor increases, efficiency also increases & efficiency is found to be maximum for 150ppm of HMIB and its efficiency decreases with acid concentration which is presented in Figure 9.8 .It reveals that in uninhibited solution, Nyquist plot yields a slightly depressed semi circles. This clearly explains that the corrosion of the mild steel in the absence of inhibitor are mainly controlled by a charge transfer process [85-86]. The simplest circuit fit for these experimental data was a Randles circuit which consists of a solution resistance, R_s in series to a parallel combination of resistor, R_{ct} and a double layer capacitor, C_{dl}. R_{ct} representing the charge transfer resistance and C_{dl} representing the electrode capacitance. It may be noted from Nyquist plots that R_{ct} values increased with inhibitor concentration, which can be attributed to the formation of a protective layer at the metal surface and this layer acts as a barrier for the mass and the charge transfers.

9.1.4 Adsorption studies

The adsorption isotherm provides information pertaining to the interaction of inhibitor with metal surface [87-88]. Adsorption behaviour of HMIB on mild steel is presented in the Table. 9.8. The surface coverage values (θ) for different concentrations of inhibitor in 0.5M, 1M, and 1.5M HCl obtained from electrochemical measurements were used in adsorption isotherm. Using these data different graphs have been constructed to find out the most suitable

adsorption isotherm. The plot C/ θ Vs C gives a straight line, providing that the adsorption of HMIB on mild steel surface obeys Langmuir adsorption isotherm and the same for mild steel in 0.5M, 1M &1.5M HCl in the absence and presence of HMIB at 303K is shown in Fig. 9.9. The values of K_{ads} and ΔG^{0}_{ads} of HMIB is given in Table 9.7.The negative value of ΔG^{0}_{ads} ensures the spontaneity of adsorption process and stability of the adsorbed layer on the mild steel surface. Generally the value of ΔG^{0}_{ads} around -20 kJ mol^{-1} or lower are consistent with physisorption, while those around -40kJmol^{-1} or higher value involve chemisorptions [89]. Based on the calculated ΔG^{0}_{ads} values, it could be concluded that adsorption involved is physisorption.

9.1.5 Computational studies

Quantum chemical parameters like energy of highest occupied molecular orbital (E_{HOMO}), energy of the lowest unoccupied molecular orbital (E_{LUMO}), energy gap (ΔE) i.e. E_{HOMO}-E_{LUMO}, ionization potential, I which is -E_{HOMO}, electron affinity, A which is –E_{LUMO}, electro negativity, χ which is (I+A)/2 and hardness, η which is (I-A)/2 were calculated and optimized the geometry of the molecule using Gaussian 09 program package.. The calculated values of quantum chemical parameters are listed in Table 9.8. The optimized geometry of the inhibitor HMIB is given in Fig. 9.10 .HOMO and LUMO of HMIB are given in Fig. 9.11.It is generally said that the efficiency of inhibitors increase with decrease in energy gap, ΔE, increase in E_{HOMO} and decrease in E_{LUMO}. Higher E_{HOMO} value enhances the adsorption of inhibitors thereby increasing the inhibition efficiency. Smaller the E_{LUMO} value greater will be the probability of molecules to accept

electrons. Higher the ionization energy, easier will be the removal of electrons from the molecule.

9.1.6 Scanning electron microscopy

SEM studies were carried out to understand the effect of inhibitor molecules on the surface of mild steel. The SEM images of a bare polished mild steel, mild steel after immersion in 1M HCl medium without inhibitor & with HMIB for a period of 24 hours were given in Fig. 9.12. SEM studies revealed that the metal surface was smooth and free from depressions in the case of mild steel immersed in HCl which contains the inhibitor HMIB where as the surface is damaged in the case of mild steel which is immersed in HCl which is kept free from the inhibitor.

9.2. Conclusions.

1) The schiff base acts as an effective inhibitor for the corrosion protection of mild steel in HCl and the efficiency increased with the increase in inhibitor concentration. Highest inhibition efficiency is obtained at 150ppm concentration of the inhibitor.

2) Potentiodynamic polarization study indicates that the inhibitors act as mixed type. Quantum chemical parameters also support the inhibition efficiency of the inhibitor.

3) The adsorption of the inhibitor obeys Langmuir adsorption isotherm model.

4) The charge transfer resistance increased and the double layer capacitance decreased with the increase in inhibitor concentration.

Table 9.1: Data on Electrochemical parameters of mild steel obtained from polarisation curves in 0.5 M, 1 M & 1.5 M HCl at 303K

HCl	HMIB (ppm)	E_{corr} (mV)	β_a (mV dec-1)	β_c (mV dec-1)	Icorr (mA cm^{-2})	CR (mils/yr)	(%IE)
	Blank	-470.58	192.90	231.08	0.059	61.54	-------
	50	-496.98	79.65	172.93	0.030	25.88	49.15
0.5M	100	-517.48	85.45	190.30	0.022	21.77	62.71
	150	-511.43	111.09	241.54	0.015	16.14	74.57
	Blank	-466.61	88.68	90.18	1.015	63.63	------
	50	-466.66	40.44	44.35	0.530	27.20	47.78
1 M	100	-480.88	33.42	54.52	0.460	22.89	54.67
	150	-485.71	41.11	48.24	0.375	18.68	62.12
	Blank	-450.38	43.02	50.05	1.017	75.00	----
1.5 M	50	-471.27	27.82	38.44	0.559	35.16	45.03
	100	-472.12	27.72	36.36	0.480	32.23	52.80
	150	-476.49	28.48	41.31	0.496	30.25	60.12

Table 9.2: Data on Electrochemical parameters of mild steel obtained from polarisation curves in 0.5 M, 1 M & 1.5 M HCl at 308K

HCl	HMIB (ppm)	E_{corr} (mV)	β_a (mV dec-1)	β_c (mV dec-1)	Icorr (mA cm^{-2})	CR (mils/yr)	(%IE)
	Blank	-470.58	192.90	231.08	0.065	298.34	-------
	50	-496.98	79.65	172.93	0.035	135.46	46.15
0.5M	100	-517.48	85.45	190.30	0.028	112.36	56.92
	150	-511.43	111.09	241.54	0.060	99.17	69.23
	Blank	-466.61	88.68	90.18	1.020	567.64	------
	50	-466.66	40.44	44.35	0.565	228.98	44.60
1 M	100	-480.88	33.42	54.52	0.486	221.81	52.35
	150	-485.71	41.11	48.24	0.400	142.65	60.78
	Blank	-450.38	43.02	50.05	1.025	576.79	----
1.5 M	50	-471.27	27.82	38.44	0.590	238.86	42.43
	100	-472.12	27.72	36.36	0.550	231.44	46.34
	150	-476.49	28.48	41.31	0.475	226.36	53.65

Table 9.3: Data on Electrochemical parameters of mild steel obtained from polarisation curves in 0.5 M, 1 M & 1.5 M HCl at 313K

HCl	HMIB (ppm)	E_{corr} (mV)	β_a (mV dec-1)	β_c (mV dec-1)	Icorr (mA cm^{-2})	CR (mils/yr)	(%IE)
	Blank	-498.16	48.274	74.659	0.080	769.49	-------
	50	-501.41	52.126	65.740	0.045	291.24	43.75
0.5 M	100	-488.36	61.796	152.43	0.037	243.93	53.75
	150	-500.95	58.891	181.74	0.030	230.59	62.50
	Blank	-471.27	70.689	164.78	1.027	908.46	--------
	50	-475.47	35.739	58.992	0.590	317.47	41.86
1 M	100	-472.12	28.66	42.205	0.550	251.35	46.44
	150	-450.72	25.33	29.435	0.540	248.17	47.03
	Blank	-475.88	80.477	101.83	1.030	927.47	-------
1.5 M	50	-451.89	62.866	125.22	0.650	393.61	36.89
	100	-430.46	51.588	45.011	0.630	280.58	38.83
	150	-370.18	92.013	167.12	0.600	286.50	41.74

Table 9.4:AC impedance data on mild steel with HMIB in 0.5 M, 1 M & 1.5 M HCl at 303K

HCl	HMIB (ppm)	R_{ct} (Ω cm^2)	C_{dl} (μF cm^{-2})	i_{corr} (mA cm^{-2})	C.R (mils/yr)	(%IE)
	Blank	218	36	0.119	54.00	--------
	50	823	77	0.031	14.45	73.00
	100	1186	60	0.022	10.04	82.00
0.5M	150	1550	43	0.016	7.68	85.93
	Blank	164.2	47	0.15	72.70	------
	50	447.2	57	0.05	26.80	63.17
	100	629.6	111	0.04	19.40	74.13
1M	150	981	54	0.023	10.68	83.20
	Blank	155.2	89	0.16	76.70	-----
	50	402	62	0.06	29.61	61.42
1.5M	100	592	66	0.05	19.21	73.00
	150	711	45	0.03	16.74	78.19

Table 9.5: AC impedance data on mild steel with HMIB in 0.5 M, 1 M & 1.5 M HCl at 308K.

HCl	HMIB (ppm)	R_{ct} (Ω cm^2)	C_{dl} (μF cm^{-2})	i_{corr} (mA cm^{-2})	C.R (mils/yr)	(%IE)
0.5M	Blank	153	93	0.170	64.00	------
	50	415	48	0.060	20.00	63.00
	100	588	47	0.040	14.00	74.00
	150	788	36	0.030	11.00	80.50
1M	Blank	129	108	0.201	92.13	------
	50	262	57	0.099	45.33	50.76
	100	390	55	0.066	30.51	67.00
	150	639	41	0.040	18.62	79.84
1.5M	Blank	122	88	0.213	97.33	-------
	50	239	45	0.100	45.93	48.90
	100	361	46	0.067	31.01	66.20
	150	544	48	0.043	19.71	77.50

Table 9.6: AC impedance data on mild steel with HMIB in 0.5 M, 1 M & 1.5 M HCl at 313K

HCl	HMIB (ppm)	R_{ct} (Ω cm^2)	C_{dl} (μF cm^{-2})	i_{corr} (mA cm^{-2})	C.R (mils/yr)	(%IE)
0.5M	Blank	195	62	0.13	60.83	-------
	50	510	62	0.04	20.00	61.76
	100	713	50	0.031	14.19	72.65
	150	927	52	0.025	11.62	78.96
1M	Blank	121	101	0.214	97	--------
	50	214	50	0.127	55	43.00
	100	379	42	0.068	31	68.00
	150	512	46	0.046	21	76.36
1.5M	Blank	51	118	0.511	233	----
	50	77	92	0.337	153	33.76
	100	108	95	0.240	109	52.70
	150	153	72	0.169	77	66.60

Table 9.7: Adsorption parameters of inhibitor (HMIB) for corrosion of mild steel at various temperatures and concentration.

HCl	Temperature (K)	ΔG^{o}_{ads} (kJ mol^{-1})& K_{ads} x 10^{4}(mol^{-1}) HMIB (ppm)					
		50		100		150	
0.5M	303	-17.32	17.46	-16.89	14.71	-12.05	12.22
	308	-16.42	10.99	-15.96	9.18	-15.80	8.62
	313	-16.47	10.09	-15.96	8.31	-15.74	7.63
1M	303	-16.16	10.99	-15.70	9.18	-16.04	10.21
	308	-15.06	2.15	-15.10	6.56	-15.64	8.10
	313	-14.56	4.85	-14.40	4.57	-15.44	6.81
1.5M	303	-15.94	10.09	-15.57	8.73	-15.24	7.63
	308	-15.85	5.95	-14.99	6.72	-15.34	7.20
	313	-13.46	3.18	-13.70	3.49	-14.17	4.18

Table 9.8: Calculated quantum chemical properties for inhibitor

Inhibitor	E_{HOMO} (eV)	E_{LUMO}(eV)	ΔE (eV)	I (eV)	A (eV)	χ(eV)	η (eV)
HMIB	- 5.91	- 2.00	3.91	5.91	2.00	3.95	1.91

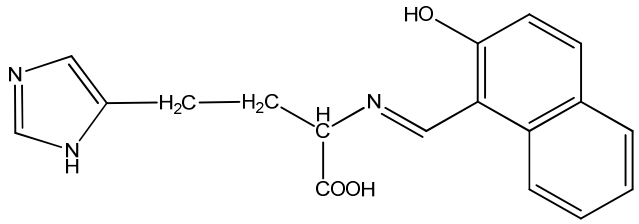

Figure 9.1: Structure of the inhibitor

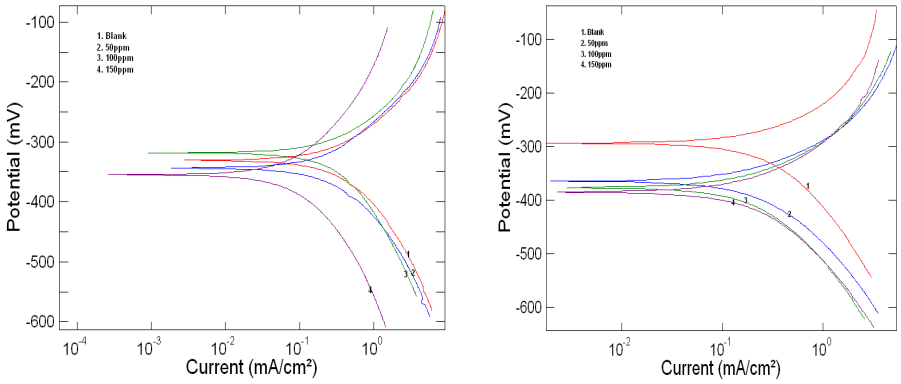

(a) (b)

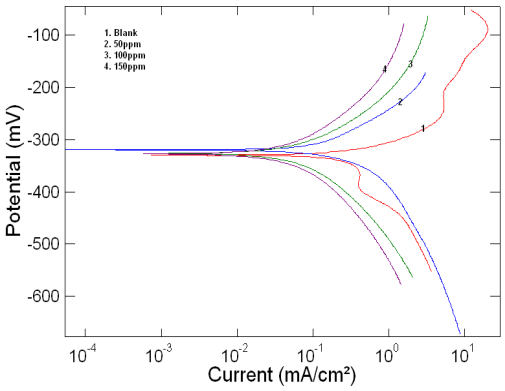

(c)

Figure 9.2 : Polarization curves of mild steel in 0.5, 1 and 1.5M HCl in the absence and presence of different concentrations of HMIB at 303K.

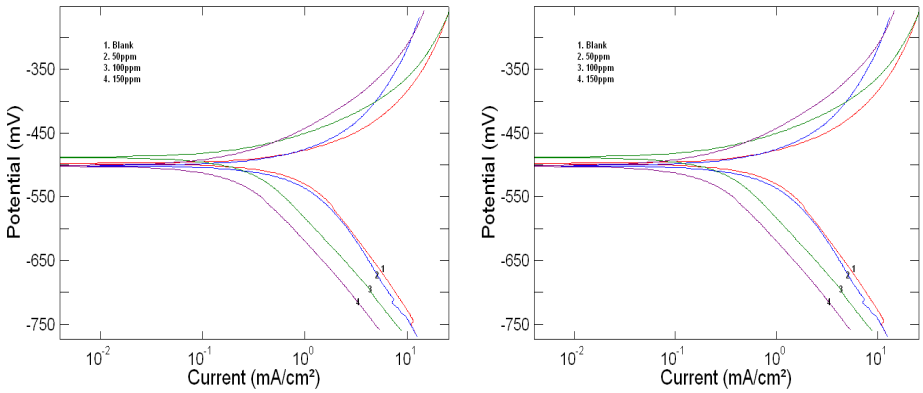

(a) (b)

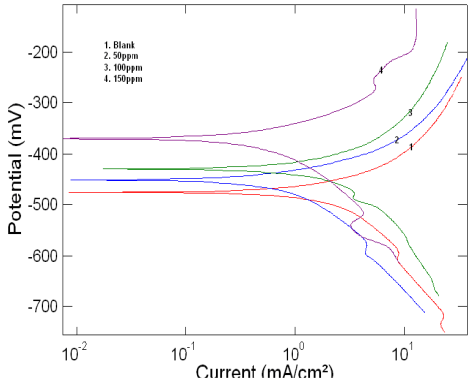

(c)

Figure 9.3: Polarization curve of mild steel in 0.5, 1 and 1.5M HCl in the absence and presence of different concentrations of HMIB at 308K.

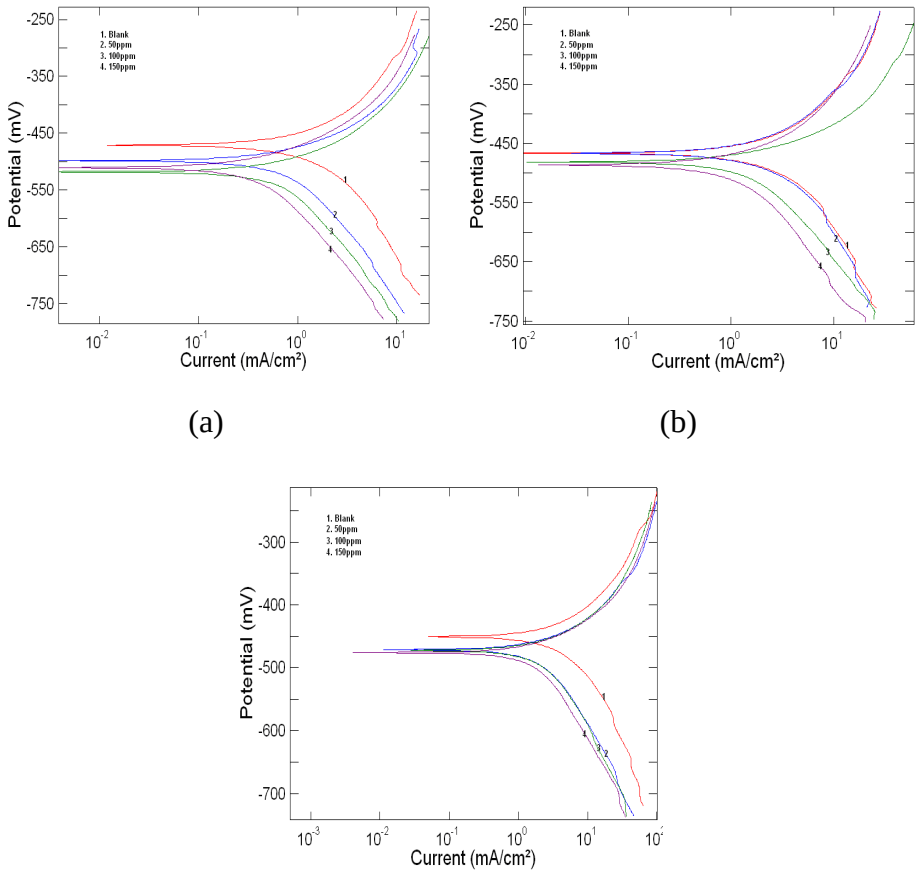

Figure. 9.4: Polarization curve of mild steel in 0.5, 1 and 1.5M HCl in the absence and presence of different concentrations of HMIB at 313 K.

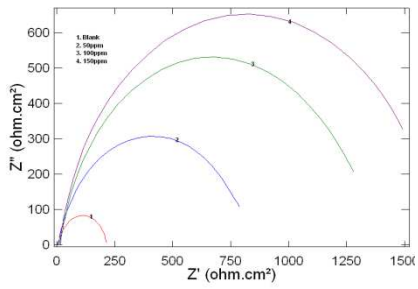

(a)

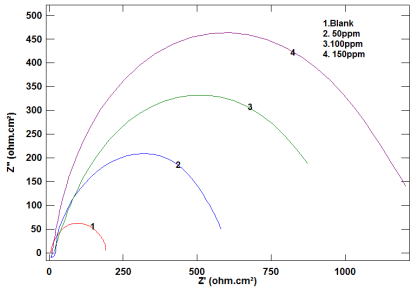

(b)

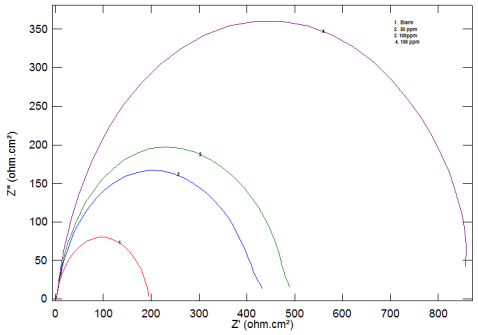

(c)

Figure.9.5: Nyquist plots of mild steel in 0.5, 1, 1.5 M HCl in different concentrations of HMIB at 303K.

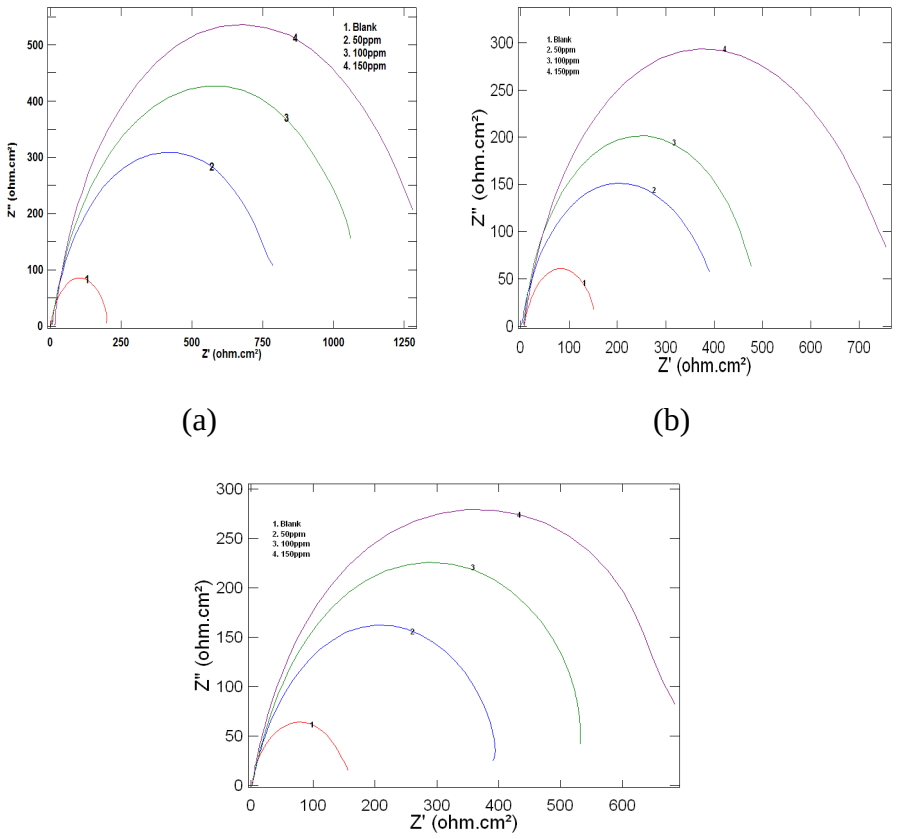

Figure 9. 6: Nyquist plots of mild steel in 0.5, 1, 1.5 M HCl in different concentrations of HMIB at 308K.

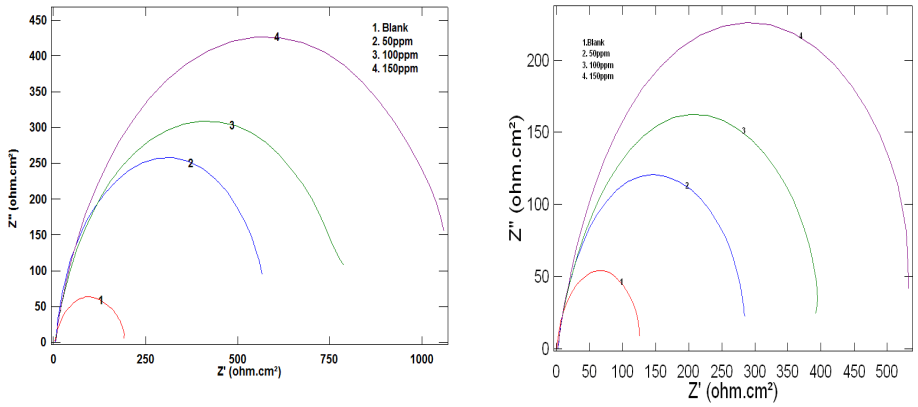

(a) (b)

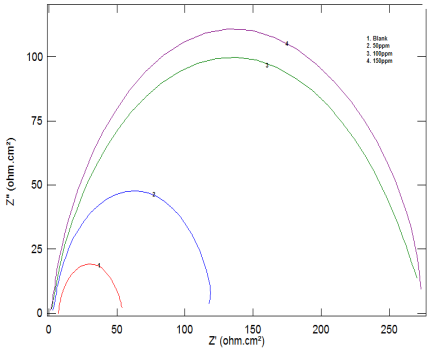

(c)

Figure.9.7: Nyquist plots of mild steel in 0.5, 1, 1.5 M HCl in different concentrations of HMIB at 313K.

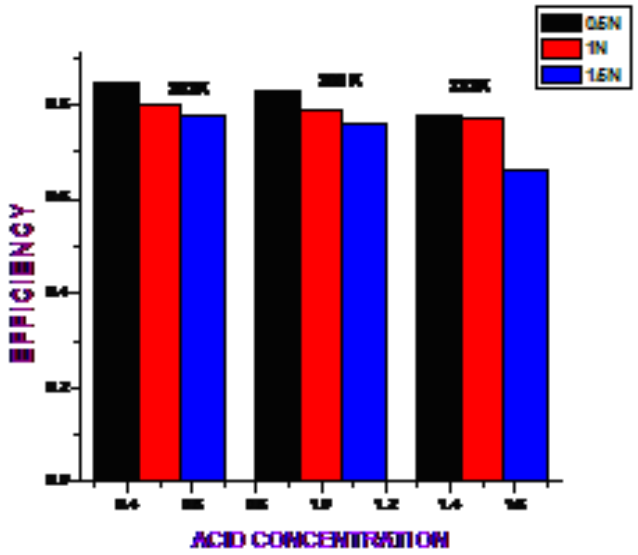

Figure 9.8: Plot of acid concentration Vs efficiency at 150 ppm of HMIB

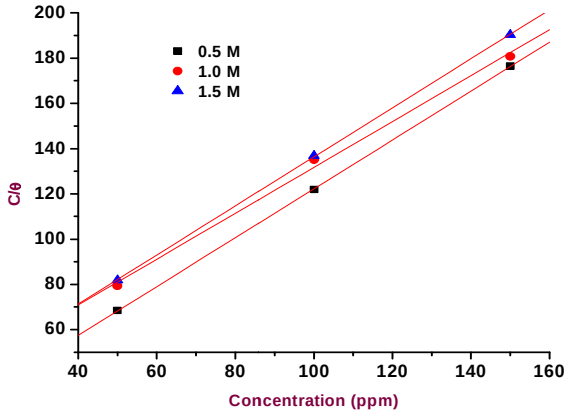

Figure 9.9: Langmuir adsorption isotherm for mild steel in 0.5M, 1M & 1.5M HCl in inhibitor HMIB at 303 K

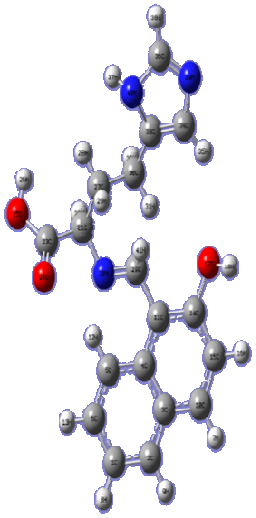

Figure. 9.10: Optimized geometry of inhibitor HMIB

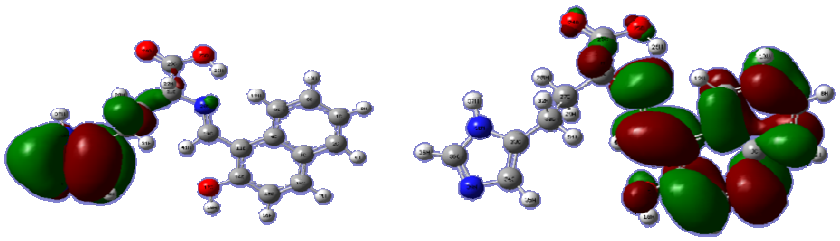

(a) (b)

Figure 9.11: HOMO and LUMO of the inhibitor HMIB

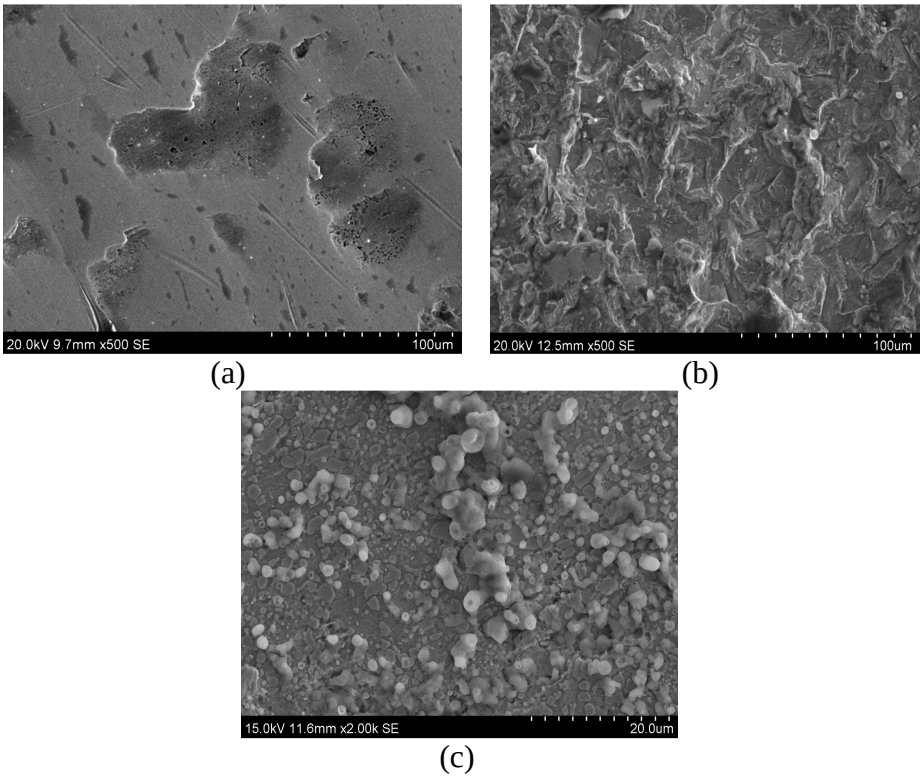

(a) (b)

(c)

Figure 9.12: SEM images of (a) blank mild steel, (b) mild steel in 1M HCl without inhibitor (c) mild steel in the presence of 150 ppm of HMIB after 24 hour.

Chapter

10

ELECTROCHEMICAL AND THEORETICAL STUDIES ON THE INTERACTION OF DL-METHIONINE WITH MILD STEEL IN SULPHURIC ACID

Contents

10.1. Results and Discussion

10.1.1. Weight loss studies

Weight loss under different time intervals (24, 48, 72 and 96 hours) at varying concentrations of DL- methionine (0.5 M, 1.0 M, 1.5M) were studied. Analysis of the results revealed that in all the concentrations of DL - methionine the inhibition efficiency was high up to 24 hour and thereafter efficiency declined gradually. The inhibition efficiency increased in accordance with the inhibitor concentration. However, with the advancement of time, inhibition efficiency declined irrespective of the concentrations of the acid.

10.1.2. Potentiodynamic polarization studies

Potentiodynamic polarization behaviour of the mild steel in 0.5M, 1.0M &1.5M acid with and without inhibitor at 303K, 308K and 313K are presented in Table 10.1 to Table 10.3. Results indicated that the electrochemical parameters E_{corr} & I_{corr} vary with the inhibitor and acid concentration. With the variation in temperature, the potentiodynamic polarization behaviour also varied. Tafel polarization curves for mild steel in 0.5M, 1M, & 1.5M of sulphuric acid in the absence and presence of various concentrations of DL - methionine at 303K, 308K and 313 K are presented in Fig. 10.2 to Fig. 10.4. It reveals that both the anodic metal dissolution and cathodic hydrogen evolution would exhibit Tafel type behaviour. The results emerged from these studies revealed that DL – methionine can act as mixed type inhibitor. The mechanism behind the corrosion inhibition involves blocking of the reaction sites by the inhibitor due to the adsorption of its molecule on the metal surface. The increase in the inhibitor concentration paves way to increase the surface adsorption. The formation of coatings on the metal surface provides considerable protection against corrosion.

10.1.3. Electrochemical impedance spectroscopy (EIS)

Electrochemical impedance spectroscopy (EIS) is reported to be novel technique to study organic coatings on the metal as this technology does not react with the double layer coatings of the metal / solution interface [101]. The electrochemical parameters such as R_{ct}, C_{dl} observed in the impedance studies are given in the Table 10.4 to Table 10.6. Results revealed that I_{corr} value showed decreasing trend with

increased concentrations of the inhibitor and this trend was observed in all the concentrations of the acid. Similar results were also observed in all the temperature conditions. It is worth to mention that in all the different concentrations of the acid devoid of inhibitor registered high values of I_{corr}. Nyquist plots of mild steel in sulphuric acid at various concentrations of DL - methionine after 30 minutes of immersion at different temperatures are presented in the Fig. 10.5 to Fig. 10.7. It clearly reveals that in uninhibited medium, Nyquist plot turned out to be slightly depressed semi circles. This finding explains that the corrosion of the mild steel in the absence of inhibitor are mainly controlled by a charge transfer process [85-86]. The simplest circuit fit for results obtained from these experiments was the Randles circuit which consists of a solution resistance, R_s in series to a parallel combination of resistor, R_{ct} and a double layer capacitor, C_{dl}. R_{ct} representing the charge transfer resistance and C_{dl} representing the electrode capacitance. It is evidenced from the Nyquist plots that R_{ct} values show an increasing trend with inhibitor concentration, which can be attributed to the formation of a protective layer at the metal surface and this layer acts as a barrier for the mass and the charge transfers.

10.1.4. Adsorption studies

The adsorption isotherm provides information on the inhibitor interaction with metal surface [87-88]. Data on the adsorption of DL – methionine on mild steel are presented in the Table10.7. Results revealed that corrosion behaviour varies with inhibitor concentrations under varied temperature in the acid medium. The surface coverage

values (θ) for different inhibitor concentrations obtained from electrochemical measurements were used in adsorption isotherm. Different graphs have been constructed using the above data to find out the most suitable adsorption isotherm. The plot of log (θ/1-θ) Vs log C draws a straight line, highlighting the fact that the adsorption of the DL - methionine on mild steel obeys Langmuir adsorption isotherm and the same is presented in the Fig.10.8. The correlation coefficient (R^2) was employed to select the isotherm that fit the best in accordance with the experimental results. The values of K_{ads} and ΔG^0_{ads} are given in the Table 10.8.The negative values of ΔG^0_{ads} ensure the spontaneity of adsorption process and stability of the adsorbed layer on the mild steel surface. Generally, the value of ΔG^0_{ads} around -20kJ mol^{-1} or lower are consistent with physisorption, while those around -40kJmol^{-1} or higher value involve chemisorptions [89]. Based on the calculated ΔG^0_{ads} values, it could be concluded that adsorption involved is mixed adsorption.

10.1.5. Computational studies

Computational studies enabled to bring about various quantum chemical parameters like energy of highest occupied molecular orbital (E_{HOMO}), energy of the lowest unoccupied molecular orbital (E_{LUMO}), energy gap (ΔE) i.e. E_{HOMO} -E_{LUMO}, ionization potential, I which is -E_{HOMO}, electron affinity, A which is $-E_{LUMO}$, electro negativity, χ which is (I+A)/2 and hardness, η which is (I-A)/2 and all these were calculated and optimized the geometry of the molecule using Gaussian 09 program package. The values of quantum chemical parameters calculated are listed in Table 10.8 and optimized geometry of the

inhibitor molecule is presented in Fig.10.9. HOMO and LUMO of the inhibitor molecule is given in Fig. 10.10 & 10.11. It is generally believed that the efficiency of inhibitor increase with decrease in energy gap, ΔE, increase in E_{HOMO} and decrease in E_{LUMO}. Higher E_{HOMO} value enhances the adsorption of inhibitor thereby contributing to increased inhibition efficiency. Smaller the E_{LUMO} value, greater will be the probability of molecules to accept electrons. Higher the ionization energy, removal of electrons from the molecule will become very easy.

10.1.6 Scanning electron microscopy

SEM studies was carried out to understand the effect of inhibitor molecule on the surface of mild steel. The SEM images of a bare polished mild steel, mild steel after immersion in 1M sulphuric acid without inhibitor & with inhibitor for a period of 24 hours were given in Figure 10.12. SEM studies revealed that the metal surface was smooth and free from depressions in the case of mild steel immersed in sulphuric acid which contains the inhibitor where as the surface is damaged in the case of mild steel which is immersed in sulphuric acid which is kept free from the inhibitor.

10.2. Conclusions.

Electrochemical techniques like EIS and polarization studies were used to carry out the corrosion inhibition effect of DL- methionine on mild steel in sulphuric acid. Based on the studies it can be concluded that

1) The corrosion of mild steel decreased with the increase in concentration of DL- Methionine. However the efficiency decreased with the increase in temperature and acid concentration. The maximum efficiency of the inhibitor is observed at 303K.

2) With the increase in the inhibitor concentration, corrosion inhibition efficiency and charge transfer resistance increased but double layer capacitance decreased due to more adsorption of the inhibitor.

3) Inhibitor molecule affects both the anodic and cathodic processes and this prompted the inhibitor to acts as a mixed type one. The adsorption behaviour of the inhibitor obeys Langmuir adsorption isotherm model.

Table 10.1: Data on Electrochemical parameters of mild steel obtained from polarisation curves in 0.5 M, 1 M & 1.5 M H_2SO_4 at 303K .

Sulphuric acid	DL – methionine (ppm)	E_{corr} (mV)	β_a (mV dec-1)	β_c (mV dec-1)	Icorr (mA cm^{-2})	CR (mils/yr)	(%IE)
	Blank	-470.58	192.90	231.08	1.686	61.54	-------
	50	-496.98	79.65	172.93	0.638	25.88	62.15
0.5M	100	-517.48	85.45	190.30	0.600	21.77	64.79
	150	-511.43	111.09	241.54	0.410	16.14	75.68
	Blank	-466.61	88.68	90.18	1.244	63.63	------
	50	-466.66	40.44	44.35	0.501	27.20	59.72
1 M	100	-480.88	33.42	54.52	0.486	22.89	60.86
	150	-485.71	41.11	48.24	0.312	18.68	74.90
	Blank	-450.38	43.02	50.05	1.220	75.00	----
1.5 M	50	-471.27	27.82	38.44	0.523	35.16	57.13
	100	-472.12	27.72	36.36	0.507	32.23	58.42
	150	-476.49	28.48	41.31	0.496	30.25	60.12

Table 10.2: Data on Electrochemical parameters of mild steel obtained from polarization curves in 0.5 M, 1 M & 1.5 M H_2SO_4 at 308K

Sulphuric acid	DL – methionine (ppm)	E_{corr} (mV)	β_a (mV dec-1)	β_c (mV dec-1)	Icorr (mA cm^{-2})	CR (mils/yr)	(%IE)
	Blank	-470.58	192.90	231.08	1.686	298.34	-------
	50	-496.98	79.65	172.93	0.638	135.46	62.15
0.5M	100	-517.48	85.45	190.30	0.600	112.36	64.79
	150	-511.43	111.09	241.54	0.410	99.17	75.68
	Blank	-466.61	88.68	90.18	1.244	567.64	------
	50	-466.66	40.44	44.35	0.501	228.98	59.72
1 M	100	-480.88	33.42	54.52	0.486	221.81	60.86
	150	-485.71	41.11	48.24	0.312	142.65	74.90
	Blank	-450.38	43.02	50.05	1.220	556.79	----
1.5 M	50	-471.27	27.82	38.44	0.523	238.86	57.13
	100	-472.12	27.72	36.36	0.507	231.44	58.42
	150	-476.49	28.48	41.31	0.496	226.36	60.12

Table 10.3: Data on Electrochemical parameters of mild steel obtained from polarisation curves in 0.5 M, 1 M & 1.5 M H_2SO_4 at 313K.

Sulphuric acid	DL - methionine (ppm)	Ecorr (mV)	β_a (mV dec-1)	β_c (mV dec-1)	Icorr (mA cm^{-2})	CR (mils/yr)	(%IE)
	Blank	-498.16	48.274	74.659	0.653	769.49	-------
	50	-501.41	52.126	65.740	0.296	291.24	54.67
0.5 M	100	-488.36	61.796	152.43	0.246	273.93	62.34
	150	-500.95	58.891	181.74	0.217	270.59	66.72
	Blank	-471.27	70.689	164.78	1.50	908.46	--------
	50	-475.47	35.739	58.992	0.720	317.47	52
1 M	100	-472.12	28.66	42.205	0.580	251.35	61.30
	150	-450.72	25.33	29.435	0.543	248.17	63.80
	Blank	-475.88	80.477	101.83	1.375	627.47	-------
1.5 M	50	-451.89	62.866	125.22	0.643	293.61	50.50
	100	-430.46	51.588	45.011	0.614	280.58	53.07
	150	-370.18	92.013	167.12	0.627	286.50	51.70

Table 10.4: AC impedance data on mild steel with DL – methionine in 0.5 M, 1 M & 1.5 M H_2SO_4 at 303K.

Sulphuric acid	DL -methionine (ppm)	R_{ct} (Ω cm^2)	C_{dl} (μF cm^{-2})	I_{corr} (mA cm^{-2})	C.R (mils/yr)	(%IE)
	Blank	28.55	254	0.91	416.90	-----
	50	64.47	107	0.42	199.36	55.71
0.5M	100	118	63	0.24	110.90	75.80
	150	156	23	0.16	74.68	81.69
	Blank	20.82	274	1.25	501.0	------
	50	44.74	149	0.58	220.35	53.46
1M	100	66.00	89	0.36	138.20	68.45
	150	108	87	0.20	94.50	80.74
	Blank	18.57	1063	1.40	571.3	-----
	50	39.60	322	0.65	266.1	53.10
1.5M	100	55.90	156	0.57	179.80	66.77
	150	90	117	0.25	114.80	79.36

Table 10.5: AC impedance data on mild steel with DL – methionine in 0.5 M, 1 M &1.5 M H_2SO_4 at 308K.

Sulphuric acid	DL – methionine (ppm)	R_{ct} (Ω cm^2)	C_{dl} (μF cm^{-2})	I_{corr} (mA cm^{-2})	C.R (mils/yr)	(%IE)
	Blank	20.7	117	1.14	522.50	------
	50	46.07	107	0.56	258.40	55.06
0.5M	100	74.00	104	0.38	174.20	72.02
	150	105.0	100	0.27	123.90	80.28
	Blank	19.32	363	1.26	576.70	-------
	50	40.00	176	0.70	300.60	51.70
1M	100	60.00	172	0.393	178.50	67.80
	150	94.65	126	0.278	125.60	79.58
	Blank	18	678	1.09	641.0	-------
	50	34.01	298	0.50	321.20	47.07
1.5 M	100	66.20	189	0.391	234.4	64.10
	150	85	139	0.274	141.80	78.82

Table 10.6: AC impedance data on mild steel with DL – methionine in 0.5 M, 1 M, &1.5 M H_2SO_4 at 313K.

Sulphuric acid	DL – methionine (ppm)	R_{ct} (Ωcm^2)	C_{dl} (μF cm^{-2})	I_{corr} (mA cm^{-2})	C.R (mils/yr)	(%IE)
	Blank	17.92	193	1.45	750.2	-----
	50	38.49	155	0.67	309.3	53.44
0.5M	100	47.14	142	0.55	252.5	61.98
	150	79.06	133	0.33	150.6	77.33
	Blank	15.31	632	1.70	775.00	-----
	50	30.06	172	0.83	350.40	49.50
1M	100	34.89	168	0.74	341.20	56.11
	150	67	161	0.511	233.40	77.14
	Blank	15.00	757	1.966	897.7	-----
	50	29.00	406	0.739	357.40	48.27
1.5M	100	33.00	345	0.531	351.1	54.54
	150	65.01	212	0.253	251.56	76.92

Table 10.7: Adsorption parameters of inhibitor (DL – methionine) for corrosion of mild steel at various temperatures and concentration

Sulphuric acid	Temperature (K)	ΔG^{o}_{ads} (kJ mol^{-1})& K_{ads} x 10^{4}(mol^{-1}) DL - methionine (ppm)					
		50		100		150	
0.5M	303	-14.10	4.86	-12.57	2.65	-12.87	2.98
	308	-13.76	3.88	-12.77	2.64	-12.81	2.68
	313	-13.34	3.30	-12.56	2.43	-12.16	1.93
1M	303	-13.77	4.26	-12.14	2.23	-12.73	2.82
	308	-13.64	3.71	-12.77	2.64	-12.43	2.31
	313	-13.13	3.04	-12.45	2.32	-11.63	1.69
1.5M	303	-13.57	3.94	-11.93	2.05	-11.12	1.49
	308	-25.61	3.15	-26.93	1.74	-30.96	1.23
	313	-25.29	3.94	-26.21	2.05	-28.79	1.49

Table 10.8: Calculated quantum chemical properties for DL – methionine

Inhibitor	E_{HOMO} (eV)	E_{LUMO} (eV)	ΔE (eV)	I (eV)	A (eV)	χ (eV)	η (eV)
DL - methionine	- 6.24	- 0.55	5.68	6.24	0.55	3.39	2.84

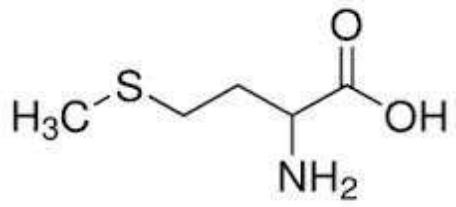

Figure 10.1: Structure of DL - methionine, the inhibitor molecule.

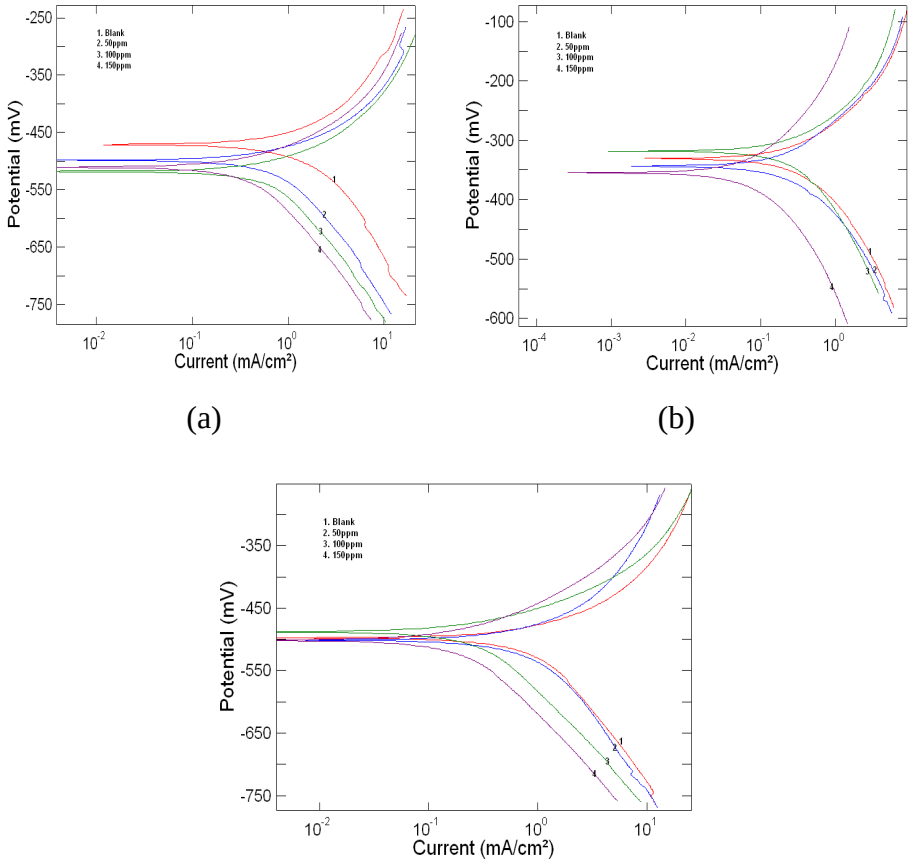

Figure 10.2: Polarization curves of mild steel in 0.5 M H_2SO_4 with different concentrations of DL - methionine at (a) 303K (b) 308K and (c) 313K.

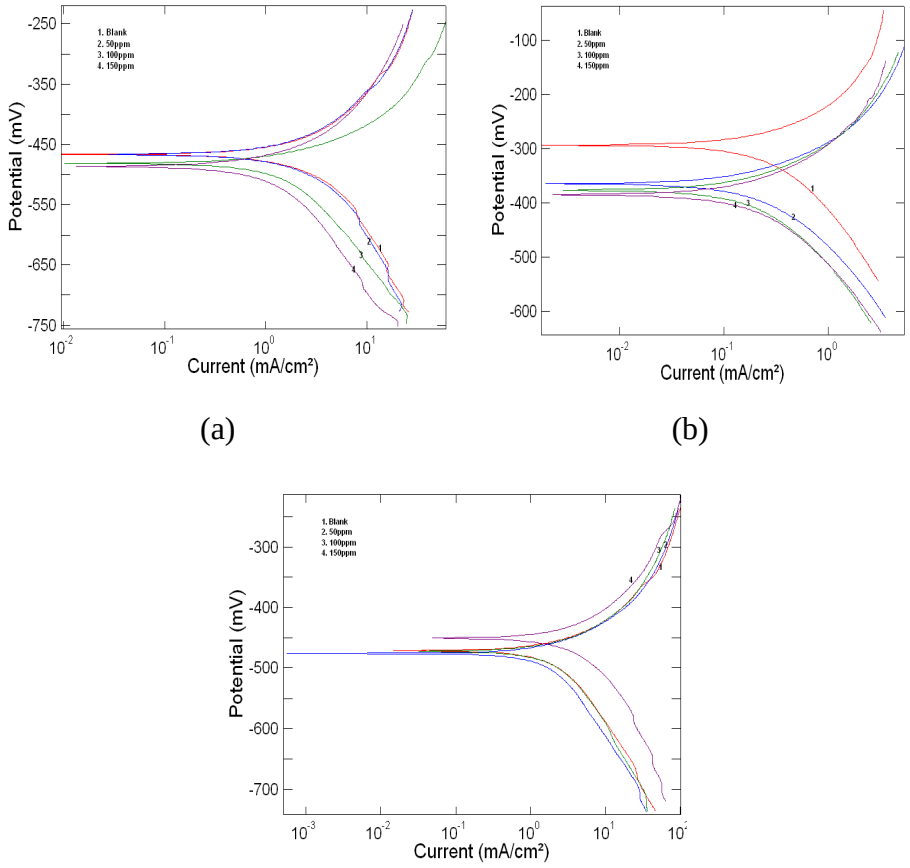

Figure 10.3 : Polarization curves of mild steel in 1 M H_2SO_4 with different concentrations of DL - methionine at (a) 303K (b) 308K (c) 313K.

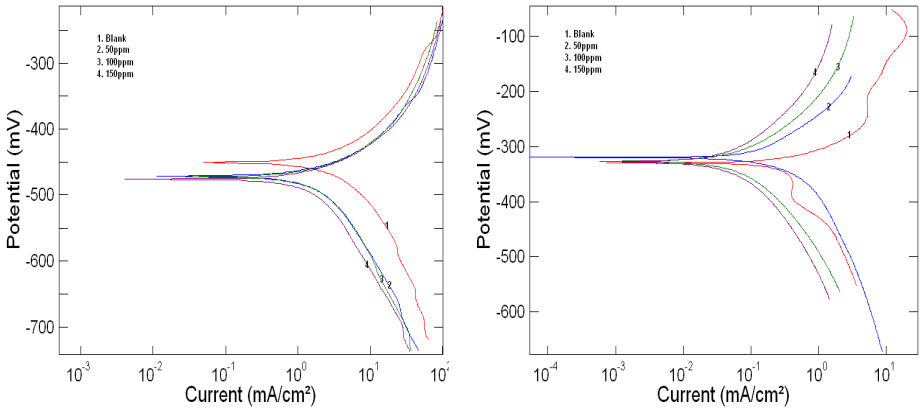

(a) (b)

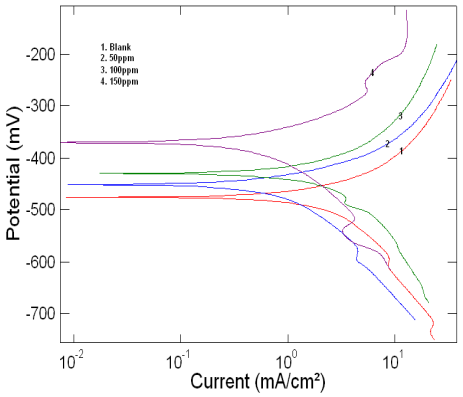

(c)

Figure 10.4 : Polarization curves of mild steel in 1.5 M H_2SO_4 with different concentrations of DL - methionine at (a) 303K (b) 308K (c) 313K.

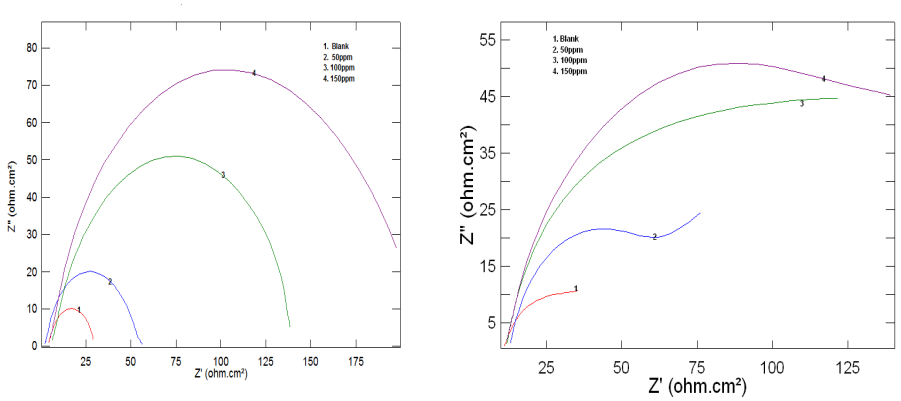

(a) (b)

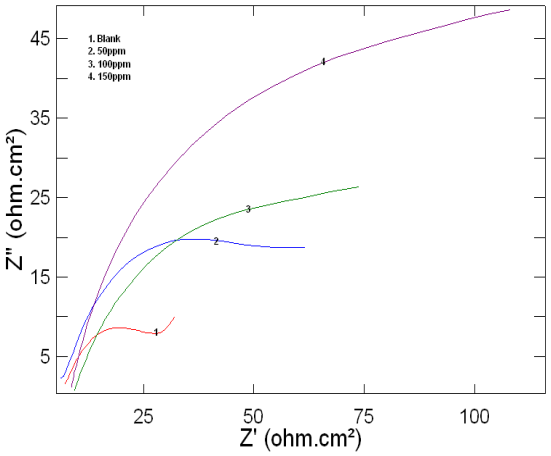

(c)

Figure 10.5: Nyquist plots of mild steel in 0.5 M H_2SO_4 with different concentrations of DL – methionine at (a) 303K (b) 308K (c) 313K.

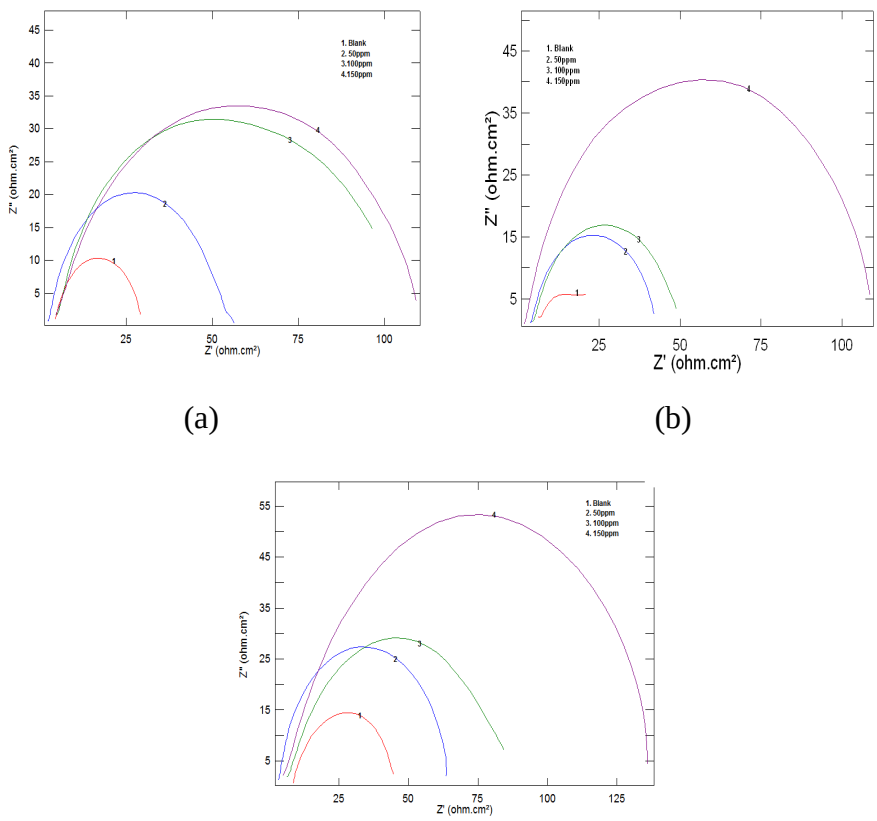

Figure 10.6: Nyquist plots of mild steel in 1M H_2SO_4 with different concentrations of DL - methionine at (a) 303K (b) 308K and (c) 313K.

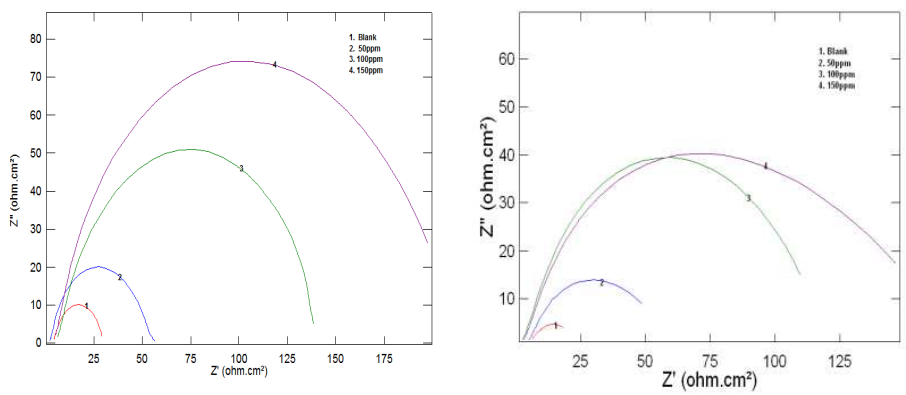

(a) (b)

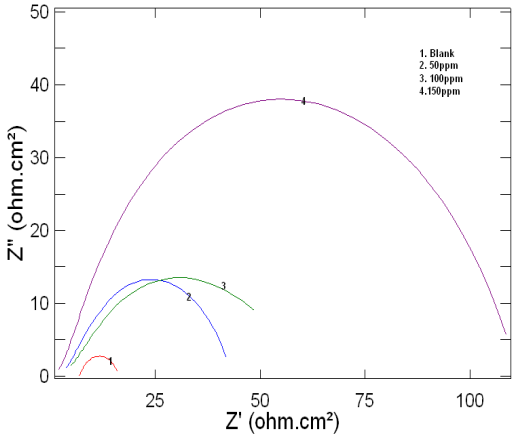

(c)

Figure 10.7: Nyquist plots of mild steel in 1.5M H_2SO_4 with different concentrations of DL – methionine at (a) 303K (b) 308K and (c) 313K

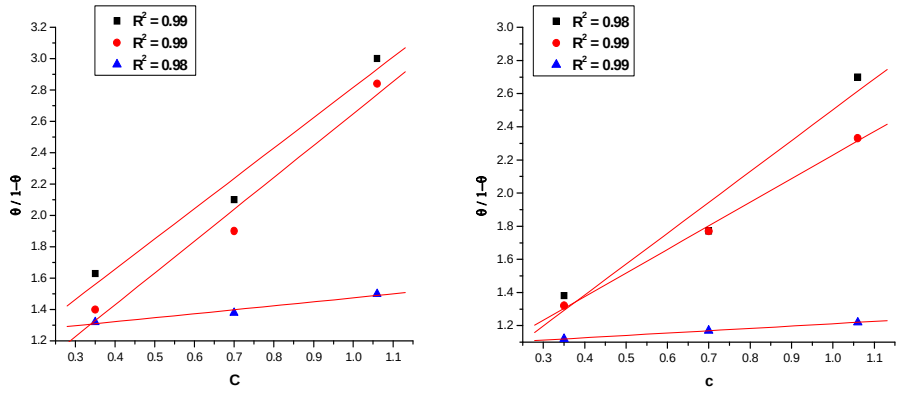

(a)

(b)

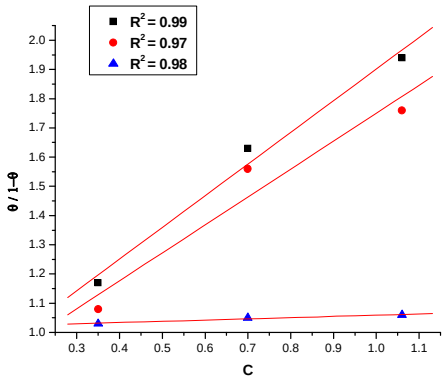

(c)

Figure 10.8: Langmuir adsorption isotherm for mild steel with 0.5M, 1M & 1.5M H_2SO_4 in DL - methionine inhibitor at (a) 303K (b) 308K (c) 313 K.

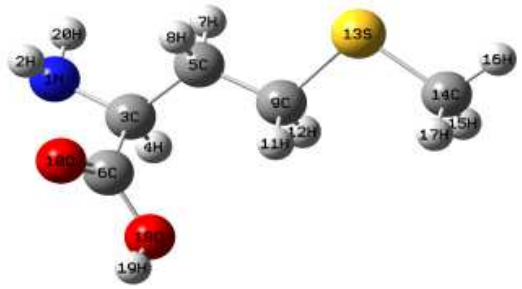

Figure. 10.9: Optimized geometry of DL – methionine.

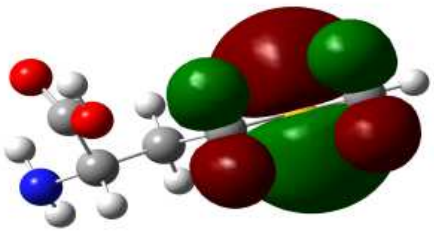

Figure. 10.10: HOMO of DL – methionine.

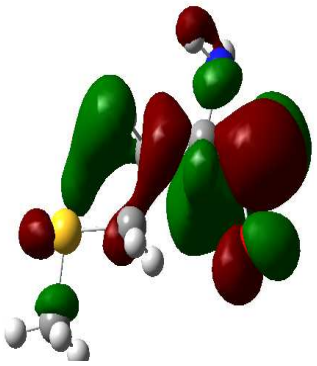

Figure. 10.11. LUMO of DL – methionine.

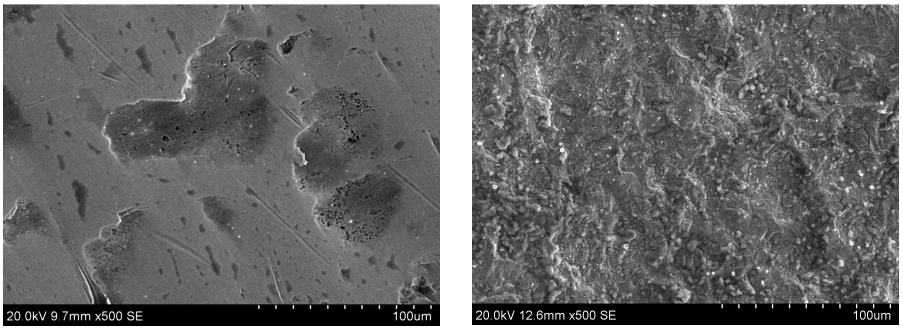

(a) (b)

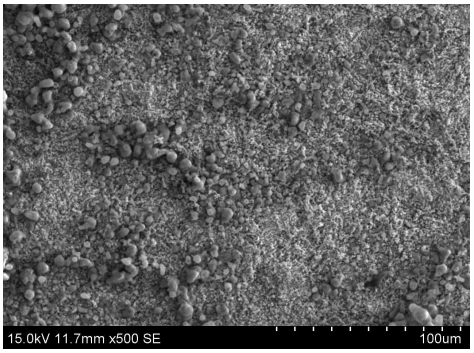

(c)

Figure. 10.12: SEM images of (a) blank mild steel, (b) mild steel in 1M H_2SO_4without inhibitor (c) mild steel in the presence of 150 ppm of DL – methionine after 24 Hour.

SUMMARY

In recent past, research efforts oriented in corrosion chemistry are mainly to identify green corrosion inhibitors which are cost effective and capable of reducing the intensity of environmental pollution. With an objective to identify the efficient green corrosion inhibitors, studies were undertaken to find out the corrosion inhibition effect of different amino acids such as L- cysteine, DL - methionine and newly synthesized schiff bases namely HDMMA, HMIB, HMMB, HHDMP, MOAB derived from the amino acids on corrosion of widely used metals in the industry *viz*. copper and mild steel. Acids like sulphuric acid and hydrochloric acid at various concentrations are employed as the medium. The standard techniques such as Weight loss, Electrochemical impedance spectroscopy (EIS), Polarization studies, Adsorption studies, Scanning electron microscope (SEM), Atomic force microscope (AFM) are employed in the studies.

The thesis is divided into ten chapters containing two parts Part – A and Part – B. First two chapters include introduction and materials and methods. Part – A deals with corrosion inhibition of copper using amino acid schiff bases and Part – B deals with corrosion inhibition of mild steel using amino acid schiff bases.

The sulphur containing amino acid L - cysteine is used to study the corrosion inhibition behaviour in copper at different concentrations (0.5M, 1M & 1.5M) of sulphuric acid under varied temperature conditions such 303K,308K and 313K. The studies revealed the

inhibition efficiency varied depending on the concentrations of inhibitor as well as acid medium concentrations. Maximum inhibition effect is recorded at 150ppm of the inhibitor at 0.5M H_2SO_4. It is evident from the adsorption studies that the adsorption of L - cysteine on copper surface obeyed Langmuir adsorption isotherm.

The corrosion inhibition effect of amino acid schiff base HHDMP synthesized from amino acid serine on copper in 1M H_2SO_4 was also studied at various temperature conditions. The results highlight that HHDMP is an ideal inhibitor for corrosion of copper as showed fairly good inhibition efficiency at room temperature and also at high temperature. The studies clearly indicated that corrosion rate and double layer capacitance decreased due to increased adsorption of the inhibitor.

HDMMA is another schiff base synthesized from the sulphur containing amino acid L – cysteine used for studies of corrosion inhibition in copper. The hydrochloric acid (1M HCl) was used as the medium. In this study, polarization technique brings about that the molecule can inhibit both cathodic and anodic reactions and behave in accordance with that of a mixed type inhibitor. It is also clear that the inhibitor molecule adsorbs on the copper surface and blocked the reaction sites. The surface area available for the attack of the corrosive species decreased in accordance with the increase of inhibitor concentration.

The synergistic effect of amino acids L- cysteine and alanine is also subjected to studies on the corrosion of copper in 1M H_2SO_4 at 303K,

308K and 313 K. The results showed corrosion inhibition efficiency increased to a great extent when two inhibitor molecules are simultaneously used to check corrosion. Higher inhibition efficiency was manifested by a combination of 150 ppm cysteine and 50 ppm alanine. It also pointed out that synergism is more pronounced at higher temperature.

Schiff base MOAB synthesized from the amino acid valine is employed to study corrosion of copper in 1M HCl at various temperature conditions such as 303K, 308K & 313K. Results showed MOAB inhibit corrosion effectively with good inhibition efficiency. The inhibition efficiency increased with increase in concentration and decreases with exposure time and temperature.SEM & AFM image reveals that the surface of the metal is protected by the adsorption of the inhibitor and thereby cracks on the surface of the metal is reduced.

Schiff base HMMB synthesized from amino acid DL – methionine is used to study the corrosion of mild steel in HCl (05M, 1M & 1.5M) at 303K, 308K and 313K. Results showed that efficiency of the inhibitor increased with concentration and the maximum corrosion efficiency is registered at a concentration of 150 ppm. Potentiodynamic polarization study indicates that the inhibitor acts as a mixed type. Quantum chemical parameters also support the inhibition efficiency of the inhibitor.

Schiff base HMIB is employed to study corrosion of mild steel in HCl (0.5M, 1M & 1.5M) at 303K, 308K and 313K. Studies revealed that the data on adsorption of inhibitor obeys Langmuir adsorption

isotherm model and the charge transfer resistance increased, double layer capacitance decreased with the increase in the inhibitor concentration.

Amino acid DL – methionine used to study the corrosion of mild steel in HCl (0.5M, 1M & 1.5M) at 303K, 308K and 313K reveals that corrosion of mild steel decreased with the increase in concentration of DL – methionine. However, the efficiency decreased with the increase in temperature and acid concentration. The maximum efficiency of the inhibitor is observed at 303K.

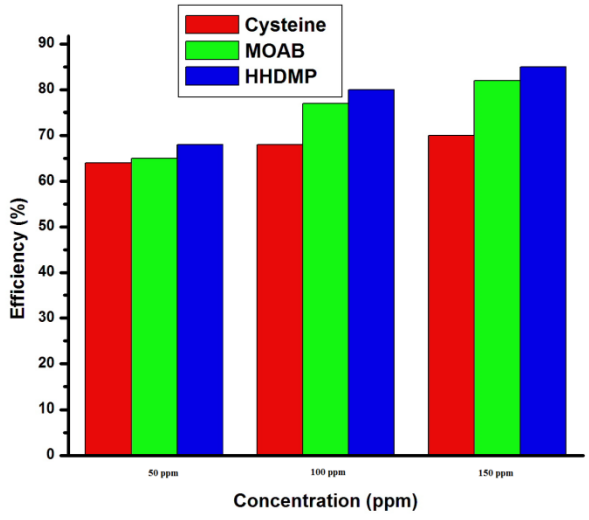

Variation of inhibition of cysteine, MOAB, HHDMP in 1M H_2SO_4 at 303K.

In the present studies, the corrosion inhition behaviour of amino acids such as cysteine and methionine on most widely used metals in the industry *viz* mild steel and copper were carried out. In addition to amino acids, schiff bases namely HDMMA, HMIB, HMMB, HHDMP, MOAB were synthesized and subjected to corrosion studies. Studies shows that the amino acids as well as schiff bases are capable of reducing corrosion level in the metals under studies irrespective of the medium and temperature conditions. However the efficiency of corrosion inhibition depends on the inhibitor concentration and temperature conditions. The studies also brought about that the synergism of the amino acids are also effective and prevent corrosion in metal. Based on the results, these inhibitors could be considered as efficient and ideal ones.

REFERENCES

1. J. Kruger in “Uhlig’s Corrosion Handbook”, R. W. Revie, Ed., p. 3, John Wiley, New York (2000).
2. Metal Progress Data Book and Advanced Materials and Processes, American Society for Metals, Metals Park, Ohio.
3. N.E. Hamner (ed.), NACE Corrosion Data Survey, Houston, TX, NACE, 1974.
4. E.D. Verink, Jr., Uhlig’s Corrosion Handbook, 2nd edn, John Wiley & Sons, Inc., NY, 2000.
5. R.W. Staehle, Life Prediction of Corrodible Structures, R.N. Parkins (ed.), NACE, Vol. 3, Texas,1994.
6. O. L. Riggs Jr., Corrosion inhibitors, C.C.Nathan (Ed.), NACE Houston, Texas, USA, 1973.
7. A. Frignani, G. Trabanelli, F. Zucchi, M. Zucchini, proceedings of 5th European symposium of corrosion inhibitors, Ferrara, Italy, 1980
8. A. Subramananian, M. Natesan, V. S. Muralidharan, K. Balakrishnan, and T. Vasudevan, Corrosion, *56*, 144(2000).
9. A. Wachter, T. Skei, and N. Stillman, Corrosion, *7*, 284 (1951).
10. S. A. Levin, S. A. Gintzbergy, I. S. Dinner and V. N. Kuchninsky, proceedings of 2nd European symposium on corrosion inhibition, Ferrara, Italy, 1965.
11. J. Kruger in “Uhlig’s Corrosion Handbook”, R. W. Revie, Ed., p. 3, John Wiley, New York (2000).
12. D.Q. Zhang, L.X. Gao, G.D. Zhou, J. Appl. Electrochem. 35 (2005) 1081.
13. K.M. Ismail, A.M. Fathi, W.A. Badawy, Corros. Sci. 48 (2006) 1912.
14. K. Barouni1, A. Kassale, A. Albourine, O. Jbara, B. Hammouti , L. Bazzi, J. Mater. Environ. Sci. 5 ((2014) 456.

15. Ana T. Simonovic, Marija B. Petrovic ,Milan B.Radovanovic, Snezana M.Milic, Milan M. Antonijevic, Chemical Papers 68 (2014)362.

16. D. Xu, Y. Li ,T. Gu, Mat. and Corro.65(2014)837.

17. Milosev, , Jasminaka, Milan, Lesar, Antonija, Journal of the Serbian Chemical Society, 78(2013)2069.

18. A.Zarrouk, B. Hammouti, A. Dafali, H. Zarrok, *Der Pharma Chemica*. 3 (2011) 266.

19. K.F. Khaled, Corros. Sci. 52 (2010) 3225.

20. Wei Luo, Yimin Xu, Qiming Wang,Peizhen Shi, Mi Yan, Corros. Sci. 52 (2010) 3509.

21. Manjula Spah, Dal Chand Spah, Balraj Deshwal, Seungmoon Lee, Yoon-Keun Chae, Jin Won Park, Corros. Sci. 51(2009) 1293.

22. M.M Antonijevic , M. B. Petrovic, Int. J. Electrochem. Sci. 3 (2008)1 .

23. K. Barouni, L. Bazzi, R. Salghi, M. Mihit, B. Hammouti , A. Albourine, S. El Issami, Mater. Let. 62 (2008)3325.

24. K.F. Khaled, Mater. Chem. Phys. 112(2008)104.

25. Khaled M. Ismail, Electrochimica Acta, 52 (2007) 7811.

26. S. Kumar, T.S Narayanan, M. S Kumar, A Manimaran, Int. J. Electrochem. Sci. 1 (2006) 456.

27. Da-quan Zhang, Li-xin Gao, Guo-ding Zhou, J.Appl. Electrochem.35 (2005)1081.

28. Matos, J.B. Pereira, L.P. Agostinho, S.M.L. Baricia, O.E. Cordeiro, G.G.O. Elia. J. Electroanal. Chem. 570(2004) 91.

29. G. Moretti, F. Guidi, Corros. Sci. 44 (2002) 1995.

30. Ishtiaque Ahamad, M A Quraish, Corros. Sci. 52 (2002) 651

31. M. Rylkina, A. Chikanova, L. Trubacheva, S. Reshetnikov, Protection of Metals 35 (1999) 23.

32. H. Baba, T. Kodama, Corros. Sci. 41 (1999) 1987.

33. Moretti G, Guidi F. Corros. Sci. 44 (1995) 2002.

34. G .Gomma, M Wahdan. Mater. Chem. Phys. 39(1994)142.

35. Qiong Deng, Hong-Wei Shi, Na-Na Ding, Bao-Qin Chen, Xiao-Peng He, Guixia Liu, Yun Tang, Yi-Tao Long, Guo-Rong Chen, Corros. Sci. 57 (2012)220.

36. M. S. Morad, J.Appl.Electochem, 38(2008)1509.

37. O. Olivares-Xometl, N.V. Likhanova, M.A. Domínguez-Aguilar, E. Arce, H. Dorantes, P. Arellanes-Lozada,110(2008)344.

38. M. S. Morad, J.Appl.Electochem, 37 (2007)1191.

39. M. S. Morad, J.Appl.Electochem, 35(2005)889.

40. M .Zerfaoui, H. Oudda, B. Hammouti, S. Kertit, M. Benkaddour. Prog. Org. Coat. 51(2004) 134.

41. G. Gomma, Bull. Electrochem. 12 (1998) 456.

42. L. Madkour, M. Ghoneim, Bull. Electrochem. 13 (1997) 1.

43. D. Kalota, D. Silverman, Corros. Sci. 50 (1994) 138.

44. I.Sakiyan, N. Gunduz, T.Gunduz, Synth. React. Inorg.Met.-Org.Chem. 31 (2001)1175

45. I.Lukovits, E.Kalman, G.Palinkas, Corrosion. 51 (1995) 201.

46. F.Bentiss, M.Lagrenee, M.Traisnel, B.Mernari, H.El Attari, J. Hetrocycl. Chem.36 (1999) 149.

47. E.Mc Cafferty, V.Pravadic, A.C. Zettlemoyer, Trans Faraday Soc. 66 (1999) 237.

48. S.K. Bag, S.B. Chakra borty, S.R.Chaudhari, J. Indian Chem Soc .70 (1993) 24.

49. W.H. Ailor, Hand book of corrosion testing and evaluation, John Wiley and Sons, New York,1971.

50. J.D.Talati, R.M. Modi, Br. Corros J. 10 (1975) 103.

51. J.D. Talati, G.A.Patel, Br. Corros J. 11 (1976) 47.

52. M. K. Pavithr, T.V. Venkatesh, K. Vathsal, K.O. Nayan, Corros. Sci. 52 (2010) 3811.

53. U. Rammelt, G. Reinhard, Prog. Org. Coat. 21 (1992) 205.

54. A. Amirudin, Prog.Org. Coat. 26 (1995) 1.

55. R. Greef, R. Peat, L. M. Peter, D. Pletcher and J. Robinson, Instrumental Methods in Electrochemistry, Eastbourne: Horwood Publishing Ltd. 2001.

56. I.O. Arukalam, I .C. Madufo, E.E Orguzie, Int.Journal of Applied Sciences and Engineering Rresearch 3(2014) 241

57. A. Chetouani, B. Hammouti, T. Benhadda, M. Daoudi, Appl. Surf. Sci. 249 (2005) 375.

58. M.G. Noack,Mater.Perform.21 (1982)26

59. A.K. Dubey, G. Singh. Port Electrochim.Acta 25 (2007) 221.

60. H.H. Uhling (1971) Corrosion and Corrosion control , 2nd edition, John wiley and sons , Newyork

61. J.C.Scully (1990) “The fundementals of corrosion” 3rd edition ,Perhamon press.

62. D.A.Jones(1996) “Principles and prevention of corrosion “ Prentice Hall Inc., New Jersy.

63. V.S.Sastri, Corrosion ,52(1996) 447

64. M. Bouklah, B. Hammouti, M. Lagrene and F. Bentiss: Corros. Sci, 48 (2006) 2831.

65. R. Agrawal and T.K.G. Namboodhiri Corros. Sci 30 (1990) 37.

66. M.J.S.Dewar , W.Thiel , J.Am Chem Soc 99 (1977) 4899.

67. R.G.Pearson, Inorg Chem 27 (1988) 734–740.

68. H. Keles, M. Keles, I. Dehri , O. Serindag, Colloid. Surface A. 320(2008) 138.

69. L. Tang, X. Li, L. Li, G. Mu, G. Liu, Mat. Chem. Phys. 97(2006) 301.

70. R. Solmaz, G. Kardas ¸ B. Yazici , B .Erbil, Prot. Met.43 (2007) 476.

71. A Popova, E .Sokolova, S. Raicheva, M. Christov, Corros. Sci. 45(2003) 33.

72. G. Kardas , R. Solmaz, Corros. Rev. 24(2006)151.

73. E. Nisek-Lisac, A. Brnada, A.D. Mance, Corros .Sci. 42(2000) 243.

74. G. Gomma, M. Wahdan, Mat. Chem. Phys. 39(1994) 142.

75. R. Braun, E. Lopez, D. Vollmer, Corros. Sci. 34(1993) 1251.

76. M. Wahdan, Mate. Chem. Phys. 49(1997)135.

77. H. Otmacic, E. Stupinusek-Lisac, Electrochim Acta. 48 (2003)985.

78. P. Yu, D-M Liao, Y-B Luo, Z-G Chen, Corrosion. 59(2003)314.

79. K.F.Khaled, S.A .Fadl-Allah, B. Hammouti, Mat. Chem Phys. 117(2009)148.

80. M. Scendo, M. Hepel, J. Electroanal. Chem. 613(2008)3.

81. F. Bentiss, M.Traisnel, M.Lagrenee. J. Appl. Electrochem. 31(2001)41.

82. F.A. Champion, *Corrosion testing procedure,* 2nd edn. (Chapman and Hall, London, 1964) 32.

83. A. Chetouani, B. Hammouti, T. Benhadda , M. Daoudi, App Surf Sci. 249(2005)375.

84. B. El Mehdi, B. Mernari, M. Traisnel, F. Bentiss, M. Lagrenee, Mat. Chem. Phys. 77(2002) 489.

85. M. El Achouri, S. Kertit, H. M. Gouttaya, B. Nciri, Y. Bensouda, L. Perez, M.R. Infante , K. Elkacemi , Prog .Org. Coat. 43(2001) 267.

86. W.J. Lorenz, F. Mansfeld, Corros Sci.31(1986)467.

87. M. Erbil, Chim Acta Turcica.1(1988)59.

88. M. A. Migahed, H. M. Mohamed, Al-Sabagh, Mat.Chem.Phys. 80 (2003)169.

89. A. Azim, Shalaby L. A. , Abbas H, Corros Sci.14(1974)21.

90. F. Rosalbino, R. Carlini, F. Soggia, G. Zanicchi, G. Scavino, Corros. Sci. 58 (2012) 139.

91. El-Sayed M. Sherif, R.M. Erasmus, J.D. Comins, J. Colloid Interf. Sci. 311 (2007) 144.

92. A. Fiala, A. Chibani, A. Darchen, A. Boulkamh, K. Djebbar, *Appl. Surf. Sci*. 2007, 253, 9347.

93. Drach, A., Tsukrov, I., DeCew, J., Aufrecht, J., Grohbauer, A., Hofmann, U. Corros. Sci. 76 (2013) 453.

94. Tian, H., Li, W., Cao, K., Hou, B. *Corros. Sci.* 73 (2013) 281.

95. F. Zucchi, G. Trabanelli, C. Monticelli, Corros. Sci. 38 (1996) 147.

96. S.H. Lee, J.G. Kim, J.Y. KooEng. Fail. Anal. 17 (2010) 1424.

97. E.M. Sherif, S.M. Park, Electrochim. Acta 48 (2006)4065.

98. S.M. Milic´, M.M. Antonijevic , Corros. Sci. 51 (2009) 28.

99. X. Wang, H. Yang, F. Wang, Corros. Sci. 53 (2011) 113.

100. T.T. Qin, J. Li, H.Q. Luo, M. Li, N.B. Li, Corros. Sci. 53 (2011) 1072.

101. A. Chetouani, B. Hammouti, T. Benhadda , M. Daoudi, App. Surf. Sci. 249 (2005) 375 .